Solar Radiation Glazing Factors for Window Panes, Glass Structures and Electrochromic Windows in Buildings - Measurement and Calculation

Bjørn Petter Jelle [ab]∗

[a] SINTEF Building and Infrastructure,
Department of Materials and Structures, NO-7465 Trondheim, Norway
[b] Norwegian University of Science and Technology (NTNU),
Department of Civil and Transport Engineering, NO-7491 Trondheim, Norway

∗ Corresponding author: bjorn.petter.jelle@sintef.no (e-mail), 47-73593377 (phone), 47-73593380 (fax)

Abstract

Window panes, glass structures and electrochromic windows in buildings may be characterized by a number of solar radiation glazing factors, i.e. ultraviolet solar transmittance, visible solar transmittance, solar transmittance, solar material protection factor, solar skin protection factor, external visible solar reflectance, internal visible solar reflectance, solar reflectance, solar absorbance, emissivity, solar factor and colour rendering factor. Comparison of these solar quantities for different glass fabrications enables one to evaluate and thus select the most appropriate glass material or system for the specific buildings and applications. Measurements and calculations were carried out on various glass materials, including three electrochromic window devices, and several two-layer and three-layer window pane configurations.

Keywords: Solar radiation glazing factor; Transmittance; Reflectance; Absorbance; Emissivity; Colour rendering factor.

Contents

1.   Introduction

Since early times when man discovered and began utilizing the glass material in their buildings, they have had an efficient means to let solar radiation into the buildings and at the same time be protected from harsh weather in the form of rain and wind outside. This has provided mankind with buildings where daylight and solar heat have given comfortable living and working spaces in a protected environment. With the following citation we may go back 4000-6000 years in history (Zerwick 1990):

"Who, when he first saw the sand or ashes ... melted into a metallic form ... would have imagined that, in this shapeless lump, lay concealed so many conveniences of life? ... Yet, by some such fortuitous liquefaction was mankind taught to procure a body ... which might admit the light of the sun, and exclude the violence of the wind ..."

The main component in glass is sand (silica, SiO_2), but to melt silica one has to use temperatures higher than 1700°C, which is not so practically done. However, adding soda ash (Na_2CO_3) reduces the melting point, e.g. to 800°C, which is a much more feasible and practical temperature. Unfortunately, this makes the resultant material into sodium silicate (water-glass, $NaSiO_3$), which is soluble in water. To obtain a non-soluble product, a stabilizer, like limestone ($CaCO_3$), is included. A typical glass composition will then consist of 65 % sand, 20 % soda ash and 15 % limestone (Flavell and Smale 1974). The glass structure is amorphous, and is in every respect like a liquid, but with such a high viscosity that at room temperature its fluid properties can not be measured, i.e. a rigid liquid. As an example a given deformation taking place in glass at 965°C in 1 second, takes 30 seconds at 742°C, 1 minute at 660°C, 1 hour at 538°C, one day at 427°C, one year at 316°C, 1000 years at 254°C and $35 \cdot 10^9$ years at room temperature (Flavell and Smale 1974). Thus, the common misinterpretation that glass is believed to slowly creep at normal temperatures is seen to be wrong, e.g. in churches and cathedrals several centuries old.

As the use of window panes and glass structures in buildings have become more and more widespread and extensive up throughout the years, the construction design and glass material properties have become more important. This is also strenghtened by the increasing tendency of often employing rather large glass areas in today's buildings. Glass with material additives and different surface coatings is tailor-made and chosen in order to fulfil the various requirements for the specific buildings. The glass and window properties are selected with respect to several, often contradictory, considerations. Generally, a window is supposed to let in as much daylight as possible, give comfortable luminance conditions, give satisfactory view out of (and often into) buildings, transmit a minimum of heat from the interior to the exterior in order to reduce the heating demand, transmit solar radiation from the exterior to the interior in order to reduce the heating demand (i.e. in winter), shut off solar radiation by reflection which otherwise might cause too much heating, not induce air current problems or give a poor thermal comfort and not induce unacceptable interior or exterior water condensation.

As is seen from the above, very much concern is taken regarding the energy aspects of window panes. The energy transfer in windows consists of solar radiation, thermal (infrared) radiation, thermal conduction in solids and gases and gas convection. The glass materials with surface coatings and window details are adapted to the actual building type and function, e.g. office building, hospital, family dwelling etc. The energy from the solar radiation will diminish the need for heating, but at the same time the energy costs due to cooling demands should be kept as low as possible. The measurement and calculation of quantities such as solar transmittance, solar reflectance and solar factor is important in this respect. The solar

factor (SF) is the sum of the solar transmittance and the emitted infrared radiation inwards the building, i.e. the total solar energy transmission through the glazing.

Electrochromic window (ECW) devices are able to control the solar radiation passage by varying the applied voltage, hence offering an elegant and dynamic way to regulate the solar transmittance. For various aspects and information on electrochromic materials and windows it is referred to the available literature, e.g. the studies by Alamri (2009), Azens et al. (2005), Baetens et al. (2010a), Bhadra et al. (2009), Bouessay et al. (2002), Carpenter et al. (1987), Carpenter and Conell (1990), K.-C. Chen et al. (2011), Z. Chen et al. (2011), Fantini and Gorenstein (1987), Geniès et al. (1990), Granqvist (1989, 1991, 1995, 2000, 2005, 2008, 2012), Granqvist et al. (1997, 2003, 2010), Green et al. (2012ab), Jelle et al. (1992ab, 1993abc, 2007), Jelle and Hagen (1993, 1999ab), Kalagi et al. (2011), Karuppasamy and Subrahmanyam (2007), Lampert (1980, 1984, 1986, 1989, 1998, 2004), Lampert and Ma (1992), Lampert et al. (1999), Lee and DiBartolomeo (2002), Lee et al. (2006ab), Leventis and Chung (1990), Makimura et al. (2006), Monk et al. (1995, 2001), Mortimer (1999), Mortimer et al. (1992, 2006), Moulki et al. (2012), Penin et al. (2006), Piccolo 2010, Rougier et al. (1999, 2002), Rougier and Blyr (2001), Sauvet et al. (2008, 2009), Stilwell et al. (1992), Syed and Dinesan (1991), Yu et al. (1987), Yu and Lampert (1989) and Zhang et al. (2011). Solar regulation may also be achieved by other smart windows than electrochromic ones, i.e. photochromic windows, thermochromic windows, gasochromic windows, liquid crystal windows and suspended particle (electrophoretic) windows, see e.g. the studies by Adami et al. (2010), Anders et al. (2008), Baetens et al. (2010a), Chen and Lo (2009), Cupelli et al. (2009), Gao et al. (2011), Gardiner et al. (2009), Georg et al. (1998), Huang et al. (2012), Lampert (1998, 2003, 2004), Li et al. (2012), Mennig et al. (1999), Mlyuka et al. (2009), Park and Hong (2009), Vergaz et al. (2008), Wittwer et al. (2004), Ye et al. (2012) and Yoshimura et al. (2009). Energy performance and life cycle cost of smart windows have been studied by Sekhar and Toon (1998), whereas an eco-efficiency evaluation of a smart window prototype has been performed by Syrrakou et al. (2006). Furthermore, an evaluation of control strategies for different smart window combinations using computer simulations has been carried out by Jonsson and Roos (2010). In order to be able to achieve as large solar regulation as possible in smart windows, dirt accumulation should be avoided as for all window panes, thus self-cleaning windows and glazing products (Midtdal and Jelle 2013) may play an important role.

Several commercial electrochromic windows are already available (Baetens et al. 2010a, Jelle et al. 2012a), and applications in combination with other technologies like solar cells, solar cell glazing and building integrated photovoltaics (BIPV) may also be possible (Ahn et al. 2007, Deb et al. 2001, Bullock et al. 1996, Gao et al. 1999, Jelle et al. 2012ab, Jelle and Breivik 2012ab, Lampert 2003), where the BIPVs also have to fulfil the requirements of the building envelope (Jelle et al. 2012b), e.g. wind-driven rain tightness (Breivik et al. 2013). For studies concerning high-performance window frames and window spacers it is referred to the works by Gustavsen et al. (2007, 2008, 2011), Jelle et al. (2012a) and Van Den Bergh et al. (2013). Grynning et al. (2013) studied the energy balance of a window addressing both heat losses and heat gains, and thus also both heating and cooling demands. As solar cells normally are covered by glass panes or other transparent materials, characterization of the solar radiation throughput in glass and other materials (e.g. transparent polymers) is also highly interesting for solar cell applications in order to be able to harvest and utilize as much as possible of the solar radiation. Furthermore, recent investigations on thermal insulation materials, which may also be applied in future high-performance window frames, have been conducted by Baetens et al. (2010b), Baetens et al. (2011), Gao et al. (2012, 2013), Jelle et al. (2009, 2010), Jelle (2011) and Sandberg et al. (2013). For ageing and durability issues concerning ECWs it is referred to the available literature, e.g. the studies by Czanderna et al. (1999), Lampert (1989), Lampert et al. (1999), Nagai et al. (1999), Tajima et al. (2012) and Tracy et al. (1999).

In general, in addition to the pure energy aspects, it is also important to emphasize the degradation of building materials by solar radiation, especially organic matter where the chemical bonds may be broken up by the more energetic parts of the solar spectrum, i.e. ultraviolet (UV) radiation (see e.g. our earlier work in Jelle et al. 2007, Jelle and Nilsen 2011, Jelle et al. 2012c, Jelle 2012). A substantial part of the UV radiation is blocked by the glass itself, but nevertheless a significant amount of UV radiation passes through the glass and into the buildings. This transmitted UV radiation affects both materials and living species inside the buildings. Typical examples may be fading, discolouration and degradation of books in book shelves (e.g. in libraries) and other paper materials, wall paintings and exhibits (e.g. in museums), wood materials in walls, floor, ceiling, window frames etc., plastic materials and surface painting in various building structures and equipment, furnitures and carpets. Other examples may be green plants and flowers (e.g. in family dwellings, atriums with large glass areas, greenhouses), livestock and pet animals in various buildings and human beings in situations with larger exposed skin areas (in winter gardens, indoor svimming and recreation areas with large glass facades, etc.) Protection of human skin from solar radiation, especially the short-wave radiation, is also interesting in other structures than buildings, e.g. in automobiles.

Generally, the most important solar radiation glazing factors are:

1. Ultraviolet Solar Transmittance, T_{uv}
2. Visible Solar Transmittance, T_{vis}
3. Solar Transmittance, T_{sol}
4. Solar Material Protection Factor, SMPF
5. Solar Skin Protection Factor, SSPF
6. External Visible Solar Reflectance, $R_{vis,ext}$
7. Internal Visible Solar Reflectance, $R_{vis,int}$
8. Solar Reflectance, R_{sol}
9. Solar Absorbance, A_{sol}
10. Emissivity, ε
11. Solar Factor, SF (from T_{sol}, R_{sol} and ε)
12. Colour Rendering Factor, CRF

In order to quantify and compare solar characteristics of different glass materials with and without coating, and also other materials transmitting solar radiation (e.g. various polymers) we will in this work present a comprehensive review of measurement and calculation of the most important solar radiation glazing factors, including several examples for various glass materials, several two-layer and three-layer window pane configurations and three electrochromic window (ECW) devices at various colouration levels.

2. Solar Radiation

The solar radiation at the earth's surface is roughly located between 300 nm and 3000 nm (0.3 μm and 3 μm, respectively), where the visible (VIS) radiation (light) lies between 380 nm and 780 nm. Ultraviolet (UV) and near infrared (NIR) radiation are located below and above the VIS region, respectively. Figure 1 depicts the solar radiation in outer space and at the earth's surface, both with and without molecular absorption in the atmosphere. Above 3000 nm, and not part of the direct solar radiation, lies the thermal radiation called infrared (IR) radiation, which all materials radiate above 0 K (peak at around 10 μm at room temperature).
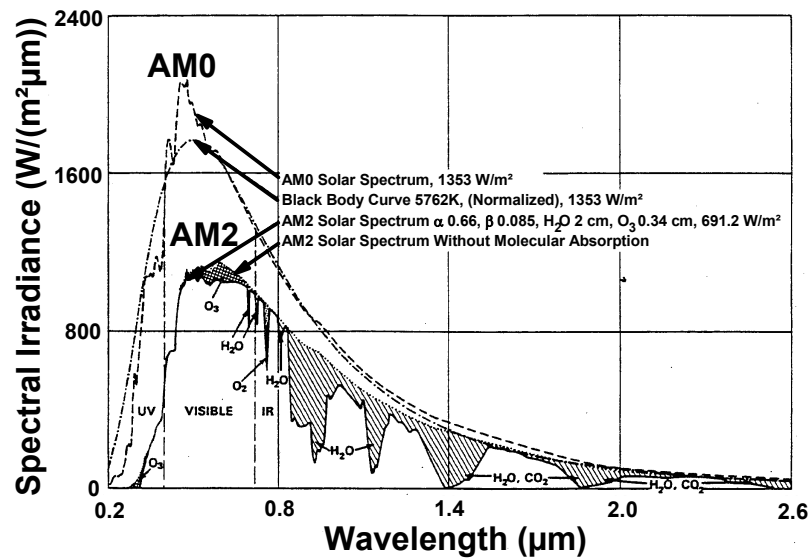
Fig.1.　　The radiation from the sun, comparing the AM0 (outer space) and AM2 (at the earth's surface, the sun 30° above the horizon) spectra. The AM2 spectrum is shown both with and without molecular absorption (in O_2, O_3, H_2O and CO_2). Somewhat redrawn from Fahrenbruch and Bube (1983).

The UV radiation is further divided into the three subregions UVA (320-400 nm), UVB (280-320 nm) and UVC (100-280 nm), where wavelength borders may have small variations in the literature (e.g. 315 nm instead of 320 nm). For examples of photodegradation processes it is referred to the studies by Croll and Skaja (2003), Fufa et al. (2012), Gerlock et al. (1998), Jelle et al. (2007), Jelle (2012), Rånby and Rabek (1975), Rabek (1995, 1996) and Tylli et al. (1989), where Jelle (2012) is treating in general accelerated climate ageing of building materials, components and structures in the laboratory.

3.　　Solar Radiation through Window Panes and Glass Structures

Solar radiation falling onto a material will be transmitted, absorbed and reflected. The amount of solar radiation transmitted, absorbed and reflected is dependent upon the wavelength (λ) of the radiation, the incident angle and the optical properties of the material. These three processes are characterized by the material's transmittance (T), absorbance (A) and reflectance (R), which denote the fraction of incident radiation intensity which is transmitted, absorbed or reflected by the material, as depicted in Fig.2. Conservation of the total energy in the solar radiation beam requires that the sum of T, A and R is given by (Andersson et al. 1990, Granqvist 1981, 1984, 1989, 1991, Hecht 1987, Jastrzebski 1987, Jelle 1993, Jelle et al. 2007, Stjerna and Granqvist 1990):

$$T(\lambda) + A(\lambda) + R(\lambda) = 1 \quad (100 \text{ %}) \tag{1}$$

For a body in thermodynamically equilibrium with its surroundings the energy absorbed in the material must be equal to the emitted energy (Kirchhoff's law of thermal radiation), i.e. (Granqvist 1981, 1984, 1989, 1991, Jelle 1993, Jelle et al. 2007):

$$E(\lambda) = A(\lambda) \tag{2}$$

where E denotes the emittance.

The diffuse transmittance, diffuse reflectance and retroreflectance have been omitted in Fig.2, i.e. only the specular (mirror) reflectance and regular transmittance are depicted. Regular reflectance may be used to refer to specular reflectance (e.g. ASTM E 179-81 (1981)). A solar radiation beam which is reflected back the same way as the incident beam is called a retroreflected radiation beam, whereas refracted radiation beam is used for a beam transmitted into a second medium.
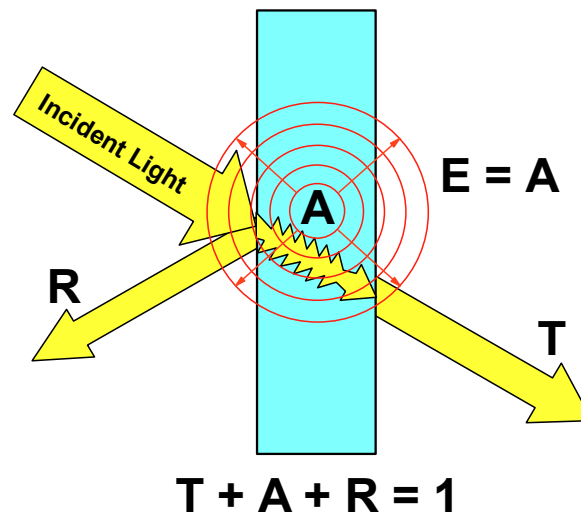
Fig.2.   The releelationship between transmittance (T), absorbance (A) and reflectance (R), in addition to emittance (E), in a single glass pane. Diffuse transmittance, diffuse reflectance and retroreflectance are not depicted, neither reflectance from the interface glass/air within the glass material.

While Fig.2 is treating a single glass pane with a simple relationship between the spectroscopic quantities, the situation is more complex in Fig.3 with multiple transmittance, absorbance and reflectance in a two-layer glass pane. Both Fig.2 and Fig.3 are simplified with respect to actual refracted radiation beam paths, e.g. parallel displacement due to different media with unequal refraction indices. In fact, contrary to real situations, this is avoided in the calculations by assuming a radiation beam with normal incidence. The real transmittance values including the total solar energy transmittance are then somewhat lower. In addition, the reflectance from the interface glass/air(gas) within the glass material is not depicted either. The calculations for a three-layer window pane will naturally be even more complex.

In a two-layer window pane which purpose is to act as a blocking screen towards solar radiation, a coating is placed on the inside of the outer glass. In a two-layer window pane which purpose is to reduce the heat loss from the inside, a coating is placed on the outside of the inner glass. In both cases, the coating is facing the window pane cavity.

Transmittance T and reflectance R as functions of wavelength λ for a ***single glass pane*** given by

$$T(\lambda) = T_1 \tag{3}$$

$$R(\lambda) = R_1 \tag{4}$$

may be calculated for a ***two-layer window pane*** by applying Fig.3 and infinite series expansion to give the following expressions (Davies 2004, ISO 9050:2003 (2003), Kimura 1977, Rubin et al. 1998):

$$T(\lambda) = \frac{T_1 T_2}{1 - R_{1b} R_2} \tag{5}$$

$$R_{ext}(\lambda) = R_1 + \frac{T_1^2 R_2}{1 - R_{1b} R_2} \tag{6}$$

$$R_{int}(\lambda) = R_{2b} + \frac{T_2^2 R_{1b}}{1 - R_2 R_{1b}} \tag{7}$$

and furthermore for a ***three-layer window pane*** the following formulas (ISO 9050:2003(E) (2003), Rubin et al. 1998):

$$T(\lambda) = \frac{T_1 T_2 T_3}{[1 - R_{1b} R_2][1 - R_{2b} R_3] - T_2^2 R_{1b} R_3} \tag{8}$$

$$R_{ext}(\lambda) = R_1 + \frac{T_1^2 R_2[1 - R_{2b} R_3] + T_1^2 T_2^2 R_3}{[1 - R_{1b} R_2][1 - R_{2b} R_3] - T_2^2 R_{1b} R_3} \tag{9}$$

$$R_{int}(\lambda) = R_{3b} + \frac{T_3^2 R_{2b}[1 - R_2 R_{1b}] + T_3^2 T_2^2 R_{1b}}{[1 - R_3 R_{2b}][1 - R_2 R_{1b}] - T_2^2 R_3 R_{1b}} \tag{10}$$

where

> T_1, T_2, T_3, R_1, R_2 and R_3 denote the transmittance and reflectance for glass number 1, 2 and 3, respectively, i.e. exterior (outer) glass towards incident radiation beam, middle glass and interior (inner) glass, respectively. The index "b" for R_{1b} and R_{2b} designates that the reflectance measurement is performed on the back (reverse) side of the glass as compared to the normal incident radiation beam direction, e.g. R_{1b} versus R_1. For simplicity reasons, the wavelength (λ) dependence of T_1, T_2, T_3, R_1, R_2 and R_3 is omitted in Eqs.3-10 above. Note that the denominators in Eqs.8-10 above are identical after some minor rearrangements in Eq.10.

$R_{ext}(\lambda)$ and $R_{int}(\lambda)$ denote the external and internal solar radiation reflectance, i.e. outdoor solar radiation reflected back to the outside and indoor solar radiation reflected back to the inside, respectively. Note that the denominators in the last term for R_{ext} and R_{int} are equal both for a two-layer and a three-layer window pane, as the apparent distinction is due to the chosen symmetrical notation.
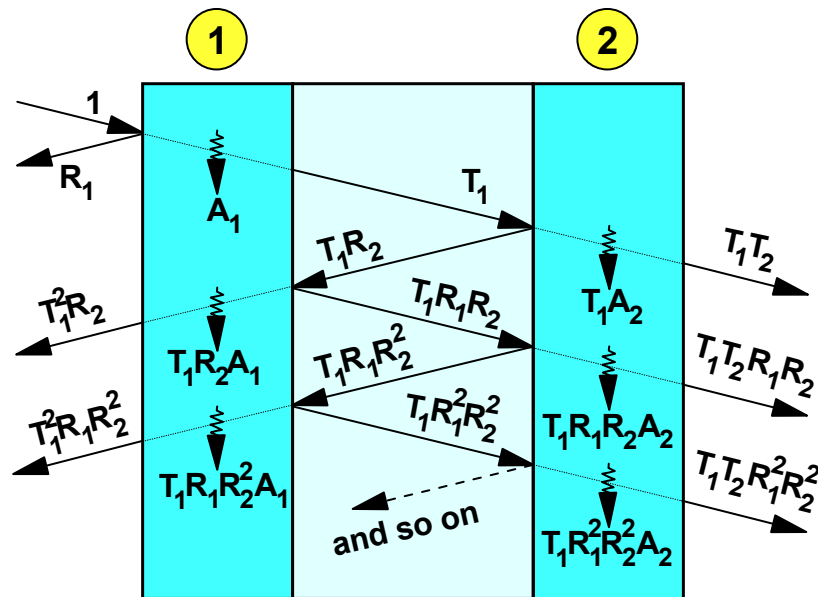
Fig.3.   Multiple transmittance (T), absorbance (A) and reflectance (R), in a two-layer glass pane. See e.g. Davies (2004) and Kimura (1977). Diffuse transmittance, diffuse reflectance and retroreflectance are not depicted, neither reflectance from the interface glass/air(gas) within the glass material.

All the calculated solar radiation glazing factors for multilayer window panes are based on transmittance and reflectance measurements carried out on single glass panes, with subsequent calculations applying Eqs.3-10 above. The absorbance is then calculated by applying the expression in Eq.1.

4.   Solar Radiation Modulation by Electrochromic Windows

Electrochromic windows (ECW) are able to control the solar radiation throughput by applying an external voltage. This solar radiation transmittance modulation is achieved either by regulation of the absorbance or the reflectance as shown in Fig.4 and Fig.5, respectively. The former one (Fig.4) represents a broadband (over a specified broad wavelength range) transmittance modulation, while the latter one (Fig.5) represents a transmittance modulation by a movable transmittance edge. See also e.g. the early studies by Goldner and Rauh (1984), Goldner et al. (1985) and Lampert (1984) in this respect. Figure 6 illustrates transmittance modulation by a combined regulation of both the absorbance and the reflectance. Note that the graphs in Figs.4-6 depict an ideal or maximum modulation, whereas real ECWs will have a much less modulation.

As of today, most of the investigations and work on ECWs have been performed with solar radiation absorbing materials, both with respect to research and commercial ECWs. See e.g. the studies by Baetens et al. (2010a) and Jelle et al. (2012a) for available state-of-the-art commercial ECWs.
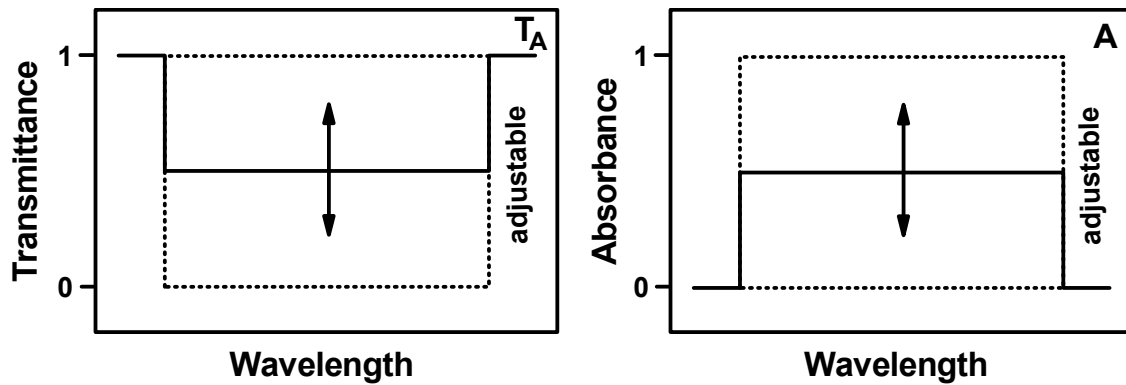
Fig.4.   Transmittance modulation (T$_A$) by regulation of the absorbance (A).
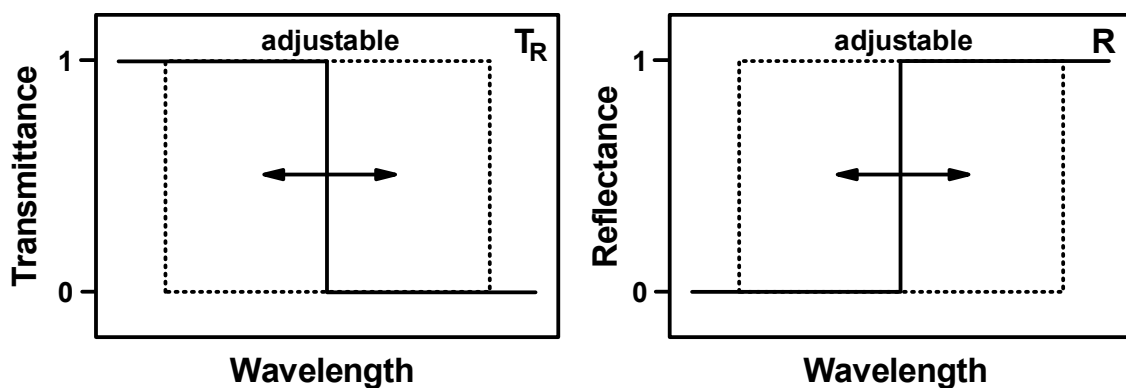
Fig.5.   Transmittance modulation (T$_R$) by regulation of the reflectance (R).
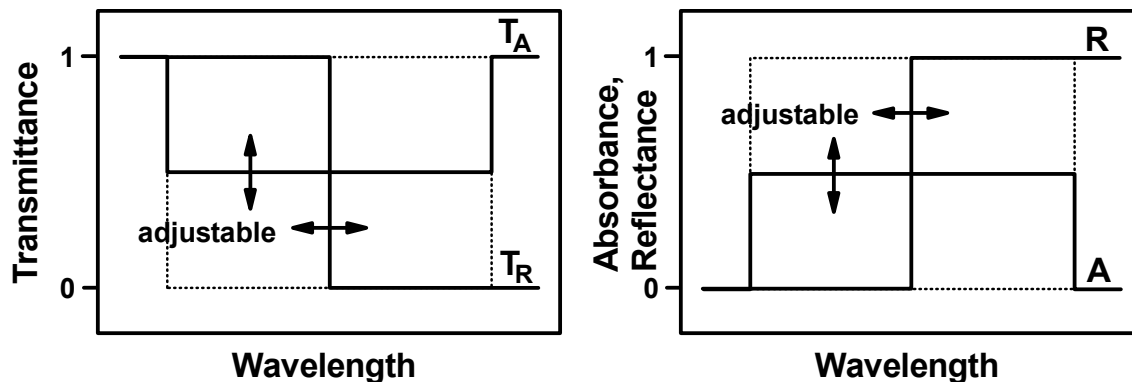
Fig.6.   Transmittance modulation (T$_A$ and T$_R$) by combined regulation of both the absorbance (A) and the reflectance (R).

It may be argued that reflectance regulation represents the best ideal way of modulating the solar radiation transmittance in ECWs. This is due to several reasons (Goldner and Rauh 1984, Goldner et al. 1985, Goldner et al. 1987, Goldner et al. 1988, Goldner et al. 1989, Goldner et al. 1990, Goldner et al. 1992, Jelle 1993):

- Absorbance regulating window panes may become unacceptable hot, and the thermally induced strain may lead to degradation of the different layers (with different thermal expansion coefficients) in the ECWs.

- Absorbance regulating window panes have a lower thermal transfer efficiency since 50 % of what is absorbed is reradiated both into and out of the building, i.e. resulting in undesirable heat gains which can not be controlled.

- Absorbance regulation requires thicker films than reflectance regulation, leading to higher manufacturing and operation costs, i.e. amount of materials and consumed electrical charge and energy. The absorbance is dependent upon the film thickness as well as the absorption coefficient according to the Beer-Lambert law, while the reflectance depends upon the density and dynamics of the free charge carriers. Except from interference effects, the reflectance should be relatively independent of the film thickness for thicknesses larger than about 10-50 nm. In addition, thinner films will lead to shorter switching times.

- Spectrally selective modulation (filtering) is believed to be more readily achieved by reflectance regulation than by bound electron absorbance regulation, see e.g. the difference in Fig.4 (absorbance regulation) and Fig.5 (reflectance regulation).

As an example it may be mentioned that reflectance regulation may be obtained in crystalline tungsten oxide (c-WO$_3$), while amorphous tungsten oxide (a-WO$_3$) exhibit practically only absorbance regulation. In c-WO$_3$ free electrons give rise to the reflectance regulation, while the absorbance in a-WO$_3$ is due to bound or highly localized electrons. That is, the reflectance may be changed by variation of the free carrier (electron) density, which alters the plasma wavelength λ_p given by the following expression (Goldner et al. 1987, Goldner et al. 1988, Goldner et al. 1989, Goldner et al. 1990, Jelle 1993):

$$\lambda_p = 2\pi c / \omega_p = (2\pi c/q_e)(m_e \varepsilon_0/n_e)^{1/2} \tag{11}$$

where ω_p, c, q_e, m_e, ne and ε_0 denote the plasma frequency, the velocity of light, the electron charge, the free electron effective mass, the free electron density and the dielectric coefficient of vacuum, respectively. Materials with a high free electron density (short λ_p) will be highly reflecting materials with a low emissivity, whereas a low free electron density (long λ_p) corresponds to a low reflectivity and thus a high emissivity. By changing λ_p, i.e. changing the free electron density, one may regulate the reflectance with an adjustable vertical reflectance edge as e.g. depicted in Fig.5, where λ_p is located at just this vertical reflectance edge.

Thus, in order to be able to regulate the reflectance the electrochromic materials should be crystalline so that the injected or extracted electrons can be free. Changing the free electron density changes the plasma wavelength λ_p, thereby making it possible to regulate the reflectance. Increasing the electron density, decreases λ_p and moves the reflectance edge from higher to lower wavelengths (Fig.5), i.e. a material with a high free electron density is a highly reflecting material. And vice versa, decreasing the electron density, increases λ_p and moves the reflectance edge from lower to higher wavelengths, i.e. a material with a low free electron density has a low reflectivity.

Various studies have been conducted on tungsten oxide with respect to its crystallinity and reflectance regulating possibilities. For further details and elaborations on these and related aspects, including more general information about the plasma wavelength and frequency, it is referred to the available literature, e.g. the investigations by Ashrit et al. (1992), Beni and Shay (1982), Cogan et al. (1986), Deb (2008), Faughnan and Crandall (1980), Goldner and Rauh 1984, Goldner et al. (1985, 1987, 1988, 1989, 1990, 1992), Granqvist (1993, 2007, 2012), Hamberg and Granqvist (1984a, 1984b), Hecht (1987), Jelle (1993), Lim (1986),

Mendelsohn and Goldner (1984), Nagai et al. (1986), Schirmer et al. (1977), Schuster et al. (1986), Svensson and Granqvist (1984a, 1984b, 1985) and Yamanaka (1987).

5.   Experimental

5.1.   Glass Samples and Window Pane Configurations

To illustrate various transmittance, absorbance and reflectance levels in the solar spectrum, one float glass, one glass with low emittance coating, one dark silver coated glass, several two-layer and three-layer window pane combinations and three electrochromic window (ECW) devices, were selected as examples. Based on the spectroscopical measurements the solar radiation glazing factors were calculated. The actual fabrication and miscellaneous testing and characterization of the ECWs are described elsewhere (Jelle and Hagen 1993, Jelle and Hagen 1994, Jelle et al. 1998, Jelle and Hagen 1998, Jelle and Hagen 1999a, Jelle et al. 2007).

5.2.   UV-VIS-NIR Spectrophotometry

A Cary 5 UV-VIS-NIR spectrophotometer, with an absolute reflectance accessory (Strong-type, VW principle), was used to measure the transmittance and reflectance of the glass samples in the ultraviolet (UV), visible (VIS) and near infrared (NIR) region, from 290 nm to 3300 nm. The absorbance was calculated from the expression given in Eq.1. However, at the moment of the fabrication and characterization of the ECW devices, no laboratory resources for determining the absolute reflectance of the ECWs were available. Nevertheless, as the three ECWs consist of solar absorbing electrochromic materials, and not reflecting modulating electrochromics, the measured (low) reflectance values for float glass are applied in the calculation of the various reflectance based solar radiation glazing factors.

5.3.   Emissivity Determination by Specular IR Reflectance

The standard ISO 9050:2003(E) (2003) refers to ISO 10292:1994 (1994) for emissivity determinations, which according to ISO 10292:1994 (1994) are to be carried out with an infrared spectrometer, measuring the near normal reflectance ($\leq 10^\circ$) at a temperature of 283 K. More details of the emissivity determinations and measurements are found in EN 12898:2001 (2001). In order to minimize polarization effects, the angle of incidence with respect to the normal of the sample must be 10º or less (ASTM E 1585-93 (1993)). For other ambient temperatures than 283 K (≈ 10 ºC), the emissivity is not strongly dependent on the mean temperature (ISO 10292:1994(E) (1994)).

5.4.   Emissivity Determination by Heat Flow Meter

The emissivity may be determined by applying a heat flow meter apparatus according to the standard EN 1946-3:1999 E (1999). For theoretical considerations, referral is made to EN 1946-2:1999 E (1999) and EN 1946-3:1999 E (1999). Note that in general glass with a low emittance coating is assumed to have an emissivity value below 0.1.

In order to validate the method and to achieve a satisfactory accuracy level, five experiments have been carried out with varying thickness of the air gap between two sample glass plates

facing each other. The air gap thickness was controlled and varied by use of three columns consisting of either 1, 2, 3, 4 or 5 small squares of glass located at the outer glass sample edges as depicted in Fig.7 and Fig.8. The low emittance coating on each glass sample are facing each other towards the air gap. Each column height, i.e. from 1 to 5 glass squares, was measured and adjusted to be of the same height with an accuracy of 0.1 mm. The glass sample and removable small glass squares have dimensions 500 mm × 500 mm × 4 mm and approximately 10 mm × 10 mm × 4 mm, respectively.
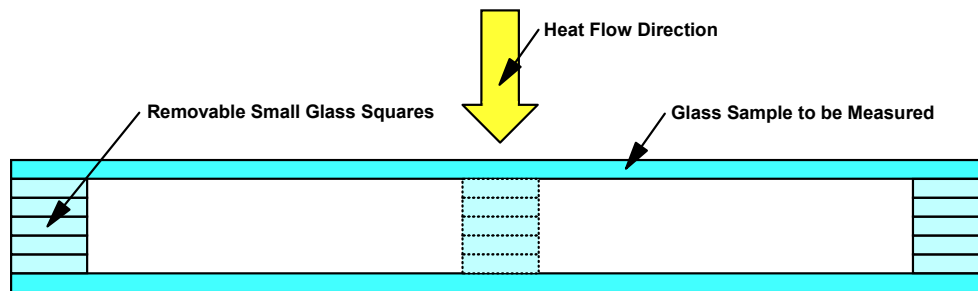
Fig.7.　　　Control of air gap thickness between two glass plates by application of three glass columns, each column with either 1, 2, 3, 4 or 5 small glass squares. The glass sample and removable small glass squares have dimensions 500 mm × 500 mm × 4 mm and approximately 10 mm × 10 mm × 4 mm, respectively. The low emittance coating on each glass sample are facing each other towards the air gap. Vertical cross-section.
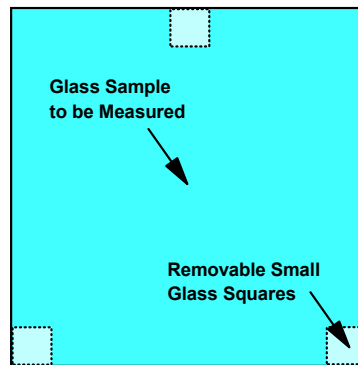
Fig.8.　　　Control of air gap thickness between two glass plates by application of three glass columns, each column with either 1, 2, 3, 4 or 5 small glass squares. The glass sample and removable small glass squares have dimensions 500 mm × 500 mm × 4 mm and approximately 10 mm × 10 mm × 4 mm, respectively. The low emittance coating on each glass sample are facing each other towards the air gap. Horizontal cross-section.

5.5. Emissivity Determination by Hemispherical Reflectance

The emissivity may also be determined by measuring the directional hemispherical reflectance (DHR, direct mode) or the hemispherical directional reflectance (HDR, reciprocal mode). In the DHR method the sample is illuminated from a single direction and all the reflected radiation into the hemisphere surrounding the sample is measured. In the HDR method the sample is uniformly illuminated from all directions by use of a hemisphere and the radiation reflected into a single direction is measured. For both the DHR and HDR

methods the single direction may be varied and controlled for miscellaneous instruments, i.e. illuminating or detecting at varying angles, respectively.

5.6.   Actual Emissivity Determinations within this Work

A float glass, a low emittance glass and a dark silver coated glass were measured by the hemispherical directional reflectance method by applying a SOC-100 HDR Hemispherical Directional Reflectometer from Surface Optics Corporation connected to a Thermo Nicolet 8700 FTIR Spectrometer. The reflected radiation from the sample was detected at the following incident angles: 10, 20, 30, 40, 45, 50, 55, 60, 65, 70, 75 and 80º. 32 scans were performed with 2 repeats at a resolution of 16 cm^{-1} in the wavelength range 2 – 25 μm. The IR source temperature was 704ºC (maximum). The results were $\varepsilon_{float} = 0.836$, $\varepsilon_{lowe} = 0.071$ and $\varepsilon_{silver} = 0.543$, for the float glass, low emittance glass and dark silver coated glass, respectively. The ε_{float} value was directly applied in the calculation of the solar factor (SF) as the ε value in the SF calculations is with respect to the inside facing surface (of building) of the innermost glass pane, i.e. normally a float glass, whereas the ε_{lowe} and ε_{silver} values were indirectly applied in the SF calculations through the calculations of the thermal conductance Λ. At the moment of the fabrication and characterization of the ECW devices, no laboratory resources for determining the emissivity of the ECW glass materials were available, so hence the value $\varepsilon_{float} = 0.836$ for float glass is applied in the calculation of SF for the ECWs as the electrochromic materials are surrounded by float glass.

6.   Measurement and Calculation Method

6.1.   Ultraviolet Solar Transmittance

The *Ultraviolet Solar Transmittance* (T_{uv}) is given by the following expression (ISO 9050:2003(E) (2003)):

$$T_{uv} = \frac{\sum\limits_{\lambda=300nm}^{380nm} T(\lambda)S_{\lambda}\Delta\lambda}{\sum\limits_{\lambda=300nm}^{380nm} S_{\lambda}\Delta\lambda} \tag{12}$$

where

S_{λ} = relative spectral distribution of ultraviolet solar radiation (ISO 9050:2003(E) (2003), ISO 9845-1:1992(E) (1992))

$T(\lambda)$ = spectral transmittance of the glass

λ = wavelength

$\Delta\lambda$ = wavelength interval

$S_{\lambda}\Delta\lambda$ values at different wavelengths are given in Table A1 in Appendix A (ISO 9050:2003(E) (2003))

The T_{uv} value will thus be a number between 0 and 1, calculated in the ultraviolet part of the solar spectrum, i.e. 300-380 nm. A low number indicates a low transmission of ultraviolet solar radiation, whereas a high number represents a high ultraviolet solar radiation

transmission. In common usage the T_{uv} values may often be chosen in percentage, i.e. between 0 and 100 %.

It should be noted that the whole ultraviolet solar spectrum is not covered in the calculation of T_{uv}, and in future versions of ISO 9050:2003(E) (2003) the wavelength range may favourably be extended to cover an even larger part of the ultraviolet solar radiation, e.g. from 290 nm to 380 nm. Note also that T_{uv} is not directly correlated to solar radiation damage of materials and human skin (see the following chapters on SMPF and SSPF).

6.2.   Visible Solar Transmittance

The *Visible Solar Transmittance* (T_{vis}), often denoted *Light Transmittance*, is given by the following expression (ISO 9050:2003(E) (2003)):

$$T_{vis} = \frac{\sum\limits_{\lambda=380nm}^{780nm} T(\lambda)D_\lambda V(\lambda)\Delta\lambda}{\sum\limits_{\lambda=380nm}^{780nm} D_\lambda V(\lambda)\Delta\lambda} \tag{13}$$

where

D_λ = relative spectral distribution of illuminant D65 (ISO 9050:2003(E) (2003), ISO 10526:1999(E) (1999))

$V(\lambda)$ = spectral luminous efficiency for photopic vision defining the standard observer for photometry (ISO 9050:2003(E) (2003), ISO/CIE 10527:1991(E) (1991))

$T(\lambda)$ = spectral transmittance of the glass

λ = wavelength

$\Delta\lambda$ = wavelength interval

$D_\lambda V(\lambda)\Delta\lambda$ values at different wavelengths are given in Table A2 in Appendix A (ISO 9050:2003(E) (2003))

The T_{vis} value will thus be a number between 0 and 1, calculated in the visible part of the solar spectrum, i.e. 380-780 nm. A low number indicates a low transmission of visible light, whereas a high number represents a high visible light transmission. In common usage the T_{vis} values may often be chosen in percentage, i.e. between 0 and 100 %.

6.3.   Solar Transmittance

The *Solar Transmittance* (T_{sol}) is given by the following expression (ISO 9050:2003(E) (2003)):

$$T_{sol} = \frac{\sum\limits_{\lambda=300nm}^{2500nm} T(\lambda)S_\lambda\Delta\lambda}{\sum\limits_{\lambda=300nm}^{2500nm} S_\lambda\Delta\lambda} \tag{14}$$

where

S_λ = relative spectral distribution of solar radiation (ISO 9050:2003(E) (2003), ISO 9845-1:1992(E) (1992))

$T(\lambda)$ = spectral transmittance of the glass

λ = wavelength

$\Delta\lambda$ = wavelength interval

$S_\lambda\Delta\lambda$ values at different wavelengths are given in Table A3 in Appendix A (ISO 9050:2003(E) (2003), ISO 9845-1:1992(E) (1992))

The T_{sol} value will thus be a number between 0 and 1, calculated in the main part of the solar spectrum, i.e. 300-2500 nm. A low number indicates a low transmission of solar radiation, whereas a high number represents a high solar radiation transmission. In common usage the T_{sol} values may often be chosen in percentage, i.e. between 0 and 100 %.

It should be noted that the whole solar spectrum is not covered in the calculation of T_{sol}, and in future versions of ISO 9050:2003(E) (2003) the wavelength range may favourably be extended to cover an even larger part of the solar radiation, e.g. from 290 nm to 3000 nm.

6.4.   Solar Material Protection Factor (SMPF)

The *Solar Material Protection Factor* (SMPF) is given by the following expression (Jelle et al. 2007):

$$SMPF = 1 - \tau_{df} = 1 - \frac{\sum_{\lambda=300nm}^{600nm}T(\lambda)C_\lambda S_\lambda \Delta\lambda}{\sum_{\lambda=300nm}^{600nm}C_\lambda S_\lambda \Delta\lambda} \qquad (15)$$

where

τ_{df} = CIE damage factor (ISO 9050:2003(E) (2003), CIE No 89/3:1990 (1991))

$C_\lambda = e^{-0.012\lambda}$ (λ given in nm)

S_λ = relative spectral distribution of solar radiation (ISO 9050:2003(E) (2003), ISO 9845-1:1992(E) (1992))

$T(\lambda)$ = spectral transmittance of the glass

λ = wavelength

$\Delta\lambda$ = wavelength interval

$C_\lambda S_\lambda\Delta\lambda$ values at different wavelengths are given in Table A4 in Appendix A (ISO 9050:2003(E) (2003))

The SMPF value will thus be a number between 0 and 1, similar to and consistent with related values like solar transmittance, emissivity, solar factor, etc. A low number indicates a low material protection, whereas a high number represents a high degree of material protection. One should also note that both SMPF and SSPF (next section) are protection factors. The word "protection" promotes positive associations, while "damage", e.g. in CIE damage factor, may give negative associations. It may be easier and better for a potential window customer to look for a window with the highest protection factor, and not the lowest damage factor, which would probably sell far more windows also. In common usage the SMPF values may often be chosen in percentage, i.e. between 0 and 100 %.

One should notice that the wavelength region for the calculation of SMPF recently has been extended from the earlier 500 nm upper limit till today's value of 600 nm (ISO 9050:2003(E) (2003)), demonstrating an increased awareness that a much larger part of the visible solar spectrum also contributes to the degradation of materials. Earlier a Krochmann damage factor for materials was calculated, with integration between 300 nm and 500 nm (ISO/DIS 9050:2001 (2001)).

It should further be noted that some of the short-wavelength part of the ultraviolet solar spectrum is not covered in the calculation of SMPF, and in future versions of ISO 9050:2003(E) (2003) the wavelength range may favourably be extended to cover an even larger part of the ultraviolet and visible solar radiation, e.g. from 290 nm to 600 nm.

6.5.   Solar Skin Protection Factor (SSPF)

The *Solar Skin Protection Factor* (SSPF) is given by the following expression (Jelle et al. 2007):

$$SSPF = 1 - F_{sd} = 1 - \frac{\sum\limits_{\lambda=300\,nm}^{400\,nm} T(\lambda) E_\lambda S_\lambda \Delta\lambda}{\sum\limits_{\lambda=300\,nm}^{400\,nm} E_\lambda S_\lambda \Delta\lambda} \qquad (16)$$

where

> F_{sd} = skin damage factor (ISO 9050:2003(E) (2003), McKinlay and Diffey (1987))
>
> E_λ = CIE erythemal effectiveness spectrum
>
> S_λ = relative spectral distribution of solar radiation (ISO 9050:2003(E) (2003), ISO 9845-1:1992(E) (1992))
>
> $T(\lambda)$ = spectral transmittance of the glass
>
> λ = wavelength
>
> $\Delta\lambda$ = wavelength interval
>
> $E_\lambda S_\lambda \Delta\lambda$ values at different wavelengths are given in Table A5 in Appendix A (ISO 9050:2003(E) (2003))

The SSPF value will thus be a number between 0 and 1, similar to and consistent with related values like solar transmittance, emissivity, solar factor, etc. A low number indicates a low skin protection, whereas a high number represents a high degree of skin protection. One should also note that both SSPF and SMPF (previous section) are protection factors. The word "protection" promotes positive associations, while "damage", e.g. in skin damage factor, may give negative associations. It may be easier and better for a potential window customer to look for a window with the highest protection factor, and not the lowest damage factor, which would probably sell far more windows also. In common usage the SSPF values may often be chosen in percentage, i.e. between 0 and 100 %.

The calculation of the SSPF extends over the ultraviolet spectrum (at earth's surface) and the low wavelength part of the visible spectrum, which may contribute to the solar radiation damage of the human skin. It may be noted that earlier there existed another definition of a skin protection factor, denoted SPF (ISO/DIS 9050:2001 (2001)), with the following correlation between the different terms: SSPF = 1 - (1/SPF) = 1 - F_{sd} = (SPF - 1)/SPF.

It should further be noted that some of the short-wavelength part of the ultraviolet solar spectrum is not covered in the calculation of SSPF, and in future versions of ISO 9050:2003(E) (2003) the wavelength range may favourably be extended to cover an even larger part of the ultraviolet and visible solar radiation, e.g. from 290 nm to 400 nm.

6.6.   External Visible Solar Reflectance

The *External Visible Solar Reflectance* ($R_{vis,ext}$), often denoted *External Light Reflectance*, is given by the following expression (ISO 9050:2003(E) (2003)):

$$R_{vis,ext} = \frac{\sum_{\lambda=380nm}^{780nm} R_{ext}(\lambda) D_\lambda V(\lambda) \Delta\lambda}{\sum_{\lambda=380nm}^{780nm} D_\lambda V(\lambda) \Delta\lambda} \tag{17}$$

where

D_λ = relative spectral distribution of illuminant D65 (ISO 9050:2003(E) (2003), ISO 10526:1999(E))

$V(\lambda)$ = spectral luminous efficiency for photopic vision defining the standard observer for photometry (ISO 9050:2003(E) (2003), ISO/CIE 10527:1991(E) (1991))

$R_{ext}(\lambda)$ = external spectral reflectance of the glass

λ = wavelength

$\Delta\lambda$ = wavelength interval

$D_\lambda V(\lambda) \Delta\lambda$ values at different wavelengths are given in Table A2 in Appendix A (ISO 9050:2003(E) (2003))

The $R_{vis,ext}$ value will thus be a number between 0 and 1, calculated in the visible part of the solar spectrum, i.e. 380-780 nm. A low number indicates a low reflection of visible light, whereas a high number represents a high visible light reflection. In common usage the $R_{vis,ext}$ values may often be chosen in percentage, i.e. between 0 and 100 %.

6.7.   Internal Visible Solar Reflectance

The *Internal Visible Solar Reflectance* ($R_{vis,int}$), often denoted *Internal Light Reflectance*, is given by the following expression (ISO 9050:2003(E) (2003)):

$$R_{vis,int} = \frac{\sum_{\lambda=380nm}^{780nm} R_{int}(\lambda) D_\lambda V(\lambda) \Delta\lambda}{\sum_{\lambda=380nm}^{780nm} D_\lambda V(\lambda) \Delta\lambda} \tag{18}$$

where

D_λ = relative spectral distribution of illuminant D65 (ISO 9050:2003(E) (2003), ISO 10526:1999(E))

$V(\lambda)$ = spectral luminous efficiency for photopic vision defining the standard observer for photometry (ISO 9050:2003(E) (2003), ISO/CIE 10527:1991(E) (1991))

$R_{int}(\lambda)$ = internal spectral reflectance of the glass

λ = wavelength

$\Delta\lambda$ = wavelength interval

$D_\lambda V(\lambda)\Delta\lambda$ values at different wavelengths are given in Table A2 in Appendix A (ISO 9050:2003(E) (2003))

The $R_{vis,int}$ value will thus be a number between 0 and 1, calculated in the visible part of the solar spectrum, i.e. 380-780 nm. A low number indicates a low reflection of visible light, whereas a high number represents a high visible light reflection. In common usage the $R_{vis,int}$ values may often be chosen in percentage, i.e. between 0 and 100 %.

6.8. Solar Reflectance

The *Solar Reflectance* (R_{sol}), implicitly external solar reflectance, is given by the following expression (ISO 9050:2003(E) (2003)):

$$R_{sol} = \frac{\sum\limits_{\lambda=300nm}^{2500nm} R_{ext}(\lambda)S_\lambda\Delta\lambda}{\sum\limits_{\lambda=300nm}^{2500nm} S_\lambda\Delta\lambda} \tag{19}$$

where

S_λ = relative spectral distribution of solar radiation (ISO 9050:2003(E) (2003), ISO 9845-1:1992(E) (1992))

$R_{ext}(\lambda)$ = external spectral reflectance of the glass

λ = wavelength

$\Delta\lambda$ = wavelength interval

$S_\lambda\Delta\lambda$ values at different wavelengths are given in Table A3 in Appendix A (ISO 9050:2003(E) (2003))

The R_{sol} value will thus be a number between 0 and 1, calculated in the main part of the solar spectrum, i.e. 300-2500 nm. A low number indicates a low reflection of solar radiation, whereas a high number represents a high solar radiation reflection. In common usage the R_{sol} values may often be chosen in percentage, i.e. between 0 and 100 %.

It should be noted that the whole solar spectrum is not covered in the calculation of R_{sol}, and in future versions of ISO 9050:2003(E) (2003) the wavelength range may favourably be extended to cover an even larger part of the solar radiation, e.g. from 290 nm to 3000 nm.

6.9. Solar Absorbance

The *Solar Absorbance* (A_{sol}) is calculated from the expression in Eq.1, which is transformed into the following:

$$A_{sol} = 1 - T_{sol} - R_{sol} \tag{20}$$

where insertion of T_{sol} and R_{sol} from Eq.14 and Eq.19 give:

$$A_{sol} = 1 - \frac{\sum\limits_{\lambda=300nm}^{2500nm} T(\lambda)S_{\lambda}\Delta\lambda}{\sum\limits_{\lambda=300nm}^{2500nm} S_{\lambda}\Delta\lambda} - \frac{\sum\limits_{\lambda=300nm}^{2500nm} R_{ext}(\lambda)S_{\lambda}\Delta\lambda}{\sum\limits_{\lambda=300nm}^{2500nm} S_{\lambda}\Delta\lambda} \qquad (21)$$

where

S_{λ} = relative spectral distribution of solar radiation (ISO 9050:2003(E) (2003), ISO 9845-1:1992(E) (1992))

$T(\lambda)$ = spectral transmittance of the glass

$R_{ext}(\lambda)$ = external spectral reflectance of the glass

λ = wavelength

$\Delta\lambda$ = wavelength interval

$S_{\lambda}\Delta\lambda$ values at different wavelengths are given in Table A3 in Appendix A (ISO 9050:2003(E) (2003))

The A_{sol} value will thus be a number between 0 and 1, calculated in the main part of the solar spectrum, i.e. 300-2500 nm. A low number indicates a low absorption of solar radiation, whereas a high number represents a high solar radiation absorption. In common usage the A_{sol} values may often be chosen in percentage, i.e. between 0 and 100 %.

It should be noted that the whole solar spectrum is not covered in the calculation of A_{sol}, and in future versions of ISO 9050:2003(E) /2003) the wavelength range may favourably be extended to cover an even larger part of the solar radiation, e.g. from 290 nm to 3000 nm.

Note also that A_{sol} is a calculated value from measured $T(\lambda)$ and $R(\lambda)$ spectra, i.e. no direct measurements of absorbance $A(\lambda)$ spectra are performed.

6.10. Emissivity

6.10.1. Emissivity in General

The emissivity (ε) is a measure of a material's radiative properties, i.e. the emission of infrared radiation. The higher emissivity, the higher emission. Highly reflective materials of infrared radiation have low emissivity values, e.g. polished surfaces of gold, silver, aluminium or copper.

The ε value will be a number between 0 and 1. Oxidation of metallic surfaces will increase the emissivity substantially, e.g. polished aluminium with $\varepsilon = 0.05$ (reflectance 0.95) and oxidized aluminium with $\varepsilon = 0.30$ (reflectance 0.70). Confer Eq.1 and Eq.2 with zero transmittance and the emittance equal to the absorbance.

Determination of the emissivity is required in order to further determine the solar factor (SF) and the thermal transmittance (U-value).

6.10.2. Emissivity by Specular IR Reflectance Measurements

According to ISO 9050:2003(E) (2003) by referring to ISO 10292:1994(E) (1994), the emissivity may to be determined with an infrared spectrometer, measuring the near normal reflectance ($\leq 10^{\circ}$) at a temperature of 283 K. Further details of the emissivity determinations and measurements are found in EN 12898:2001 E (2001). The normal emissivity (ε_n) is given by (ISO 10292:1994(E) (1994), EN 12898:2001 E (2001)):

$$\varepsilon_n = 1 - R_n = 1 - \frac{1}{30}\sum_{i=1}^{30} R_n(\lambda_i) \tag{22}$$

where

> R_n = average spectral reflectance calculated by summation of spectral reflectance values at 30 distinct wavelengths and divided by 30 as shown in Eq.22 above
>
> λ_i = wavelength
>
> λ_i values for the 30 wavelengths are given in Table A6 in Appendix A (ISO 10292:1994(E) (1994), EN 12898:2001 E (2001))

The corrected emissivity (ε) is determined from:

$$\varepsilon = c_{corr} \cdot \varepsilon_n = \frac{\varepsilon}{\varepsilon_n}\varepsilon_n \tag{23}$$

where

> $c_{corr} = \varepsilon/\varepsilon_n$ = correction coefficient found in Table A7 in Appendix A (ISO 10292:1994(E) (1994), EN 12898:2001 E (2001)) for corresponding ε_n values
>
> ε_n = normal emissivity from Eq.22

In order to minimize polarization effects, the angle of incidence with respect to the normal of the sample must be 10° or less (ASTM E 1585-93 (1993)). For other ambient temperatures than 283 K ($\approx 10 \ ^{\circ}$C), the emissivity is not strongly dependent on the mean temperature (ISO 10292:1994(E) (1994)).

6.10.3. Emissivity by Heat Flow Meter Apparatus

The emissivity may be determined by applying a heat flow meter apparatus according to the standard EN 1946-3:1999 E (1999). For theoretical considerations, referral is made to EN 1946-2:1999 E (1999) and EN 1946-3:1999 E (1999). A short excerpt is given in the following.

The total heat flow density q_{tot} (in W/m^2) between two parallel, flat infinite isothermal surfaces may be written as (EN 1946-2:1999 E (1999), EN 1946-3:1999 E (1999)):

$$q_{tot} = q_{rad} + \frac{\kappa}{d}\Delta T \tag{24}$$

where

$$q_{rad} = \frac{4\sigma T_m^3 \Delta T}{\dfrac{1}{\varepsilon_1} + \dfrac{1}{\varepsilon_2} - 1} = \text{radiation flow density (W/m}^2) \tag{25}$$

κ = thermal conductivity of the medium separating the two surfaces (W/(mK))

d = distance between the two surfaces (m)

ΔT = temperature difference between the two surfaces (K)

T_m = mean temperature of the two surfaces

$\sigma = \pi^2 k^4/(60\hbar^3 c^2) \approx 5.67 \cdot 10^{-8}$ W/(m^{2}K^4) = Stefan-Boltzmann's constant $\tag{26}$

k = Boltzmann's constant $\approx 1.38 \cdot 10^{-23}$ J/K

c = velocity of light $\approx 3.00 \cdot 10^8$ m/s

$\hbar = h/(2\pi) \approx 1.05 \cdot 10^{-34}$ Js = reduced Planck's constant

h = Planck's constant $\approx 6.63 \cdot 10^{-34}$ Js

ε_1 = emissivity of surface 1

ε_2 = emissivity of surface 2

Equation 25 is in reality an approximation of Stefan-Boltmann's law, which describes the radiation flow density q_{rad} as proportional to the fourth power of the radiant object's (with emissivity ε) absolute temperature T:

$$q_{rad} = \sigma \varepsilon T^4 \tag{27}$$

or the radiation flow density between an radiation emitting object at temperature T_1 and surroundings at temperature T_2:

$$q_{rad} = \sigma \varepsilon (T_1^4 - T_2^4) \tag{28}$$

or the radiation flow density between two radiant parallel, flat isothermal surfaces with temperatures T_1 and T_2, and emissivities ε_1 and ε_2, respectively:

$$q_{rad,12} = \frac{\sigma}{\dfrac{1}{\varepsilon_1} + \dfrac{1}{\varepsilon_2} - 1}(T_1^4 - T_2^4) \tag{29}$$

With air between the plane surfaces, κ is κ_{air} given by the following (EN 1946-2:1999 E (1999), EN 1946-3:1999 E (1999)):

$$\kappa_{air} = 0.0242396(1 + 0.003052\theta - 1.282 \cdot 10^{-6}\theta^2) \quad \text{(W/(mK))} \tag{30}$$

where

θ is given in ºC and calculated from

$$\theta = (T_m - 273.15 \text{ K})\text{ºC/K} \quad \text{(ºC)} \tag{31}$$

and values are accurate to 0.6 % between θ = 10ºC and θ = 70ºC.

With two identical glass plates, it follows that

$$\epsilon_1 = \epsilon_2 = \epsilon \tag{32}$$

Inserting Eq.32 in Eq.25 yields the following expression:

$$q_{rad} = \frac{4\sigma T_m^3 \Delta T}{\frac{2}{\epsilon} - 1} = \frac{4\epsilon\sigma T_m^3 \Delta T}{2 - \epsilon} \tag{33}$$

Furthermore, inserting Eq.33 in Eq.24 gives

$$q_{tot} = \frac{4\epsilon\sigma T_m^3 \Delta T}{2 - \epsilon} + \frac{\kappa}{d}\Delta T \tag{34}$$

Solving Eq.34 with respect to the emissivity ϵ yields

$$\epsilon = \frac{2(q_{tot} - \frac{\kappa}{d}\Delta T)}{4\sigma T_m^3 \Delta T + q_{tot} - \frac{\kappa}{d}\Delta T} \tag{35}$$

which may be used for calculation of the emissivity from heat flow meter measurements.

The uncertainty in the emissivity value, $\Delta\epsilon$, is calculated as follows:

$$\Delta\epsilon = \sqrt{(\frac{\partial\epsilon}{\partial q_{tot}}\Delta q_{tot})^2 + (\frac{\partial\epsilon}{\partial\kappa}\Delta\kappa)^2 + (\frac{\partial\epsilon}{\partial d}\Delta d)^2 + (\frac{\partial\epsilon}{\partial(\Delta T)}\Delta(\Delta T))^2 + (\frac{\partial\epsilon}{\partial\sigma}\Delta\sigma)^2 + (\frac{\partial\epsilon}{\partial T_m}\Delta T_m)^2} \tag{36}$$

where

$$\frac{\partial\epsilon}{\partial q_{tot}} = \frac{8\sigma T_m^3 \Delta T}{(4\sigma T_m^3 \Delta T + q_{tot} - \frac{\kappa}{d}\Delta T)^2} \tag{37}$$

$$\frac{\partial\epsilon}{\partial\kappa} = \frac{-8\sigma T_m^3 (\Delta T)^2 / d}{(4\sigma T_m^3 \Delta T + q_{tot} - \frac{\kappa}{d}\Delta T)^2} \tag{38}$$

$$\frac{\partial\epsilon}{\partial d} = \frac{8\sigma T_m^3 (\Delta T)^2 / d^2}{(4\sigma T_m^3 \Delta T + q_{tot} - \frac{\kappa}{d}\Delta T)^2} \tag{39}$$

$$\frac{\partial\epsilon}{\partial\Delta T} = \frac{-8\sigma T_m^3 q_{tot}}{(4\sigma T_m^3 \Delta T + q_{tot} - \frac{\kappa}{d}\Delta T)^2} \tag{40}$$

$$\frac{\partial \varepsilon}{\partial \sigma} = \frac{-8(q_{tot} - \frac{\lambda}{d}\Delta T)T_m^3 \Delta T}{(4\sigma T_m^3 \Delta T + q_{tot} - \frac{\kappa}{d}\Delta T)^2} \tag{41}$$

$$\frac{\partial \varepsilon}{\partial T_m} = \frac{-24(q_{tot} - \frac{\kappa}{d}\Delta T)\sigma T_m^2 \Delta T}{(4\sigma T_m^3 \Delta T + q_{tot} - \frac{\kappa}{d}\Delta T)^2} \tag{42}$$

The uncertainties for the different parameters, i.e. Δq_{tot}, $\Delta \kappa$, Δd, $\Delta(\Delta T)$, $\Delta \sigma$ and ΔT_m, may be estimated, and hence numerical values for the emissivity uncertainties may then be calculated.

6.10.4. Emissivity by Hemispherical Reflectance

The emissivity may be determined as the total hemispherical emissivity by applying a hemispherical reflectometer and integrating over the hemisphere by

$$\varepsilon = 2\int_0^{\pi/2} \varepsilon_t(\theta)\sin\theta\cos\theta d\theta \tag{43}$$

where

$$\varepsilon_t(\theta, \phi, \lambda) = 1 - \frac{\int_0^\infty R(\lambda)P(\lambda, T)d\lambda}{\int_0^\infty P(\lambda, T)d\lambda} \quad \text{(Surface Optics Corporation 2009)} \tag{44}$$

$$P(\lambda, T) = \frac{8\pi hc}{\lambda^5(e^{hc/(\lambda kT)} - 1)} = \text{Planck's function} \quad \text{(Surface Optics Corporation 2009)} \tag{45}$$

R = hemispherical reflectance
λ = wavelength
T = temperature (K)
θ and ϕ are integrating angles over the hemisphere
h = Planck's constant $\approx 6.63 \cdot 10^{-34}$ Js
k = Boltzmann's constant $\approx 1.38 \cdot 10^{-23}$ J/K
c = velocity of light $\approx 3.00 \cdot 10^8$ m/s

6.11.   Solar Factor (SF)

6.11.1. Solar Factor in General

The *Solar Factor* (SF) is the *Total Solar Energy Transmittance* which is given by the following (ISO 9050:2003(E) (2003)):

$$SF = T_{sol} + q_i \tag{46}$$

where

T_{sol} = solar transmittance (Eq.14)

q_i = secondary heat transfer factor towards the inside

The secondary heat transfer factor towards the inside results from heat transfer by convection and long-wave infrared radiation of the incident solar radiation part which has been absorbed by the glazing.

The solar absorbance A_{sol} may be divided into two parts:

$$A_{sol} = q_i + q_e \tag{47}$$

where

q_i = secondary heat transfer factor towards the inside

q_e = secondary heat transfer factor towards the outside

That is, the absorbed energy in the glazing, is transferred to the inside (q_i) and to the outside (q_e).

6.11.2. Heat Transfer Coefficients of Glazing Towards the Outside and Inside

In order to calculate the secondary heat transfer factor towards the inside (q_i), the heat transfer coefficients of the glazing towards the outside (h_e) and towards the inside (h_i), are required. These coefficients depend mainly on the glazing position, wind velocity, inside and outside temperatures and the temperature of the two external glazing surfaces.

Under the following assumptions:

- vertical glazing position
- wind velocity of approximately 4 m/s and corrected emissivity of 0.837 for the outside surface
- natural convection and optional emissivity for the inside surface
- unventilated air spaces

the heat transfer coefficients of the glazing towards the outside (h_e) and towards the inside (h_i) are given by the following:

$$h_e = 23 \ W/(m^2 K) \tag{48}$$

$$h_i = \left(3.6 + \frac{4.4\varepsilon}{0.837}\right) W/(m^2 K) \tag{49}$$

where

ε = corrected emissivity of the inside surface

For soda lime glass with $\varepsilon = 0.837$ it follows from Eq.49 that $h_i = 8$ W/(m^{2}K). Note that $1/h_e \approx 0.04$ m^{2}K/W and $1/h_i \approx 0.13$ m^{2}K/W express the external and internal thermal surface resistance, respectively, for soda lime glass and horizontal heat flow direction ($\pm 30^o$ from the horizontal plane). See ISO 10292:1994(E) (1994) and EN-ISO 6946:1996 (1996) for further details.

6.11.3. Secondary Heat Transfer Factor Towards the Inside for Multiple Glazing

The secondary heat transfer factor towards the inside (q_i) of a multiple glazing is given by (ISO 9050:2003(E) (2003)):

$$q_i = \frac{\dfrac{A_{sol,1} + A_{sol,2} + A_{sol,3} + ... + A_{sol,n}}{h_e} + \dfrac{A_{sol,2} + A_{sol,3} + ... + A_{sol,n}}{\Lambda_{12}} + \dfrac{A_{sol,3} + ... + A_{sol,n}}{\Lambda_{23}} + \dfrac{A_{sol,n}}{\Lambda_{(n-1)n}}}{\dfrac{1}{h_i} + \dfrac{1}{h_e} + \dfrac{1}{\Lambda_{12}} + \dfrac{1}{\Lambda_{23}} + ... + \dfrac{1}{\Lambda_{(n-1)n}}}$$

(50)

where

$A_{sol,1}$ = solar absorbance of the outer (first) pane within the n-fold glazing

$A_{sol,2}$ = solar absorbance of the second pane within the n-fold glazing

$A_{sol,n}$ = solar absorbance of the n'th (inner) pane within the n-fold glazing

h_e = heat transfer coefficient of the glazing towards the outside

h_i = heat transfer coefficient of the glazing towards the inside

Λ_{12} = thermal conductance between the outer surface of the outer (first) pane and the centre of the second pane

Λ_{23} = thermal conductance between the centre of the second pane and the centre of the third pane

$\Lambda_{(n-1)n}$ = thermal conductance between the centre of the (n-1)'th pane and the outer surface of the n'th (inner) pane

6.11.4. Thermal Conductance

As seen from the above the thermal conductance (Λ) is required in order to calculate the secondary heat transfer factor towards the inside (q_i) (Eq.50) of a multiple glazing, which is further applied in the calculation of the solar factor (SF) (Eq.46).

The thermal conductance (Λ) is defined in the expresssion for the thermal transmittance (U-value) as given by:

$$\frac{1}{U} = \frac{1}{h_e} + \frac{1}{\Lambda} + \frac{1}{h_i}$$

(51)

where the thermal conductance (Λ) then may be expressed as:

$$\Lambda = \left(\sum_{}^{N} \frac{1}{h_s} + \sum_{}^{M} d_m r_m \right)^{-1} \tag{52}$$

where

$$h_s = h_g + h_r = \text{gas space conductance} \tag{53}$$

where

h_g = gas conductance (conduction and convection)
h_r = radiation conductance
h_e = heat transfer coefficient of the glazing towards the outside
h_i = heat transfer coefficient of the glazing towards the inside
d_m = total thickness of each material (glass)
r_m = thermal resistivity of each material, 1 mK/W for glass
N = number of spaces
M = number of materials (glass panes)

Note that the last term in Eq.52, containing the material thickness and thermal resistivity, may be viewed as a material U-value.

The gas conductance (h_g) is given by:

$$h_g = \text{Nu} \frac{\kappa}{s} \tag{54}$$

and the radiation conductance (h_r) is given by:

$$h_r = \frac{4\sigma T_m^3}{\dfrac{1}{\varepsilon_1} + \dfrac{1}{\varepsilon_2} - 1} \tag{55}$$

where

κ = gas thermal conductivity (W/(mK)) as given in Table A8 in Appendix A
s = space width
$\sigma \approx 5.67 \cdot 10^{-8}$ W/(m²K⁴) = Stefan-Boltzmann's constant (Eq.26)
T_m = gas mean temperature, where $T_m = 283$ K is a principal reference value (ISO 10292:1994(E) (1994))
ε_1 = corrected emissivity for material 1 (glass 1) at the mean absolute temperature T_m of the gas space
ε_2 = corrected emissivity for material 2 (glass 2) at the mean absolute temperature T_m of the gas space

and where

$$\text{Nu} = A(\text{Gr} \cdot \text{Pr})^n = \text{Nusselt number}$$
$$\text{for Nu} > 1 \text{ (heat flow enhanced by convection)} \tag{56}$$

Nu = 1 = Nusselt number

$$\text{for Nu} \leq 1 \text{ (heat flow by conduction only, limit value of 1)} \quad (57)$$

where

$$Gr = \frac{9.81s^3\rho^2\Delta T}{\mu^2 T_m} = \text{Grashof number} \qquad (58)$$

$$Pr = \frac{\mu c_m}{\kappa} = \text{Prandtl number} \qquad (59)$$

where

A = constant depending on space inclination as given in Table A9 in Appendix A

n = constant depending on space inclination as given in Table A9 in Appendix A

ρ = mass density of gas (kg/m^3) as given in Table A8 in Appendix A

μ = gas dynamic viscosity (kg/(ms)) as given in Table A8 in Appendix A

c_m = specific heat (heat capacity per unit mass) of gas (J/(kgK)) as given in Table A8 in Appendix A

ΔT = temperature difference on either side of the glazing, where $\Delta T = 15$ K is a principal reference value (ISO 10292:1994(E) (1994))

The corrected emissivities (ε) of the surfaces bounding the enclosed gas spaces are required to calculate the radiation conductance (h_r) in Eq.55. A corrected emissivity of 0.837 is to be applied for glass surfaces. The normal emissivity (ε_n) and corrected emissivity (ε) for coated surfaces are found from the procedures described in the earlier chapters 6.10.2 and 6.10.3. The mean temperature (T_m) of the gas space is fixed at 283 K (≈ 10 ºC) for comparison purposes.

The gas properties required for calculation of the Nusselt number (Nu) (Eq.56), which is part of the calculation of the thermal conductance (Λ) (Eq.52), are found in Table A8 in Appendix A. For gas mixtures, the gas properties are proportioned in volume ratios as the following (ISO 10292:1994(E) (1994)):

$$P = R_1P_1 + R_2P_2 + ... + R_mP_m \qquad (60)$$

where

P = relevant property, i.e. mass density, dynamic viscosity, thermal conductivity or specific heat

R_1 = volume ratio of gas 1

R_2 = volume ratio of gas 2

...

R_m = volume ratio of gas m

The heat transfer coefficient of the glazing towards the outside, i.e. the external heat transfer coefficient (h_e), is dependent on the wind velocity close to the glazing according to the following approximate formula (ISO 10292:1994(E) (1994)):

$$h_e = (10.0 + 4.1v) \text{ W/(m}^2\text{K)} \qquad (61)$$

where

v = wind velocity given in m/s
h_e = 23 W/(m²K) (Eq.48)

The h_e = 23 W/(m²K) value is used for comparing U-values of window panes.

The reciprocal

$$R_e = 1/h_e = 0.04 \text{ m}^2\text{K/W} \tag{62}$$

expresses the external thermal surface resistance.

From Eq.61 it is observed that h_e increases with increasing outdoor wind velocity. That is, the external thermal surface resistance (R_e) will decrease with increasing wind velocity influencing the external window surface.

The heat transfer coefficient of the glazing towards the inside, i.e. the internal heat transfer coefficient (h_i), is given by the following expression, see Eq.49 (ISO 10292:1994(E) (1994)):

$$h_i = h_c + h_r = \left(3.6 + \frac{4.4\varepsilon}{0.837} \right) \text{W}/(\text{m}^2\text{K}) \tag{63}$$

where

$$h_c = 3.6 \text{ W/(m}^2\text{K)} \quad \text{for free convection} \tag{64}$$

and

$$h_r = \frac{4.4\varepsilon}{0.837} \text{ W}/(\text{m}^2\text{K}) \tag{65}$$

The expression for h_r in Eq.65 is only valid if there is no condensation on the coated surface. For a clear, uncoated glass, the corrected emissivity is 0.837, and Eq.65 reduces to:

$$h_r = 4.4 \text{ W/(m}^2\text{K)} \quad \text{for clear, uncoated glass} \tag{66}$$

And furthermore, Eq.63 becomes:

$$h_i = 8.0 \text{ W/(m}^2\text{K)} \quad \text{for clear, uncoated glass and free convection} \tag{67}$$

The h_i = 8.0 W/(m²K) is used as a standardized value for comparing U-values of window panes.

The reciprocal

$$R_i = 1/h_i = 0.13 \text{ m}^2\text{K/W} \tag{68}$$

expresses the internal thermal surface resistance.

The value of h_c, and thereby h_i, will be larger if a current of air is blown over the window from a fan-blown heater or similar situated below or above the window. That is, the internal

thermal surface resistance (R_i) will decrease with increasing air current over the window surface.

Actual values applied in the calculations of the thermal conductance Λ for different cases are given in Table B1 and Table B2 in Appendix B for two-layer and three-layer window pane configurations, respectively, which are hence applied in the calculations of the solar factors (SF). For the three-layer window pane each gas (air) space is treated in each column in Table B2, where a temperature difference of 7.5 K (i.e. 15 K divided by 2) is assumed over both gas spaces and with gas mean temperatures of 279.25 K and 286.75 K for the exterior and interior gas space, respectively, which are simplications as the different material configurations around one gas space will influence the temperatures around the other gas space. Nevertheless, these simplifications are assumed to not influence the thermal conductance calculations significantly. Furthermore, for the three-layer window pane the glass thickness is stated as 3 mm (2 x 3 mm = 6 mm) in Table B2 as to add up to a full glass pane (4 mm, exterior or interior side) plus half a glass pane (2 mm, to the centre of the middle pane), i.e. 6 mm in total.

6.11.5. Solar Factor for Single Glazing

The *Solar Factor* (SF) is the *Total Solar Energy Transmittance* which is given by the following for *single glazing*:

$$SF = T_{sol} + q_i \tag{69}$$

where

$$q_i = A_{sol} \frac{h_i}{h_e + h_i} \tag{70}$$

and as before

T_{sol} = solar transmittance (Eq.14)
R_{sol} = solar reflectance (Eq.19)
$A_{sol} = 1 - T_{sol} - R_{sol}$ = solar absorbance (Eq.20 and Eq.21)
$h_e = 23$ W/(m²K)   (Eq.48, see applicable assumptions)
$h_i = \left(3.6 + \dfrac{4.4\varepsilon}{0.837}\right) W/(m^2K)$ (Eq.49, see applicable assumptions)
ε = corrected emissivity of the inside surface

6.11.6. Solar Factor for Double Glazing

The *Solar Factor* (SF) is the *Total Solar Energy Transmittance* which is given by the following for *double glazing*:

$$SF = T_{sol} + q_i \tag{71}$$

where

$$q_i = \frac{\dfrac{A_{sol,1} + A_{sol,2}}{h_e} + \dfrac{A_{sol,2}}{\Lambda}}{\dfrac{1}{h_i} + \dfrac{1}{h_e} + \dfrac{1}{\Lambda}} \tag{72}$$

$A_{sol,1}$ = solar absorbance of the outer (first) pane within the double glazing given by:

$$A_{sol,1} = \frac{\displaystyle\sum_{\lambda=300\,nm}^{2500\,nm} \left\{ A_1 + \frac{A_{1b} T_1 R_2}{1 - R_{1b} R_2} \right\} S_\lambda \Delta\lambda}{\displaystyle\sum_{\lambda=300\,nm}^{2500\,nm} S_\lambda \Delta\lambda} \tag{73}$$

$A_{sol,2}$ = solar absorbance of the inner (second) pane within the double glazing given by:

$$A_{sol,2} = \frac{\displaystyle\sum_{\lambda=300\,nm}^{2500\,nm} \left\{ \frac{A_2 T_1}{1 - R_{1b} R_2} \right\} S_\lambda \Delta\lambda}{\displaystyle\sum_{\lambda=300\,nm}^{2500\,nm} S_\lambda \Delta\lambda} \tag{74}$$

Λ = thermal conductance between the outer surface of the outer (first) pane and the innermost surface of the inner (second) pane

T_1, T_2, A_1, A_2, R_1 and R_2 denote the transmittance, absorbance and reflectance for glass number 1 and 2, respectively, i.e. exterior (outer) glass towards incident radiation beam, and interior (inner) glass, respectively. The index "b" for R_{1b} designates that the reflectance measurement is performed on the back (reverse) side of the glass as compared to the normal incident radiation beam direction, i.e. R_{1b} versus R_1. For simplicity reasons, the wavelength (λ) dependence of T_1, T_2, A_1, A_2, R_1 and R_2 is omitted in Eq.73 and Eq.74 above.

and where

$$A_1 = 1 - T_1 - R_1 \tag{75}$$

$$A_{1b} = 1 - T_1 - R_{1b} \tag{76}$$

$$A_2 = 1 - T_2 - R_2 \tag{77}$$

and as before

T_{sol} = solar transmittance (Eq.14)
R_{sol} = solar reflectance (Eq.19)
$A_{sol} = 1 - T_{sol} - R_{sol}$ = solar absorbance (Eq.20 and Eq.21)
S_λ = relative spectral distribution of solar radiation (ISO 9050:2003(E) (2003), ISO 9845-1:1992(E) (1992))
λ = wavelength
$\Delta\lambda$ = wavelength interval

$S_\lambda \Delta\lambda$ values at different wavelengths are given in Table A3 in Appendix A (ISO 9050:2003(E) (2003))

$h_e = 23 \ W/(m^2K)$ (Eq.48, see applicable assumptions)

$$h_i = \left(3.6 + \frac{4.4\varepsilon_i}{0.837} \right) W/(m^2K)$$ (Eq.49, see applicable assumptions)

6.11.7. Solar Factor for Triple Glazing

The *Solar Factor* (SF) is the *Total Solar Energy Transmittance* which is given by the following for *triple glazing*:

$$SF = T_{sol} + q_i \tag{78}$$

where

$$q_i = \frac{\dfrac{A_{sol,1} + A_{sol,2} + A_{sol,3}}{h_e} + \dfrac{A_{sol,2} + A_{sol,3}}{\Lambda_{12}} + \dfrac{A_{sol,3}}{\Lambda_{23}}}{\dfrac{1}{h_i} + \dfrac{1}{h_e} + \dfrac{1}{\Lambda_{12}} + \dfrac{1}{\Lambda_{23}}} \tag{79}$$

$A_{sol,1}$ = solar absorbance of the outer (first) pane within the triple glazing given by:

$$A_{sol,1} = \frac{\displaystyle\sum_{\lambda=300 \ nm}^{2500 \ nm} \left\{ A_1 + \frac{T_1 A_{1b} R_2 (1 - R_{2b} R_3) + T_1 T_2^2 A_{1b} R_3}{(1 - R_{1b} R_2)(1 - R_{2b} R_3) - T_2^2 R_{1b} R_3} \right\} S_\lambda \Delta\lambda}{\displaystyle\sum_{\lambda=300 \ nm}^{2500 \ nm} S_\lambda \Delta\lambda} \tag{80}$$

$A_{sol,2}$ = solar absorbance of the middle (second) pane within the triple glazing given by:

$$A_{sol,2} = \frac{\displaystyle\sum_{\lambda=300 \ nm}^{2500 \ nm} \left\{ \frac{T_1 A_2 (1 - R_{2b} R_3) + T_1 T_2 A_{2b} R_3}{(1 - R_{1b} R_2)(1 - R_{2b} R_3) - T_2^2 R_{1b} R_3} \right\} S_\lambda \Delta\lambda}{\displaystyle\sum_{\lambda=300 \ nm}^{2500 \ nm} S_\lambda \Delta\lambda} \tag{81}$$

$A_{sol,3}$ = solar absorbance of the inner (third) pane within the triple glazing given by:

$$A_{sol,3} = \frac{\displaystyle\sum_{\lambda=300 \ nm}^{2500 \ nm} \left\{ \frac{T_1 T_2 A_3}{(1 - R_{1b} R_2)(1 - R_{2b} R_3) - T_2^2 R_{1b} R_3} \right\} S_\lambda \Delta\lambda}{\displaystyle\sum_{\lambda=300 \ nm}^{2500 \ nm} S_\lambda \Delta\lambda} \tag{82}$$

Λ_{12} = thermal conductance between the outer surface of the outer (first) pane and the centre of the middle (second) pane

Λ_{23} = thermal conductance between the centre of the middle (second) pane and the innermost surface of the inner (third) pane

T_1, T_2, T_3, A_1, A_2, A_3, R_1, R_2 and R_3 denote the transmittance, absorbance and reflectance for glass number 1, 2 and 3, respectively, i.e. exterior (outer) glass towards incident radiation beam, middle glass and interior (inner) glass, respectively. The index "b" for R_{1b} and R_{2b} designates that the reflectance measurement is performed on the back (reverse) side of the glass as compared to the normal incident radiation beam direction, e.g. R_{1b} versus R_1. For simplicity reasons, the wavelength (λ) dependence of T_1, T_2, T_3, A_1, A_2, A_3, R_1, R_2 and R_3 is omitted in Eqs.80-82 above.

and where

$A_1 = 1 - T_1 - R_1$ (Eq.75)
$A_{1b} = 1 - T_1 - R_{1b}$ (Eq.76)
$A_2 = 1 - T_2 - R_2$ (Eq.77)

$$A_{2b} = 1 - T_2 - R_{2b} \tag{83}$$

$$A_3 = 1 - T_3 - R_3 \tag{84}$$

and as before

T_{sol} = solar transmittance (Eq.14)

R_{sol} = solar reflectance (Eq.19)

$A_{sol} = 1 - T_{sol} - R_{sol}$ = solar absorbance (Eq.20 and Eq.21)

S_λ = relative spectral distribution of solar radiation (ISO 9050:2003(E) (2003), ISO 9845-1:1992(E) (1992))

λ = wavelength

$\Delta\lambda$ = wavelength interval

$S_\lambda\Delta\lambda$ values at different wavelengths are given in Table A3 in Appendix A (ISO 9050:2003(E) (2003))

$h_e = 23$ W/(m^{2}K)   (Eq.48, see applicable assumptions)

$h_i = \left(3.6 + \dfrac{4.4\varepsilon}{0.837}\right)$ W/(m^{2}K)   (Eq.49, see applicable assumptions)

6.12.   Colour Rendering Factor (CRF)

The *Colour Rendering Factor* (CRF) is given by the following expression (EN 410:1998 E (1998)):

$$CRF = \frac{R_a}{100} = \frac{1}{800}\sum_{i=1}^{8} R_i \tag{85}$$

where

$$R_a = \frac{1}{8}\sum_{i=1}^{8} R_i = \text{general colour rendering index (EN 410:1998 E (1998))} \tag{86}$$

$$R_i = 100 - 4.6\Delta E_i = \text{specific colour rendering index} \tag{87}$$

$$\Delta E_i = \sqrt{(U^*_{t,i} - U^*_{r,i})^2 + (V^*_{t,i} - V^*_{r,i})^2 + (W^*_{t,i} - W^*_{r,i})^2} = \text{total distortion of colour i} \quad (88)$$

$U^*_{r,i}, V^*_{r,i}$ and $W^*_{r,i}$ are given in Table A10 in Appendix A (EN 410:1998 E (1998))

where conversion into the CIE 1964 uniform colour space system are applied (EN 410:1998 E (1998)):

$$W^*_{t,i} = 25 \left(\frac{100 Y_{t,i}}{Y_t} \right)^{1/3} - 17 \quad (89)$$

$$U^*_{t,i} = 13 W^*_{t,i} (u^*_{t,i} - 0.1978) \quad (90)$$

$$V^*_{t,i} = 13 W^*_{t,i} (v^*_{t,i} - 0.3122) \quad (91)$$

where the trichromatic coordinates corrected in terms of distortion by chromatic adaption, for the eight test colours illuminated by the transmitted light, are given by:

$$u^*_{t,i} = \frac{10.872 + 0.8802 \dfrac{c_{t,i}}{c_t} - 8.2544 \dfrac{d_{t,i}}{d_t}}{16.518 + 3.2267 \dfrac{c_{t,i}}{c_t} - 2.0636 \dfrac{d_{t,i}}{d_t}} \quad (92)$$

$$v^*_{t,i} = \frac{5.520}{16.518 + 3.2267 \dfrac{c_{t,i}}{c_t} - 2.0636 \dfrac{d_{t,i}}{d_t}} \quad (93)$$

where for transmitted light:

$$c_t = \frac{1}{v_t}(4 - u_t - 10 v_t) \quad (94)$$

$$d_t = \frac{1}{v_t}(1.708 v_t + 0.404 - 1.481 u_t) \quad (95)$$

where for transmitted light, then reflected by the test colour i:

$$c_{t,i} = \frac{1}{v_{t,i}}(4 - u_{t,i} - 10 v_{t,i}) \quad (96)$$

$$d_{t,i} = \frac{1}{v_{t,i}}(1.708 v_{t,i} + 0.404 - 1.481 u_{t,i}) \quad (97)$$

where the trichromatic coordinates in the CIE 1960 uniform chromaticity diagram are calculated as (EN 410:1998 E (1998)):

for transmitted light:

$$u_t = \frac{4X_t}{X_t + 15Y_t + 3Z_t} \tag{98}$$

$$v_t = \frac{6Y_t}{X_t + 15Y_t + 3Z_t} \tag{99}$$

for transmitted light, then reflected by the test colour i:

$$u_{t,i} = \frac{4X_{t,i}}{X_{t,i} + 15Y_{t,i} + 3Z_{t,i}} \tag{100}$$

$$v_{t,i} = \frac{6Y_{t,i}}{X_{t,i} + 15Y_{t,i} + 3Z_{t,i}} \tag{101}$$

where the tristimulus values:

for transmitted light:

$$X_t = \sum_{\lambda=380nm}^{780nm} \frac{d\Phi}{d\lambda} T(\lambda) \bar{x}(\lambda) \Delta\lambda \tag{102}$$

$$Y_t = \sum_{\lambda=380nm}^{780nm} \frac{d\Phi}{d\lambda} T(\lambda) \bar{y}(\lambda) \Delta\lambda \tag{103}$$

$$Z_t = \sum_{\lambda=380nm}^{780nm} \frac{d\Phi}{d\lambda} T(\lambda) \bar{z}(\lambda) \Delta\lambda \tag{104}$$

for transmitted light, then reflected by each of the eight test colours:

$$X_{t,i} = \sum_{\lambda=380nm}^{780nm} \frac{d\Phi}{d\lambda} T(\lambda) \beta_i(\lambda) \bar{x}(\lambda) \Delta\lambda \tag{105}$$

$$Y_{t,i} = \sum_{\lambda=380nm}^{780nm} \frac{d\Phi}{d\lambda} T(\lambda) \beta_i(\lambda) \bar{y}(\lambda) \Delta\lambda \tag{106}$$

$$Z_{t,i} = \sum_{\lambda=380nm}^{780nm} \frac{d\Phi}{d\lambda} T(\lambda) \beta_i(\lambda) \bar{z}(\lambda) \Delta\lambda \tag{107}$$

where

λ = wavelength

$\Delta\lambda$ = wavelength interval

$(d\Phi/d\lambda)\Delta\lambda$ is the relative spectral energy distribution of illuminant D65 as given in Table A11 in Appendix A (EN 410:1998 E (1998))

$\beta_i(\lambda)$ is the spectral reflectance of each test colour (i from 1 to 8) as given in Table A12 in Appendix A (EN 410:1998 E (1998))

$\overline{x}(\lambda), \overline{y}(\lambda)$ and $\overline{z}(\lambda)$ are the spectral tristimulus values for the CIE 1931 colourimetric standard observer as given in Table A13 in Appendix A (EN 410:1998 E (1998))

$T(\lambda)$ = spectral transmittance of the glazing

The CRF value expresses synthetically a quantitative evaluation of the colour differences between eight test colours lighted directly by the reference illuminant D65 and by the same illuminant transmitted through the glazing.

The CRF value will thus be a number between 0 and 1, calculated in the visible part of the solar spectrum, i.e. 380-780 nm. A high number indicates a good colour rendering. Ideally, the maximum value of 1 will be obtained by glazing whose spectral transmittance is completely constant in the whole visible spectral range, i.e. no variation of transmittance with wavelength. A CRF value > 0.9 characterizes a very good colour rendering and CRF > 0.8 represents a good colour rendering (ISO 9050:2003(E) (2003), EN 410:1998 E (1998)). In common usage the CRF values may often be chosen in percentage, i.e. between 0 and 100 %. Note also the recent studies by Mortimer and Varley (2011, 2012) on colour measurements of electrochromic materials.

6.13. Additional Heat Transfer

In addition to the heat transfer directly related to the solar radiation, an additional heat transfer q_u occurs if the room (interior) temperature θ_i differs from the outside (exterior) temperature θ_e, and may be calculated as follows:

$$q_u = U(\theta_i - \theta_e) \tag{108}$$

where U denotes the U-value, i.e. the thermal transmittance, of the glazing, determined according to ISO 10291:1994(E) (1994), ISO 10292:1994(E) (1994) or ISO 10293:1997(E) (1997). Further information may be found elsewhere EN 1946-3:1999 E (1999), EN 1946-2:1999 E (1999), EN 1946-4:2000 E (2000), EN 673:1997 E (1997), EN 674:1997 E (1997), EN 675:1997-E (1997), ISO 8301:1991(E) (1991) and ISO 8302:1991(E) (1991).

6.14. Number of Glass in a Window Pane

The solar radiation glazing factors are dependent upon the number of glass in the actual window pane. Transmittance and reflectance calculations for single glass panes, two-layer window panes and three-layer window panes are given in Eqs.3-10 above. Furthermore, the corresponding absorbance calculations are carried out with Eq.1.

6.15. General for Calculation Procedures

The solar radiation glazing factors may readily be calculated by application of simple computer programs. However, with todays sophisticated data collection tools in computers and instruments, there should be no reason for not applying even higher resolutions, i.e. narrower (wavelength) data intervals, in future versions of Table A1-A5 in Appendix A. In order to simplify the programming of the calculation procedures, there should be chosen *one* wavelength interval for the whole table. For easy implementation of the table values in calculation procedures, there may be given a reference in the standard ISO 9050:2003(E) (2003) to an internet web site where the table values may be downloaded as ASCII files.

7.   Spectroscopical Measurement and Calculation of Solar Radiation Glazing Factors

In the following, spectrophotometric measurements along with calculations of the solar radiation glazing factors, will be shown for one float glass, one glass with a low emittance coating, one dark silver coated glass, several two-layer and three-layer window pane combinations and three electrochromic window (ECW) devices at various colouration levels. The absorbance spectra depicted in the following sections below comply with the absorbance definition in Eq.1, a number between 0 and 1, i.e. the absorbance is not written on the often used/measured logarithmic scale called optical density (see e.g. Jelle and Hagen 1999b).

7.1.   Spectroscopical Data for Float Glass and Low Emittance Glass

The transmittance, absorbance and reflectance in the whole solar spectrum were measured for one float glass and one glass with low emittance coating, depicted in Fig.9 and Fig.10, respectively. The measured wavelength range is from 290 nm to 3300 nm. The upper border of 3300 nm represents the spectrophotometer's long wavelength limit, while below 290 nm the absorption in glass becomes very large. The most noticeable difference is the large reflectance values, and thereby small transmittance values, in the near infrared region for the glass with the low emittance coating. By taking a closer look at the ultraviolet and visible region (Fig.11 and Fig.12) it is observed that the low emittance glass is absorbing more solar radiation at these lower wavelengths than the float glass, i.e. the transmittance is lower for the low emittance glass than the float glass in the UV-VIS region.

The drop in transmittance at around 1000 nm, with a corresponding absorbance peak, as seen in Fig.9, is due to a certain impurity amount of ferric oxide (Fe_2O_3) in the glass. The sharp transmittance cutoffs located around 400 nm and 2700 nm are due to the large absorption in glass into the ultraviolet and infrared region, respectively, see Fig.9 and Fig.10. The sharp transmittance cutoff, with corresponding absorbance increase, at around 2700 nm, is also observed in Fig.10 for the low emittance glass, but much smaller in value since the largest part of the incoming radiation in this wavelength region is reflected from the low emittance coating (the coating surface is facing the incident radiation beam in the spectrophotometer).
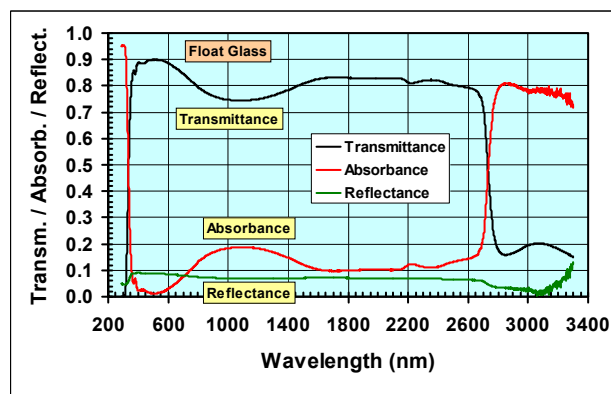
Fig.9.   Transmittance, absorbance and reflectance versus wavelength in the whole solar spectrum measured for a float glass.
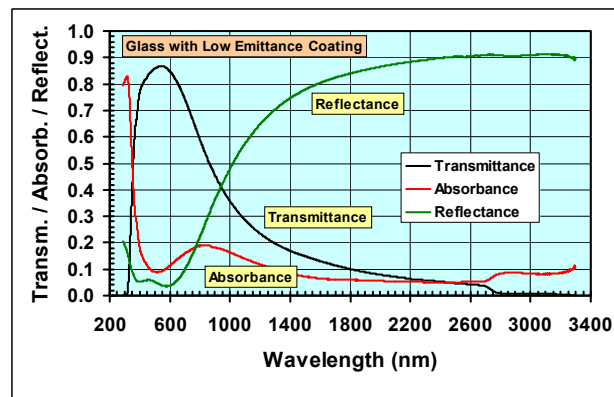
Fig.10.   Transmittance, absorbance and reflectance versus wavelength in the whole solar spectrum measured for a glass with low emittance coating. Incident radiation beam towards surface coating during reflectance measurements.
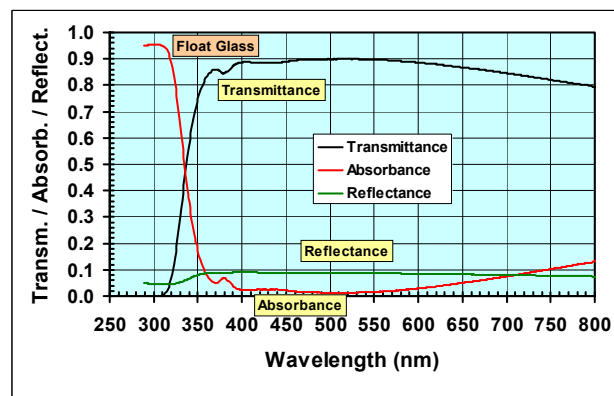
Fig.11.   Transmittance, absorbance and reflectance versus wavelength in the ultraviolet and visible region measured for a float glass.
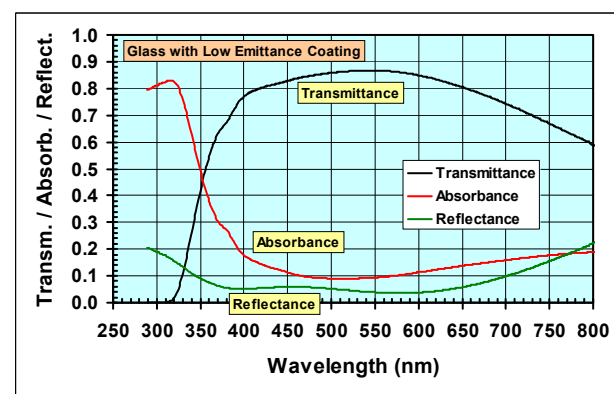
Fig.12.   Transmittance, absorbance and reflectance versus wavelength in the ultraviolet and visible region measured for a glass with low emittance coating. Incident radiation beam towards surface coating during reflectance measurements.

7.2.   Spectroscopical Data for Dark Silver Coated Glass

The transmittance, absorbance and reflectance in the whole solar spectrum were measured for one dark silver coated glass, which is depicted in Fig.13. In addition, the ultraviolet and

visible regions are shown in Fig.14. The transmittance is found to be rather low, between 0 to 0.2, in the whole UV-VIS-NIR region. Both the reflectance and absorbance are quite high in the whole UV-VIS-NIR region, with the absorbance dominating in the UV-VIS region (0.45-0.7) while still retaining a substantial reflectance (0.3-0.4), which gives rise to the dark absorbing and reflecting colour. As will be seen later (Table 1), this coating will result in high SMPF and SSPF values, i.e. high material and skin protection.
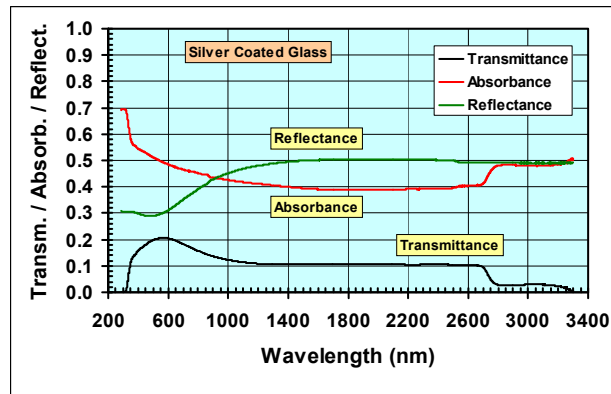
Fig.13.   Transmittance, absorbance and reflectance versus wavelength in the whole solar spectrum measured for a dark silver coated glass. Incident radiation beam towards surface coating during reflectance measurements.
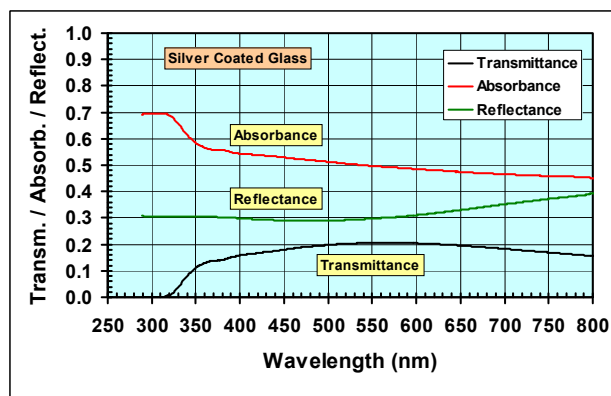
Fig.14.   Transmittance, absorbance and reflectance versus wavelength in the ultraviolet and visible region measured for a dark silver coated glass. Incident radiation beam towards surface coating during reflectance measurements.

7.3.   Spectroscopical Data for Electrochromic Windows

Electrochromic windows (ECW) are able to control the colour of the window, thereby also the solar radiation throughput, by varying the applied electrical potential. Schematic drawings of two ECWs (ECW1 and ECW2) are shown in Fig.15, constructed in a sandwich form from the electrochromic materials polyaniline (PANI), prussian blue (PB) and tungsten oxide (WO$_3$), transparent conducting glass plates with an indium-tin oxide coating (indium oxide doped with tin, In$_2$O$_3$(Sn), ITO, typical surface resistivity of 90 $\Omega/\square$) and the solid state polymer electrolyte poly(2-acrylamido-2-methyl-propane-sulphonic acid) (PAMPS) as an ionic conductor. Both the PANI, PB and WO$_3$ coating thicknesses were less than 1 μm, while the PAMPS layer thickness was about 0.1 mm. Applying a positive potential to the PANI/PB

electrode, both PANI, PB and WO_3 turn to a blue colour, while the window is bleached (made almost transparent) by reversing the polarity of the electrodes. Only a small charge density of about 3 mC/cm^2, corresponding to a low energy consumption of about 5 mWh/m^2, is required for either the colouring or the bleaching process (Jelle et al. 1998). The third electrochromic device ECW3 is similar to ECW1, however with a specific geometrical difference, where further information and details are given by Jelle and Hagen (1994).
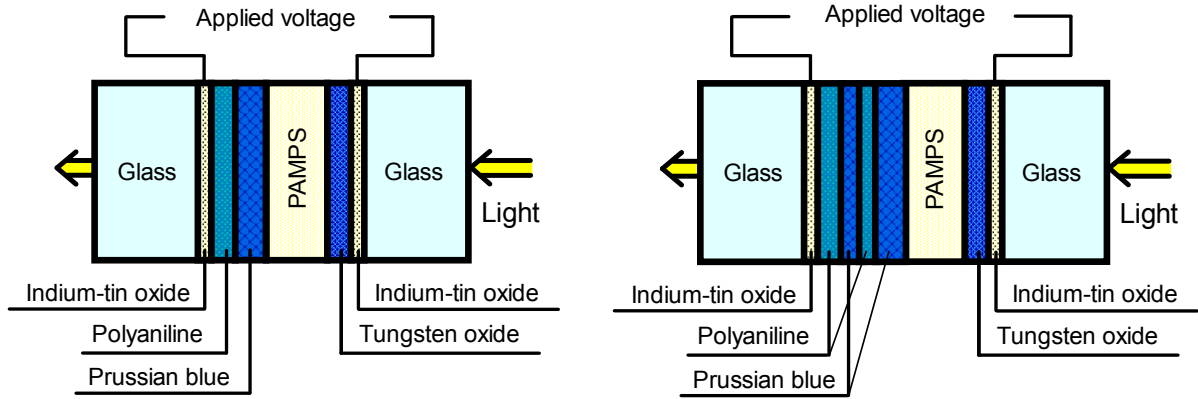
Fig.15.   Schematic drawings of electrochromic window configurations ECW1 (left) and ECW2 (right, PANI-PB multilayer) based on the electrochromic materials polyaniline (PANI), prussian blue (PB) and tungsten oxide (WO_3). From Jelle and Hagen (1999a).

The schematic cell reactions in the ECW devices including the three electrochromic materials PANI, PB and WO_3, also indicating the colour changes, may be written as (Jelle and Hagen 1999):

$$\begin{array}{c} \text{(transparent)} \\ WO_3 + (PANI)(yH^+A^-) + (x\text{-}y)K_2Fe^{II}[Fe(CN)_6] + (x\text{-}y)H^+ \\ \leftrightarrow \\ H_xWO_3 + (PANI^{y+})(A^-)_y + (x\text{-}y)KFe^{III}[Fe(CN)_6] + (x\text{-}y)K^+ \\ \text{(blue)} \end{array} \quad (109)$$
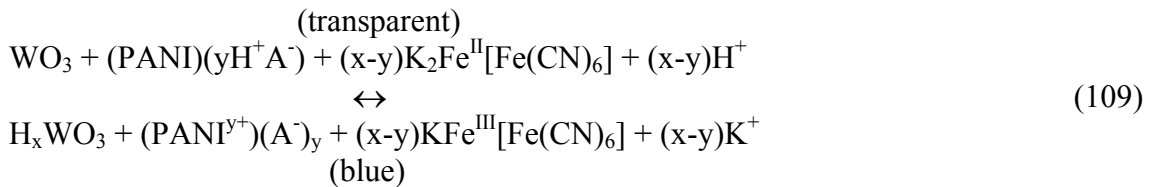
where x denotes the number of protons (H^+) exchanged at the WO_3 electrode, whereas y and (x-y) are the numbers of cations, H^+ and K^+, transferred in the PANI and PB matrix, respectively. Setting y = x in Eq.109 we obtain the cell reaction in an ECW device including only PANI and WO_3 as electrochromic materials (Jelle and Hagen 1999):

$$WO_3 + (PANI)(xH^+A^-) \leftrightarrow H_xWO_3 + (PANI^{x+})(A^-)_x \quad (110)$$
$$\text{(transparent)} \qquad\qquad \text{(blue)}$$
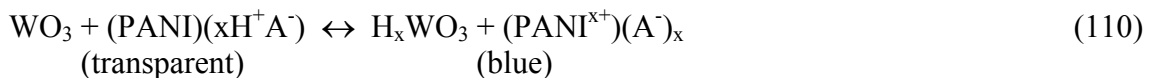
Experiments conducted by the hole method by characterization of individual electrochromic layers in solid state ECWs based on PANI, PB and WO_3 (Jelle et al. 1998) revealed that (a) PANI regulates the transmittance in the whole VIS and NIR region, with a characteristic shift in modulation from the NIR to the VIS region by application of high positive potentials, while (b) PB modulates the transmittance only in the VIS and the start of the NIR region (400-1300 nm), and (c) WO_3 regulates the transmittance in the whole VIS and NIR region where the modulation in the VIS region is largest at the longest wavelengths.

A high transmission regulation and solar modulation (solar regulation ΔT_{sol} = 53 %, T_{sol} calculated based on the solar spectral irradiance given in CRC Handbook of Chemistry and Physics (1989-1990)) (Jelle et al. 1998) have been achieved with this type of ECW (ECW1, left Fig.15), which is depicted in Fig.16 (whole solar spectrum) and Fig.17 (UV-VIS region). Note that applying the solar spectral irradiance given in ISO 9050:2003(E) (2003) gives a somewhat higher ΔT_{sol} = 57 % for ECW1 (Table 3).

The inclusion of PB in PANI enhances the colouration (wavelength dependent absorption), while the adhesion of PB is improved by PANI, i.e. in this respect there exists a symbiotic relationship between PANI and PB (Jelle et al. 1998, Jelle and Hagen 1999a).

Transmittance curves for a second ECW (ECW2, right Fig.15) of the same construction, though with PANI-PB multilayers and a very dark colour in the coloured state, are shown in Fig.18 and Fig.19. The solar regulation is ΔT_{sol} = 49 % (Jelle and Hagen 1998) with solar spectral irradiance from CRC Handbook of Chemistry and Physics (1989-1990) and somewhat higher ΔT_{sol} = 51 % (Table 3) with solar spectral irradiance given in ISO 9050:2003(E) (2003) for ECW2.

Transmittance curves for a third ECW (ECW3) of a similar construction (not depicted here) as ECW1, though with a specific geometrical difference and a very dark colour in the coloured state (measured at a location with thick electrochromic coatings, see Jelle and Hagen 1994), are shown in Fig.20 and Fig.21. The solar regulation is ΔT_{sol} = 56 % (Jelle and Hagen 1994) with solar spectral irradiance from CRC Handbook of Chemistry and Physics (1989-1990) and somewhat higher ΔT_{sol} = 59 % (Table 3) with solar spectral irradiance given in ISO 9050:2003(E) (2003) for ECW3. Note that the ΔT_{sol} = 59 % for ECW3 is very high.
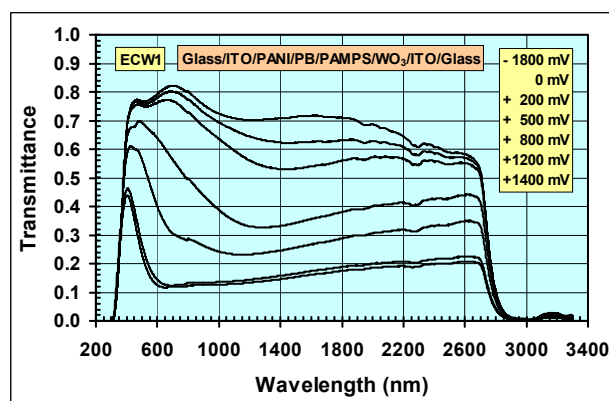
Fig.16.   Transmittance versus wavelength in the whole solar spectrum measured for an electrochromic window ECW1 at different applied potentials. Highest colouration level is at +1400 mV. Redrawn from Jelle et al. (1998).
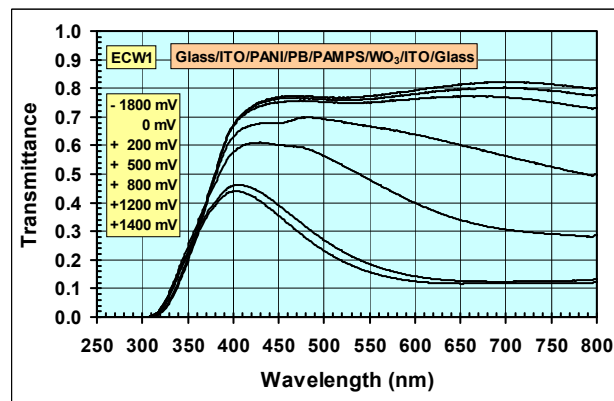
Fig.17.   Transmittance versus wavelength in the ultraviolet and visible region measured for an electrochromic window ECW1 at different applied potentials. Highest colouration level is at +1400 mV.
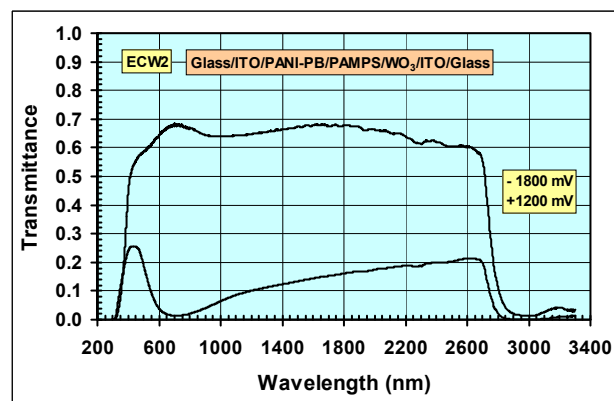
Fig.18.   Transmittance versus wavelength in the whole solar spectrum measured for a second electrochromic window ECW2 (PANI-PB multilayer) at different applied potentials. Highest colouration level is at +1200 mV. Redrawn from Jelle and Hagen (1998).
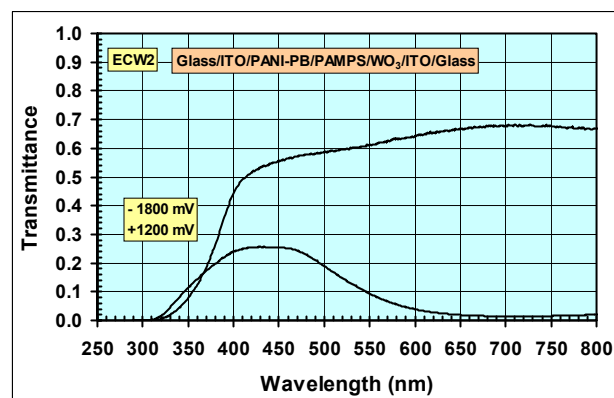
Fig.19.   Transmittance versus wavelength in the ultraviolet and visible region measured for a second electrochromic window ECW2 (PANI-PB multilayer) at different applied potentials. Highest colouration level is at +1200 mV.
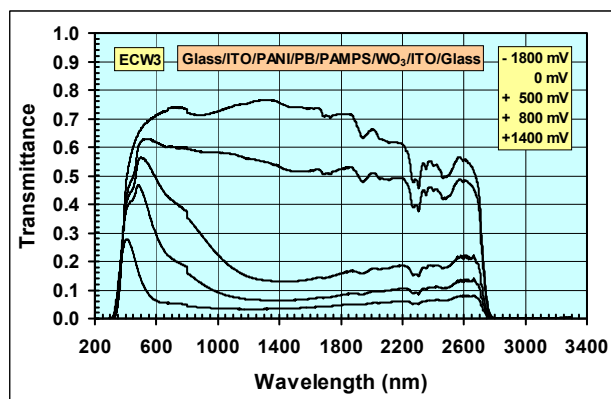
Fig.20.   Transmittance versus wavelength in the whole solar spectrum measured for a third electrochromic window ECW3 at different applied potentials. Highest colouration level is at +1400 mV. Redrawn from Jelle and Hagen (1994).
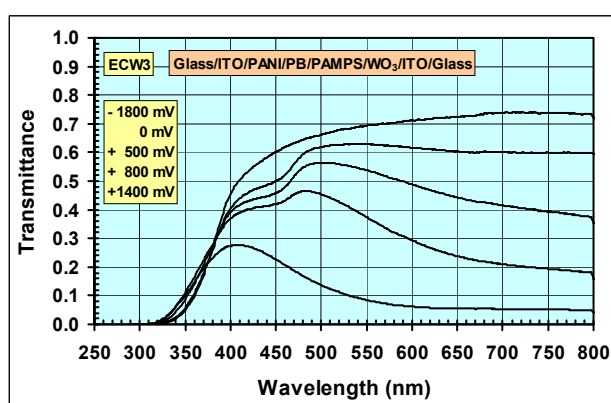
Fig.21.   Transmittance versus wavelength in the ultraviolet and visible region measured for a third electrochromic window ECW3 at different applied potentials. Highest colouration level is at +1400 mV.

It is observed that both ECW2 and ECW3 are considerably darker than ECW1 in the coloured state as depicted by Figs.16-21. Comparing ECW2 and ECW3, it is seen that ECW2 absorbs very much of the solar radiation around 700 nm, whereas ECW3 absorbs substantially more into the NIR region than ECW2. In that respect, note that the solar irradiance decreases rapidly into the NIR region (Fig.1), so the further out into the NIR region the less solar radiation energy there is to modulate by the ECWs.

The doping mechanisms in PANI include both redox processes and proton doping (Chiang and MacDiarmid 1986, Huang et al. 1986, Jelle et al. 1993c), and the characteristic absorbance shift from the NIR to the VIS region for PANI makes it appropriate to plot the absorbance versus both wavelength and applied electrical potential in 3 dimensions in order to enhance the visualization of the absorbance changes. Hence, 2- and 3-dimensional graphical plots of light absorbance versus wavelength for PANI on ITO glass in an aqueous solution of 0.1 M $Na_2SO_4 \cdot 10H_2O$ and 0.001 M H_2SO_4 (pH 3.7) at different applied potentials versus Ag/AgCl (3.5 M KCl) are depicted in Fig.22 (Jelle et al. 1993c, Jelle and Hagen 1999).
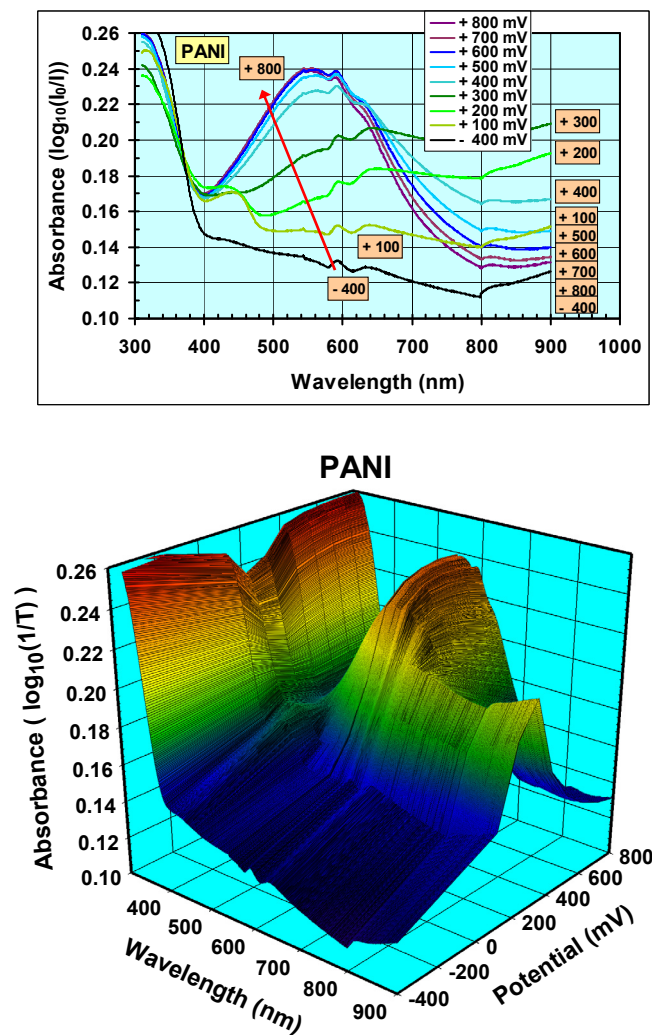
Fig.22.   2- and 3-dimensional graphical plots of light absorbance versus wavelength for PANI on ITO glass in an aqueous solution of 0.1 M $Na_2SO_4 \cdot 10H_2O$ and 0.001 M H_2SO_4 (pH 3.7) at different applied potentials versus Ag/AgCl (3.5 M KCl). The absorbance in the ITO glass, electrolyte and cell has been subtracted by the use of a reference cell in the double beam spectrophotometer. Replotted from Jelle and Hagen (1999).

In addition to their evident potential benefits and savings in solar energy control, the ECWs may also be employed in order to achieve the desired protection of materials and human skin inside buildings during direct solar radiation. That is, the dynamic characteristics of ECWs may allow diffuse daylight through the window panes in the required amount in order to obtain a satisfactory room illumination, whereas at direct solar radiation exposure, the SMPF and SSPF values for the window panes may be increased to a sufficient high protection level.

Several experimental investigations have been performed on these ECWs with PANI, PB and WO$_3$. Transmission properties for individual electrochromic layers in solid state ECWs based on PANI, PB and WO$_3$ have been studied by applying the described hole method by Jelle et al. (1998). Correlation between light absorption and electric charge in solid state ECWs based on PANI, PB and WO$_3$ has been explored by Jelle and Hagen (1999b), including memory effect, electrochromic efficiency and impedance spectra investigations. The reduction factor for PANI films has been investigated and determined from both cyclic voltammetry and visible absorption spectra, showing in general good agreement, by Jelle et al. (1993c). Furthermore, a solar material protection factor (SMPF) and a solar skin protection factor (SSPF) have been

defined and studied for solid state ECWs based on PANI, PB and WO$_3$ by Jelle et al. (2007), where also various examples of photodegradation processes have been shown.

7.4.   Solar Radiation Glazing Factors for Float Glass, Low Emittance Glass, Dark Silver Coated Glass and Two-Layer and Three-Layer Window Pane Configurations

Table 1 gives calculated solar radiation glazing factor values for one float glass, one low emittance glass, one dark silver coated glass and several two-layer and three-layer window pane combinations.

From Table 1 it is seen that the float glass and the low emittance glass have rather large and similar T_{vis} values, i.e. 0.89 and 0.86, respectively. However, the T_{sol} value for float glass is substantially higher than the T_{sol} value for the low emittance glass, i.e. 0.83 vs. 0.59. This is readily observed from the transmittance spectra in Fig.9 and Fig.10.

Furthermore, it is also observed that the float glass has substantially lower R_{sol} value than the low emittance glass, i.e. 0.08 vs. 0.27, which is also confirmed by inspecting the reflectance spectra in Fig.9 and Fig.10. Thereby, the float glass have a larger SF value than the low emittance glass, i.e. 0.85 vs. 0.62.

The A_{sol} values for float glass and low emittance glass are 0.10 and 0.14, respectively, which are considerably lower values than the A_{sol} value of 0.47 for dark silver coated glass. The dark silver glass has furthermore a higher R_{sol} (0.38) value, and lower T_{vis} (0.20), T_{sol} (0.16) and SF (0.28) values than both the float glass and the low emittance glass.

The glass with the low emittance coating has SMPF and SSPF values of 0.32 and 0.89, respectively, which gives better protection than the float glass with SMPF and SSPF values of 0.20 and 0.81, respectively. The dark silver coated glass has SMPF and SSPF values of 0.85 and 0.97, respectively, which gives a far better material protection and also substantially better skin protection than both the float glass and the low emittance glass.

The observed large differences in transmittance, absorbance and reflectance spectra for the float glass, low emittance glass and dark silver coated glass are also expressed through the solar radiation glazing factors, e.g. compare $T_{sol} = 0.83$, $A_{sol} = 0.10$ and $R_{sol} = 0.08$ for float glass with $T_{sol} = 0.59$, $A_{sol} = 0.14$ and $R_{sol} = 0.27$ for low emittance glass and $T_{sol} = 0.16$, $A_{sol} = 0.47$ and $R_{sol} = 0.38$ for dark silver coated glass. For further comparisons of these three single glass panes it is referred to Table 1, and comparison of transmittance spectra in Fig.9, Fig.10 and Fig.13 for the whole solar region and Fig.11, Fig.12 and Fig.14 for close-up of the ultraviolet and visible region.

Table 1.   Calculated solar radiation glazing factor values for one float glass, one glass with low emittance coating, one dark silver coated glass and several two-layer and three-layer window pane configurations. All coatings on each glass are facing towards the outside, except the low emittance coating on the outermost glass pane, which is facing towards the inside. In the table the glass pane sequence from left to right corresponds to from outside to inside. Corresponding transmittance spectra are given in Figs.9-14. The emissivity of the float glass was determined to $\varepsilon_{float} = 0.836$ by hemispherical directional reflectance measurements and was directly applied in the calculation of SF as the emissivity value in the SF calculations is with respect to the inside facing surface (of building) of the innermost glass pane, i.e. normally a float glass, whereas $\varepsilon_{lowe} = 0.071$ and

$\varepsilon_{silver} = 0.543$ were indirectly applied in the SF calculations through the calculations of the thermal conductance Λ. G = glass, LE = low emittance coating, S = dark silver coating, A = air cavity.

Glass Configuration	n	T_{uv}	T_{vis}	T_{sol}	SMPF	SSPF	$R_{vis,ext}$	$R_{vis,int}$	R_{sol}	A_{sol}	ε	SF	CRF
Float Glass G	1	0.65	0.89	0.83	0.20	0.81	0.09	0.09	0.08	0.10	0.836	0.85	0.99
Low Emittance Glass LE/G	1	0.41	0.86	0.59	0.32	0.89	0.04	0.04	0.27	0.14	0.836	0.62	0.98
Dark Silver Glass S/G	1	0.10	0.20	0.16	0.85	0.97	0.30	0.30	0.38	0.47	0.836	0.28	0.97
Float/Float G/A/G	2	0.50	0.80	0.69	0.31	0.87	0.16	0.04	0.13	0.17	0.836	0.76	0.97
Float/LowE G/A/LE/G	2	0.32	0.77	0.50	0.41	0.92	0.12	0.03	0.26	0.24	0.836	0.60	0.96
Float/Silver G/A/S/G	2	0.08	0.19	0.14	0.87	0.98	0.33	0.00	0.34	0.52	0.836	0.42	0.97
LowE/LowE G/LE/A/LE/G	2	0.22	0.74	0.43	0.48	0.94	0.09	0.01	0.26	0.31	0.836	0.52	0.95
LowE/Float G/LE/A/G	2	0.32	0.77	0.50	0.41	0.92	0.12	0.02	0.24	0.25	0.836	0.55	0.96
Silver/Float G/S/A/G	2	0.08	0.19	0.14	0.87	0.98	0.26	0.15	0.24	0.62	0.836	0.21	0.97
Silver/LowE G/S/A/LE/G	2	0.05	0.18	0.11	0.88	0.99	0.26	0.04	0.24	0.65	0.836	0.18	0.96
Silver/Silver G/S/A/S/G	2	0.01	0.05	0.03	0.97	1.00	0.27	0.00	0.25	0.72	0.836	0.16	0.95
Float/Float/Float G/A/G/A/G	3	0.40	0.73	0.59	0.40	0.90	0.21	0.17	0.17	0.24	0.836	0.68	0.96
Float/Float/LowE G/A/G/A/LE/G	3	0.26	0.69	0.44	0.48	0.93	0.18	0.10	0.25	0.31	0.836	0.55	0.95
Float/LowE/LowE G/A/LE/G/A/LE/G	3	0.18	0.66	0.37	0.54	0.95	0.15	0.09	0.29	0.34	0.836	0.50	0.94
LowE/LowE/LowE G/LE/A/LE/G/A/LE/G	3	0.12	0.63	0.33	0.59	0.97	0.11	0.08	0.28	0.39	0.836	0.45	0.93
Silver/Float/Float G/S/A/G/A/G	3	0.06	0.17	0.12	0.88	0.98	0.26	0.26	0.24	0.64	0.836	0.18	0.96
Silver/Float/LowE G/S/A/G/A/LE/G	3	0.04	0.16	0.09	0.89	0.99	0.26	0.15	0.24	0.66	0.836	0.15	0.95
Silver/LowE/LowE G/S/A/LE/G/A/LE/G	3	0.03	0.15	0.08	0.91	0.99	0.26	0.14	0.25	0.67	0.836	0.14	0.94
Silver/Silver/Silver G/S/A/S/G/A/S/G	3	0.00	0.01	0.01	0.99	1.00	0.27	0.26	0.25	0.74	0.836	0.11	0.93

Naturally, the two-layer and three-layer window panes transmit less solar radiation than their single glass pane counterparts. For example (Table 1), a single float glass pane has $T_{vis} = 0.89$ and $T_{sol} = 0.83$, whereas the two-layer float/float window pane has $T_{vis} = 0.80$ and $T_{sol} = 0.69$, and the three-layer float/float/float window pane has $T_{vis} = 0.73$ and $T_{sol} = 0.59$. Furthermore, a single low emittance glass pane has $T_{vis} = 0.86$ and $T_{sol} = 0.59$, whereas the two-layer LowE/LowE window pane has $T_{vis} = 0.74$ and $T_{sol} = 0.43$, and the three-layer LowE/LowE/LowE window pane has $T_{vis} = 0.63$ and $T_{sol} = 0.33$. On the more extreme dark side, a single dark silver coated glass pane has $T_{vis} = 0.20$ and $T_{sol} = 0.16$, whereas the two-layer dark silver/silver window pane has $T_{vis} = 0.05$ and $T_{sol} = 0.03$, and the three-layer dark silver/silver/silver window pane has $T_{vis} = 0.01$ and $T_{sol} = 0.01$. Normally, only one or two

low emittance coated glass panes, and only maximum one dark silver coated glass pane, are applied in a two-layer or three-layer window pane unit. Several configurations are calculated and given in Table 1. Note that all the calculated configurations here have glass (i.e. not a coating) as the outermost surface both at the exterior and interior side of the window pane, i.e. outside and inside the building, respectively, i.e. all coatings are then protected from the exterior and interior environments by the glass.

The two-layer window panes give an even better material and skin protection compared with their single pane counterparts, with SMPF values of 0.31, 0.41 and 0.87, and with SSPF values of 0.87, 0.92 and 0.98, for float/float, float/LowE and float/silver, respectively. Note that the SMPF is as high as 0.87 for the two-layer window pane consisting of one float glass and one dark silver coated glass. The three-layer window pane counterparts have even higher SMPF and SSPF values, e.g. note the very high SMPF and SSPF values of 0.88 and 0.98 for the three-layer dark silver/float/float window pane, and 0.99 and 1.00 for the three-layer dark silver/silver/silver window pane, respectively. It is also clear that materials inside buildings are far better protected with the two-layer or three-layer window pane with one dark silver coated surface than with the float or low emittance coating alternatives. However, the dark silver coated window pane alternatives admit far less visible solar radiation and also total solar radiation as demonstrated by the much lower T_{vis} and T_{sol} values.

Comparing the relatively low SMPF (with dark silver coated glass as an exception) and relatively high SSPF values, gives evident reasons for the everyday observation that some materials like e.g. books in book shelves and various wood and paint materials become discoloured and bleached, whereas we human beings usually do not get tanned or sunburnt behind glass inside buildings. It should be mentioned that with the earlier upper wavelength limit of 500 nm (compared with 600 nm today) in calculation of SMPF, the material protection values were apparently larger, 0.34, 0.52 and 0.89 for the single float glass, the low emittance glass and the dark silver coated glass, respectively. That is, a much larger part of the visible solar radiation is considered today to contribute to the solar deterioration of materials. For further details and visual comparison of SMPF and SSPF values with T_{vis} values it is referred to the work by Jelle et al. (2007). It should be noted that all glass configurations in Table 1 have very high CRF values, including float glass, low emittance glass and dark silver coated glass in single, two-layer and three-layer window pane combinations, with CRF values ranging from 0.93 to 0.99, i.e. a very good colour rendering, even for the various dark silver coated glass combinations.

In Fig.23 there is depicted an example of applying measured transmittance and reflectance spectra for single float glass panes (Eq.3 and Eq.4) for calculating the transmittance spectra through two-layer and three-layer window panes according to Eq.5 and Eq.8, respectively. It is observed that the addition of extra glass panes decreases the transmittance in the whole solar spectral range. That is, adding more glass panes to a window or glass structure decreases the available amount of daylight and solar radiation to be exploited and utilized inside a building. The two-layer and three-layer window pane transmittance spectra have been calculated with the full spectral resolution and wavelength range as applied in the spectrophotometric measurements, i.e. not with the considerably lower resolution and narrower wavelength range as applied when calculating the solar radiation glazing factors like e.g. T_{sol} (Table A3).
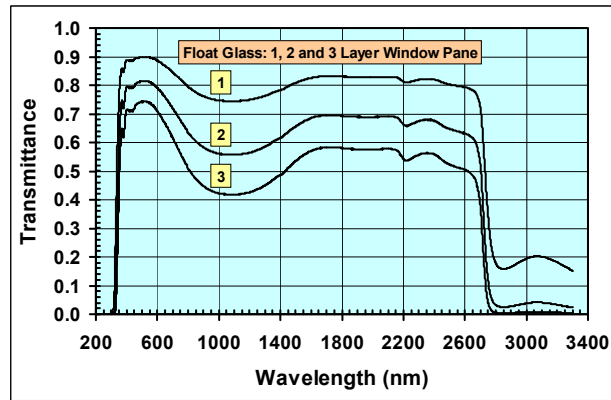
Fig.23.   Transmittance versus wavelength in the whole solar spectrum measured for a float glass and calculated for two-layer and three-layer float glass window panes (Eq.5 and Eq.8).

When designing and choosing the appropriate window glass or glass structure, many considerations and evaluations have to be made, e.g. with respect to solar material protection, solar skin protection, solar energy aspects, thermal radiation aspects, daylight, visual appearance, etc., where many of these parameters are influencing each other. Measurement and calculation of the solar radiation glazing factors represent the adequate and best tool for making quantitative evaluations and hence the appropriate and best decisions in this regard.

7.5.   Solar Radiation Glazing Factors for Electrochromic Windows

Table 2 gives the solar radiation glazing factors for different colouration levels, i.e. at different applied electrical potentials, for three electrochromic windows (ECW1, ECW2 and ECW3), in addition to selected two-layer and three-layer window pane configurations with incorporated electrochromic materials.

Table 2.   Calculated solar radiation glazing factors for three different electrochromic windows (ECW) at different colouration levels, i.e. at different applied potentials, and selected two-layer and three-layer window pane configurations with ECWs. Highest colouration level is at +1400 mV (ECW1 and ECW3) and +1200 mV (ECW2, PANI-PB multilayer). Corresponding transmittance spectra are given in Figs.16-19. Reflectance values of the ECWs have not been measured, but as the (absorbing) electrochromic coatings are located between two glass plates, the (low) reflectance values will be close to the values for float glass, and these are hence employed in the current calculations. The emissivity of the float glass was determined to $\varepsilon_{float} = 0.836$ by hemispherical directional reflectance measurements and was directly applied in the calculation of SF as the emissivity value in the SF calculations is with respect to the inside facing surface (of building) of the innermost glass pane, i.e. normally a float glass, whereas $\varepsilon_{lowe} = 0.071$ and $\varepsilon_{silver} = 0.543$ were indirectly applied in the SF calculations through the calculations of the thermal conductance Λ. G = glass, LE = low emittance coating, A = air cavity, EC1 = ECW device between two glass plates, EC2 = ECW2 device between two glass plates (PANI-PB multilayer), T or C behind EC1 and EC2 denote transparent or coloured state, respectively.

Glass Configuration	n	T_{uv}	T_{vis}	T_{sol}	SMPF	SSPF	$R_{vis,ext}$	$R_{vis,int}$	R_{sol}	A_{sol}	ε	SF	CRF
ECW1 (-1800 mV)	1	0.23	0.78	0.74	0.43	0.93	0.09	0.09	0.08	0.18	0.836	0.79	0.98
ECW1 (0 mV)	1	0.23	0.77	0.72	0.43	0.93	0.09	0.09	0.08	0.21	0.836	0.77	0.98
ECW1 (+200 mV)	1	0.24	0.75	0.68	0.44	0.93	0.09	0.09	0.08	0.24	0.836	0.74	0.99
ECW1 (+500 mV)	1	0.25	0.66	0.52	0.48	0.93	0.09	0.09	0.08	0.40	0.836	0.62	0.95
ECW1 (+800 mV)	1	0.26	0.47	0.36	0.54	0.92	0.09	0.09	0.08	0.56	0.836	0.51	0.82
ECW1 (+1200 mV)	1	0.24	0.19	0.19	0.68	0.93	0.09	0.09	0.08	0.73	0.836	0.38	0.68
ECW1 (+1400 mV)	1	0.23	0.17	0.17	0.71	0.93	0.09	0.09	0.08	0.75	0.836	0.37	0.68
ECW2 (-1800 mV)	1	0.10	0.62	0.61	0.61	0.97	0.09	0.09	0.08	0.31	0.836	0.69	0.95
ECW2 (+1200 mV)	1	0.12	0.10	0.10	0.82	0.97	0.09	0.09	0.08	0.82	0.836	0.31	0.31
ECW3 (-1800 mV)	1	0.08	0.69	0.67	0.59	0.97	0.09	0.09	0.08	0.25	0.836	0.74	0.96
ECW3 (+1400 mV)	1	0.12	0.09	0.08	0.83	0.97	0.09	0.09	0.08	0.84	0.836	0.30	0.59
EC1/Float (-) EC1T/A/G	2	0.18	0.70	0.62	0.50	0.95	0.14	0.04	0.12	0.26	0.836	0.67	0.99
EC1/Float (+) EC1C/A/G	2	0.18	0.15	0.15	0.75	0.95	0.09	0.04	0.08	0.77	0.836	0.25	0.67
EC1/LowE (-) EC1T/A/LE/G	2	0.12	0.67	0.45	0.55	0.97	0.11	0.03	0.23	0.32	0.836	0.55	0.99
EC1/LowE (+) EC1C/A/LE/G	2	0.12	0.14	0.11	0.78	0.97	0.09	0.03	0.09	0.80	0.836	0.19	0.68
EC1/Float/Float (-) EC1T/A/G/A/G	3	0.15	0.63	0.53	0.55	0.96	0.18	0.17	0.15	0.32	0.836	0.60	0.99
EC1/Float/Float (+) EC1C/A/G/A/G	3	0.14	0.14	0.13	0.78	0.96	0.09	0.17	0.08	0.79	0.836	0.20	0.67
EC1/Float/LowE (-) EC1T/A/G/A/LE/G	3	0.10	0.60	0.39	0.60	0.97	0.16	0.10	0.22	0.39	0.836	0.50	0.98
EC1/Float/LowE (+) EC1C/A/G/A/LE/G	3	0.10	0.13	0.10	0.81	0.97	0.09	0.10	0.09	0.82	0.836	0.16	0.67
EC1/LowE/LowE (-) EC1T/A/LE/G/A/LE/G	3	0.07	0.58	0.33	0.64	0.98	0.13	0.09	0.25	0.41	0.836	0.45	0.97
EC1/LowE/LowE (+) EC1C/A/LE/G/A/LE/G	3	0.07	0.12	0.08	0.83	0.98	0.09	0.09	0.09	0.83	0.836	0.14	0.67
EC2/LowE/LowE (-) EC2T/A/LE/G/A/LE/G	3	0.03	0.46	0.26	0.74	0.99	0.11	0.09	0.22	0.52	0.836	0.37	0.96
EC2/LowE/LowE (+) EC2C/A/LE/G/A/LE/G	3	0.03	0.07	0.04	0.89	0.99	0.09	0.09	0.08	0.87	0.836	0.10	0.30

From Table 2 it is observed that various solar radiation glazing factors may obtain both high and low values depending upon the applied electrical potential in the ECWs, e.g. changing the T_{vis} value from 0.78 to 0.17 for the ECW1 device and from 0.62 to 0.10 for the darker ECW2 device. It is also noted that these ECWs contain solar radiation absorbing electrochromic materials, i.e. not reflecting materials, as the changes with applied potential occur in the transmittance (e.g. T_{sol}) and absorbance (e.g. A_{sol}) values, and not in the reflectance (e.g. R_{sol}) values. The ECW3 device changes T_{vis} from 0.69 in the transparent state to 0.09.in the coloured state.

As expected, the highest colouration level gives the largest SMPF values, i.e. the best protection of materials is achieved with the darkest ECW, e.g. compare a SMPF value of 0.71 for ECW1, 0.82 for ECW2 and 0.83 for ECW3 in the coloured state, with 0.43 (ECW1), 0.61 (ECW2) and 0.59 (ECW3) in the transparent (bleached) state, respectively.

Incorporating the ECWs into two-layer and three-layer window pane configurations reduces the total solar energy throughput in the windows, e.g. as seen in the T_{sol} and SF values, as several layers of glass and coatings will increase the total reflectance and absorbance. Note that some of the reflectance values $R_{vis,ext}$, $R_{vis,int}$ and R_{sol} may have errors due to parallel displacement of solar radiation through glass causing parts of the radiation to not enter the spectrophotometer detector during the measurements.

The CRF values are very high, i.e. a very good colour rendering, for all the ECW configurations in the transparent (bleached) state, with CRF values ranging from 0.95 to 0.99, also including two-layer and three-layer window pane combinations. ECW2 has the lowest CRF value in the transparent state, i.e. a CRF = 0.95. However, in the coloured state, the CRF values are substantially reduced for all the three different ECWs. ECW1 has CRF = 0.68, ECW2 has CRF = 0.31 and ECW3 has CRF = 0.59 in the coloured state. Note that especially ECW2 has a very low CRF (0.31) value. The large differences between the CRF values for the three ECWs in the coloured state may be deduced from comparing the transmittance spectra in the visible region between 380 nm and 780 nm (Figs.16-21).

Furthermore, based on values in Table 2, solar radiation glazing factor modulations (regulations) are calculated for the three different ECWs and selected two-layer and three-layer window pane configurations with ECWs as given in Table 3. The modulation level is calculated by subtracting the solar radiation glazing factors for the same ECW at the high and low potentials given in Table 2, e.g. as for ΔT_{sol}:

$$\Delta T_{sol} = T_{sol}(bleached) - T_{sol}(coloured) \tag{111}$$

where the T_{sol} values in Table 2 are calculated from Eq.14 and likewise for the other solar radiation glazing factors.

Table 3.   Calculated solar radiation glazing factor modulations for three different electrochromic windows (ECW) and selected two-layer and three-layer window pane configurations with ECWs. The modulation level is calculated by subtracting the solar radiation glazing factors for the same ECW at the high and low potentials given in Table 2 (e.g. Eq.111).

Glass Configuration	n	ΔT_{uv}	ΔT_{vis}	ΔT_{sol}	$\Delta SMPF$	$\Delta SSPF$	$\Delta R_{vis,ext}$	$\Delta R_{vis,int}$	ΔR_{sol}	ΔA_{sol}	ε	ΔSF	ΔCRF
ECW1 (-1800 mV) ECW1 (+1400 mV)	1	0.00	0.61	0.57	-0.28	0.00	0.00	0.00	0.00	-0.57	-	0.42	0.30
ECW2 (-1800 mV) ECW2 (+1200 mV)	1	-0.02	0.52	0.51	-0.21	0.00	0.00	0.00	0.00	-0.51	-	0.38	0.64
ECW3 (-1800 mV) ECW3 (+1400 mV)	1	-0.04	0.60	0.59	-0.24	0.00	0.00	0.00	0.00	-0.59	-	0.44	0.37
EC1/Float (-) EC1T/A/G EC1/Float (+) EC1C/A/G	2	0.00	0.55	0.47	-0.25	0.00	0.05	0.00	0.04	-0.51	-	0.42	0.32
EC1/LowE (-) EC1T/A/LE/G EC1/LowE (+) EC1C/A/LE/G	2	0.00	0.53	0.34	-0.23	0.00	0.02	0.00	0.14	-0.48	-	0.36	0.31

EC1/Float/Float (-) EC1T/A/G/A/G EC1/Float/Float (+) EC1C/A/G/A/G	3	0.01	0.49	0.40	-0.23	0.00	0.09	0.00	0.07	-0.47	-	0.40	0.32
EC1/Float/LowE (-) EC1T/A/G/A/LE/G EC1/Float/LowE (+) EC1C/A/G/A/LE/G	3	0.00	0.47	0.29	-0.21	0.00	0.07	0.00	0.13	-0.43	-	0.34	0.31
EC1/LowE/LowE (-) EC1T/A/LE/G/A/LE/G EC1/LowE/LowE (+) EC1C/A/LE/G/A/LE/G	3	0.00	0.46	0.25	-0.19	0.00	0.04	0.00	0.16	-0.42	-	0.31	0.30
EC2/LowE/LowE (-) EC2T/A/LE/G/A/LE/G EC2/LowE/LowE (+) EC2C/A/LE/G/A/LE/G	3	0.00	0.39	0.22	-0.15	0.00	0.02	0.00	0.14	-0.35	-	0.27	0.66

The ECW1, ECW2 and ECW3 devices have rather large solar radiation modulation abilities, e.g. $\Delta T_{vis} = 0.61$ and $\Delta T_{sol} = 0.57$ for ECW1, $\Delta T_{vis} = 0.52$ and $\Delta T_{sol} = 0.51$ for ECW2 and $\Delta T_{vis} = 0.60$ and $\Delta T_{sol} = 0.59$ for ECW3, where the transmittance modulation is assumed to be due to absorbance regulation, i.e. $\Delta A_{sol} = -0.57$ for ECW1, $\Delta A_{sol} = -0.51$ for ECW2 and $\Delta A_{sol} = -0.59$ for ECW3. Note that reflectance values of the ECWs have not been measured, but as the (absorbing) electrochromic coatings are located between two glass plates, the (low) reflectance values will be close to the values for float glass, and these are hence employed in the current calculations.

Although the solar factor modulations are lower than their solar transmission counterparts for the ECWs, the solar factor modulations are still quite high, i.e. $\Delta SF = 0.42$, $\Delta SF = 0.38$ and $\Delta SF = 0.44$ for ECW1, ECW2 and ECW3, respectively.

As mentioned in the above, applying the ECWs into two-layer and three-layer window pane configurations reduces the total solar energy throughput modulation in the windows, e.g. as also seen in the ΔT_{sol} and ΔSF values, as several layers of glass and coatings will increase the total reflectance and absorbance, i.e. less solar radiation left for the ECWs to modulate (regulate). That is, the solar radiation modulation by an ECW will decrease with the number of glass panes and low emittance coatings added to the total window configuration. For example, the single glass ECW1 values $\Delta T_{vis} = 0.61$ and $\Delta T_{sol} = 0.57$ are decreased to the two-layer EC1/float window pane values $\Delta T_{vis} = 0.55$ and $\Delta T_{sol} = 0.47$ and three-layer EC1/float/float window pane values $\Delta T_{vis} = 0.49$ and $\Delta T_{sol} = 0.40$. Nevertheless, even if these values are lower they still represent a large solar modulation by the electrochromic window. Employing one or two low emittance coatings in the window configurations will decrease e.g. ΔT_{vis} and ΔT_{sol} even further, where especially the ΔT_{sol} value is decreased. For example, the three-layer EC1/LowE/LowE window pane has $\Delta T_{vis} = 0.46$ and $\Delta T_{sol} = 0.25$. For further comparisons of solar radiation glazing factors for various electrochromic window pane configurations is referred to Table 3.

It is observed that the $\Delta SSPF$ modulation is more or less insignificant for the ECW glass configurations given in Table 3, as the change in ECW colouration state at low wavelengths is almost negligible due to the highly increasing absorption in the glass system from 400 nm and below (see Figs.16-21). It should be noted that the above referred ECWs were constructed in order to achieve the highest possible solar energy regulation, with no optimization with respect to SMPF and SSPF values. Direct investigation in this area may therefore improve the SMPF regulation in ECWs substantially (but not SSPF due to the already high absorption in

glass as mentioned above). For further details and visual comparison of SMPF and SSPF values with T_{vis} values for ECWs it is referred to the work by Jelle et al. (2007).

Applying glass panes with low emittance coatings together with ECWs decreases the solar modulation abilities of the ECWs, as there is much less solar radiation to be regulated due to the large reflectance in the near infrared region caused by the low emittance coating (Fig.10). Nevertheless, the combined ECW low emittance window pane alternatives represent appropriate and useful window configurations as the low emittance coating is reducing the heat loss (infrared radiation) through windows, and hence examples are given in Table 2 and Table 3. Applying glass panes with dark silver coatings together with ECWs decreases the solar modulation abilities of the ECWs also, as there is much less solar radiation to be regulated due to the large absorbance and reflectance in both the visible and the near infrared region caused by the dark silver coating (Fig.13). However, as the combined ECW dark silver coated window pane alternatives normally do not represent appropriate and useful window configurations, no such examples are given in Table 2 and Table 3.

In Fig.24 there is depicted an example of applying measured transmittance and reflectance spectra for the ECW1 single glass pane structure (Eq.3 and Eq.4) for calculating the transmittance spectra through two-layer and three-layer ECW1 window panes according to Eq.5 and Eq.8, respectively. It is observed that the addition of extra glass panes decreases the transmittance in the whole solar spectral range. That is, adding more glass panes to an ECW structure decreases the available amount of daylight and solar radiation to be controlled and regulated by the electrochromic window or smart window in general. The two-layer and three-layer window pane transmittance spectra have been calculated with the full spectral resolution and wavelength range as applied in the spectrophotometric measurements, i.e. not with the considerably lower resolution and narrower wavelength range as applied when calculating the solar radiation glazing factors like e.g. T_{sol} (Table A3).
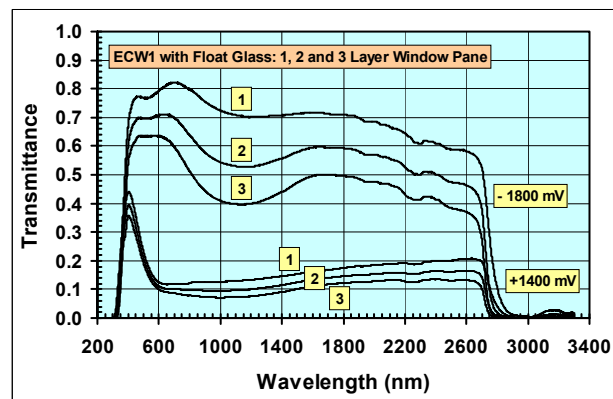
Fig.24.   Transmittance versus wavelength in the whole solar spectrum measured for an electrochromic window ECW1 and calculated for two-layer and three-layer ECW1 float glass window pane combinations (Eq.5 and Eq.8) at two different applied potentials. Highest colouration level is at +1400 mV.

Hence, the ECWs may contribute to elegant, flexible glazing systems with dynamical control of the solar radiation, both with regard to daylight, solar energy aspects and protection of materials inside buildings. The ECWs may readily be characterized by spectroscopical measurements and subsequent calculations of the solar radiation glazing factors.

7.6.   Miscellaneous Other Electrochromic Properties

7.6.1.   General

The solar radiation glazing factors represent some of the most important properties for electrochromic windows (ECW). In addition, there are also miscellaneous other electrochromic properties which are crucial for the performance of ECWs. As for solar radiation transmittance modulation by regulation of either the absorbance or reflectance, it is referred to the earlier discussion related to Figs.4-6. Furthermore, nor the production, transport, installation, operation, maintenance or demolition of ECWs should pose any hazard to the nearby surroundings or to the environment in general, e.g. the environmental impact should be as low as possible.

7.6.2.   Colour Coordinates

Colour measurements involve the determination of among others the colour coordinates L, a and b in a three-dimensional colour space, where higher positive values denote a more light colour (on a white-black scale, i.e. higher luminance), a more reddish colour (on a red-green scale) and a more yellowish colour (on a yellow-blue scale), respectively (Jelle 2012). Furthermore, a higher gloss value denotes a more glossy (shiny) material. One may also calculate a colour difference ΔE as:

$$\Delta E = \sqrt{(\Delta L)^2 + (\Delta a)^2 + (\Delta b)^2} \tag{112}$$

where $\Delta L = L_2 - L_1$, $\Delta a = a_2 - a_1$ and $\Delta b = b_2 - b_1$, where (L_2, a_2, b_2) and (L_1, a_1, b_1) represent two colours or colour coordinates in the three-dimensional CIELab colour space. Thus, the colour difference ΔE represents the distance between two colours, e.g. a colour difference between a non-aged and an aged condition, or e.g. a colour difference for an ECW changing colour between two coloured states. However, these colour coordinates have not been measured for the treated ECWs here, as the solar radiation glazing factors including the colour rendering factor (CRF) are the important factors for window applications, i.e. also requiring a transparent state with as low colour distortion as possible. For colour displays the L, a and b coordinates would be interesting, though.

7.6.3.   Electrochromic Efficiency

One characteristic quantity for ECWs is the bleaching and colouring efficiency at a specific wavelength λ, the electrochromic efficiency η defined by (Beni and Shay 1982, Cogan et al. 1990, Córdoba de Torresi et al. 1991, Córdoba de Torresi and Gorenstein 1992, Jelle 1993, Jelle and Hagen 1994, Jelle and Hagen 1999b, Kitao et al. 1992, Seike and Nagai 1991, Zhang et al. 1993):

$$\eta(\lambda) = \Delta OD(\lambda)/Q = \log_{10}(T_{bleach}(\lambda)/T_{col}(\lambda))/Q \tag{113}$$

where ΔOD is the change in optical density and Q is the consumed electrical charge density stepping from a bleached state (with transmittance T_{bleach}) to a coloured state (with transmittance T_{col}) or vice versa. The optical density OD is defined as the absorbance A' written on a logarithmic form by (Jelle 1993, Jelle and Hagen 1999b):

$$OD = A' = \log_{10}(1/T) = \log_{10}(I_0/I) = \alpha \log_{10}(e)x = \alpha'x \tag{114}$$

which is deduced from the well-known Beer-Lambert law given by (Batchelder 1988, Gale 1988, Hecht 1987, Jastrzebski 1987, Jelle 1993, Loudon 1990, Silverstein et al. 1981):

$$I = I_0 e^{-\alpha x} \tag{115}$$

where the transmittance T is given by:

$$T = I/I_0 \tag{116}$$

where the transmitted radiation intensity I decreases exponentially with the penetration length or depth x, I_0 is the incident radiation intensity, and α and α' denote absorption coefficients depending what form is used.

In order to account for the whole visible solar radiation spectral region, and the whole solar radiation spectral region, visible and solar spectral electrochromic efficiencies η_{vis} and η_{sol} may be respectively defined by:

$$\eta_{vis} = \Delta OD_{vis}/Q = \log_{10}(T_{vis}(\text{bleached})/T_{vis}(\text{coloured}))/Q \tag{117}$$

$$\eta_{sol} = \log_{10}(T_{sol}(\text{bleached})/T_{sol}(\text{coloured}))/Q \tag{118}$$

where T_{vis} and T_{sol} denote the visible solar transmittance (Eq.13) and the solar transmittance (Eq.14), respectively. Note that the term optical density (OD) is not used in the expression for η_{sol} as optical normally refers to the visible region.

Electrochromic efficiencies have been calculated from measurements on the ECW3 configuration (transmittance spectra in Fig.20), yielding the following bleaching and colouring efficiencies (Jelle and Hagen 1994): $\eta_{bleach}(1000\ nm) = 200\ cm^2/C$, $\eta_{col}(1000\ nm) = 120\ cm^2/C$, $\eta_{bleach}(550\ nm) = 120\ cm^2/C$ and $\eta_{col}(550\ nm) = 70\ cm^2/C$. The observed longer colouring time compared to the bleaching time, is reflected in the lower colouring efficiency versus the bleaching efficiency (Jelle and Hagen 1994). Assuming approximately the same consumed electrical charge densities as utilized in the calculations above (see Jelle and Hagen 1994 for details), and $T_{vis}(\text{bleached}) = 0.69$, $T_{vis}(\text{coloured}) = 0.09$, $T_{sol}(\text{bleached}) = 0.67$ and $T_{sol}(\text{coloured}) = 0.08$ for ECW3 given in Table 2, the following approximate electrochromic efficiencies are obtained: $\eta_{vis}(\text{bleached}) = 150\ cm^2/C$, $\eta_{vis}(\text{coloured}) = 90\ cm^2/C$, $\eta_{sol}(\text{bleached}) = 160\ cm^2/C$ and $\eta_{sol}(\text{coloured}) = 90\ cm^2/C$.

7.6.4.   Energy Consumption, Memory and Switching Time

The energy consumption in ECWs represent an important value with respect to the energy savings and overall performance of ECWs. Typically for the ECWs discussed in this work, only a small charge density of about 3 mC/cm^2, corresponding to a low energy consumption of about 5 mWh/m^2, is required for either the colouring or the bleaching process, i.e. about 0.01 Wh/m^2 for one whole cycle including both bleaching and colouring (Jelle and Hagen 1993, Jelle and Hagen 1994, Jelle et al. 1998).

The memory of ECWs, i.e. the ability to maintain the bleached and coloured states without any applied voltage, is another important property. However, the lower the required energy consumption for intended bleaching and colouring, the less important is the memory of the ECWs. Jelle and Hagen (1994, 1999b) present memory experiments for ECWs based on PANI and WO$_3$ and based on PANI, PB and WO$_3$.

Switching times, i.e. bleaching and colouring times, are also crucial properties for ECWs. The shorter switching times, the better. Nevertheless, for ECW applications switching times of some minutes may be acceptable. Typical switching times for the ECWs discussed in this work are in the order of half a minute, although repeated cycling may increase the switching time to several minutes (Jelle et al. 1993b, Jelle and Hagen 1993, Jelle and Hagen 1994). However, for display applications, switching times considerably shorter than a second may be required.

7.6.5. Durability

A satisfactory durability of ECWs is crucial. The durability comprises:

- Climate exposure durability.
- Cycling durability.
- Elapsed time durability.

Climate exposure durability covers resistance towards various climate exposure factors the ECWs may be subjected to during their lifetime, including the production, transport, installation and operational period until planned demolition. In general, these climate exposure factors are solar radiation (i.e. ultraviolet (UV), visible (VIS) and near infrared (NIR) radiation), ambient infrared (IR) heat radiation (the resulting elevated temperature increases the rate of chemical degradation reactions, and also the rate of growth of rot and fungus up to limiting temperatures), high and low temperatures, temperature changes/cycles (relative temperature movements between different materials, number of freezing point passes during freezing/thawing), water (e.g. moisture, relative air humidity, rain (precipitation) and wind-driven rain), physical strains (e.g. snow loads), wind, erosion (also from above factors), pollutions (e.g. gases and particles in air), microorganisms, oxygen, and time (determining the effect for all the factors above to work). For a general overview of these climate strains and the role of accelerated climate ageing of building materials, components and structures in the laboratory, including new materials and solutions, it is referred to the work by Jelle et al. (2012c) and Jelle (2012).

Cycling durability covers the ability of the ECWs to be cycled (or stepped) back and forth between various colouration levels, i.e. highly transparent and very dark coloured states, during bleaching and colouring of the ECWs, without any significant degradation. The highest number of complete cycles (from transparent to coloured and then back to transparent state) for typical ECWs based on PANI, PB and WO_3 as reported herein was 3745 cycles (52 days), then with a significantly increased switching time, especially the colouring time (Jelle and Hagen 1993). Note that in the available literature there are also reported much longer cycling lifetimes, e.g. 10^7 cycles at 22°C and $5 \cdot 10^6$ cycles at 50°C without any failure detection for an ECW based on WO_3 and a solid polymer electrolyte (PAMPS) (Lampert 1989).

Elapsed time durability addresses the ECWs durability performance with respect to elapsed time independent of any external strains, i.e. including the durability during no climate exposure and no applied voltage (no cycling), often termed the shelf-life of ECWs and other devices.

The studies by Czanderna et al. (1999), Lampert (1989), Lampert et al. (1999), Nagai et al. (1999), Tajima et al. (2012) and Tracy et al. (1999) investigate miscellaneous ageing and

durability issues concerning ECWs, where also general considerations and several specific ECW configurations are treated.

7.6.6. Electrochromic Window Configuration

In principle, an ECW normally consists of an electrochromic (EC) material or coating, an ionic conductor (IC) and a counter electrode (CE) interposed between two glass panes each with a transparent conductor (TC). By applying a voltage over the two transparent conductors, ions will go through the ionic conductor between the electrochromic coating and the counter electrode, and thereby change the colour of the electrochromic layer. The counter electrode acts as an ion storage, supplying the necessary ions for the electrochromic reaction, which, via the ionic conductor, are injected into or withdrawn from the electrochromic layer depending on the polarity of the applied voltage. The counter electrode may also have electrochromic properties complementary to the electrochromic coating (CE = EC*), thus enhancing the colour changes (Jelle 1993). Such a synergetic complementary electrochromic material pair is sometimes called a *rocking chair* configuration (Armand 1980, Passerini 1990, Pietro et al. 1982).

Naturally, the properties of all these layers and their interactions have to optimized. The ionic conductor should have a low electrical conductivity and a high ionic conductivity in order to prevent loss of electrons (short circuit) and to obtain satisfactory fast bleaching and colouring times. Transparent ionic conductors are required for use in electrochromic windows, and solid state ionic conductors are preferred before liquid ones. As the name indicates, the transparent conductor has to provide both a high transparency and a high electrical conductivity, i.e. a low electrical surface resistance. A lower electrical surface resistance for a specific material is obtained by increasing the thickness of the transparent conductor, which unfortunately in turn is decreasing the transparency. An obvious requirement for window applications, is that the electrochromic material has to have a clear and transparent state, which is not required in display devices. In addition to the solar energy regulation of ECWs, on may also exploit the visible colour changes in an architectural way, i.e. so-called *fancy windows* as introduced by Jelle and Hagen (1993, 1994).

7.6.7. Reflectance Induced Limitations

Reflection of solar radiation from each air/glass interface places limitations to how transparent a glass and window pane configuration may become, and hence also limits the total solar radiation modulation potential of ECWs. The solar radiation is reflected at every boundary, and is dependent upon the refractive indices n_1 and n_2 for the ambient and substrate medium, respectively. For normal incidence and in a spectral range where the absorbance is low, the reflectance is given by the following expression (Gale 1988, Hecht 1987, Jastrzebski 1987):

$$R \approx \frac{(n_2 - n_1)^2}{(n_2 + n_1)^2} \tag{119}$$

Setting $n_1 = 1$ for air and $n_2 = 1.5$ for glass (typical), we obtain R = 0.04, i.e. 4 % of the radiation is reflected at each air/glass and glass/air interface. Hence, the maximum transmittance through a single glass pane (two air/glass interfaces) becomes 92 %, and in fact as low as about 84 % for a two-layer window pane configuration (with air between the two glass panes). For normal incidence and low absorbance, the transmittance may be written as (Hecht 1987):

$$T \approx \frac{4n_2 n_1}{(n_2 + n_1)^2} \qquad (120)$$

Applying $n_1 = 1$ for air and $n_2 = 1.5$ for glass again and inserting in Eq.120, a transmittance of 96 % is obtained, which is in agreement with the results from Eq.119 above (assuming normal incidence and low absorbance). These results clearly demonstrates the limitations to achieve as large transmittance (and transparency) as possible in windows in general and in ECWs in particular, especially when applying several glass panes.

8.   Commercial Electrochromic Windows and the Path Ahead

Commercial electrochromic windows (ECW) are already available from several manufacturers. A comprehensive state-of-the-art review of these commercial ECWs is given in the work by Baetens et al. (2010a), depicting various properties and among them several important solar radiation glazing factors. Furthermore, a review on fenestration products of today and tomorrow, including ECWs, is given by Jelle et al. (2012a). Materials exhibiting both photovoltaic and electrochromic properties may be envisioned, manufactured and applied, or various combinations of building integrated photovoltaic products like solar cell glazing with electrochromic materials. However, a window still needs a transparent (in some cases translucent) state, and when in the transparent state such a photovoltaic window can not produce electricity from the visible part of the solar spectrum as the visible light is transmitted through the window, i.e. one single photon at a specific wavelength can not be used simultaneously for both electricity generation and daylighting. Nevertheless, other parts of the solar radiation (ultraviolet and near infrared) may still in principle be exploited in the transparent state. Furthermore, in the coloured state all the solar radiation including the visible part may be utilized.

Unfortunately, as stated by Jelle et al. (2012ab), it is often hard to obtain all the desired information concerning the commercial product properties from all the manufacturers. In general, many property values are often not available at the manufacturers' websites or other open information channels, including the solar radiation glazing factors. Hopefully, the addressing of this fact in these studies could act as an incentive for the manufacturers to state all the important properties of their products at their websites and other information channels, and also as an incentive and reminder for the contractors, consumers and users to demand these values from the respective manufacturers.

In addition to the solar radiation glazing factors, and with regard to increased application of ECWs in the years ahead, it should be stressed that the durability of commercial ECWs is essential. The durability of ECWs should therefore be rigorously tested and characterized with respect to (a) climate exposure durability, (b) cycling durability and (c) elapsed time durability. Hence, the durability of ECWs should also be stated by the manufacturers.

As discussed earlier herein (see e.g. Figs.4-6) and noted by Jelle et al. (2012a), as today's commercial and almost all research ECWs are solar radiation absorbing ECWs, research carried out on reflecting ECWs may pay off as these have a large potential in solar energy control. Reflecting ECWs avoid any heating problems that absorbing ECWs may be subjected to. Furthermore, reflecting ECWs may in principle regulate more of the solar energy as these windows block off the solar radiation by reflecting it back towards the outside, while absorbing ECWs reemit the absorbed solar radiation in all directions both towards the outside and towards the inside, the latter process hence decreasing the overall solar energy regulation for absorbing ECWs.

Finally, a lowered ECW cost and increased awareness of potential savings and enhanced indoor comfort would contribute to facilitate the application of ECWs in the buildings of tomorrow, also with respect to retrofitting of existing buildings.

9. Increased Application of Solar Radiation Glazing Factors

As of today miscellaneous window panes, glass structures and electrochromic windows are applied in buildings for various specific purposes and with different desired levels for solar radiation transmittance, absorbance and reflectance, and new glass products are continuously emerging on the market. However, all too often the various glass products have not been characterized by the solar radiation glazing factors. And if some products have been characterized to some extent, often they have not been characterized sufficiently or satisfactorily with respect to the comprehensive characterization the solar radiation glazing factors represent.

The solar radiation glazing factors represent a comprehensive, versatile and valuable characterization method of glass products, also including various two-layer and three-layer window pane structures, giving a set of specific and crucial parameters for the glass products with regard to transmittance, absorbance and reflectance of solar radiation in selected wavelength areas and in addition with respect to the protection level of materials and human skin. Hence, in order to be able to evaluate and choose the most appropriate and suitable glass material or product for the specific building application, the desire and demand for available solar radiation glazing factors are believed to increase. This is important with respect to daylight, solar energy aspects and protection of materials inside buildings. The dynamic solar radiation control enabled by electrochromic windows or other smart windows may readily and beneficially be characterized by spectroscopical measurements and subsequent calculations of the solar radiation glazing factors.

10. Conclusions

Solar radiation glazing factors, i.e. ultraviolet solar transmittance, visible solar transmittance, solar transmittance, solar material protection factor, solar skin protection factor, external visible solar reflectance, internal visible solar reflectance, solar reflectance, solar absorbance, emissivity, solar factor and colour rendering factor, characterize window panes, glass structures and electrochromic windows in buildings. These factors may readily be compared for different glass fabrications in order to select the most appropriate glass material for the specific building application. Spectroscopical measurements and corresponding calculations of the solar radiation glazing factors were performed on various glass materials, three electrochromic windows and several two-layer and three-layer window pane configurations.

Acknowledgements

References

N. Adami, D. Fazzi, A. Bianco, C. Bertarelli and C. Castiglioni, "Enhancing the light driven modulation of the refractive index in organic photochromic materials: A quantum chemical strategy", *Journal of Photochemistry and Photobiology A: Chemistry*, **214**, 61-68, 2010.

K.-S. Ahn, S.J. Yoo, M.-S. Kang, J.-W. Lee and Y.-E. Sung, "Tandem dye-sensitized solar cell-powered electrochromic devices for the photovoltaic-powered smart window", *Journal of Power Sources*, **168**, 533-536, 2007.

S.N. Alamri, "The temperature behavior of smart windows under direct solar radiation", *Solar Energy Materials and Solar Cells*, **93**, 1657-1662, 2009.

A. Anders, J.L. Slack and T.J. Richardson, "Electrochromically switched, gas-reservoir metal hydride devices with application to energy-efficient windows", *Thin Solid Films*, **517**, 1021-1026, 2008.

A.M. Andersson, A. Talledo, C.G. Granqvist and J.R. Stevens, "Electrochromic coatings and devices for large-area transmittance control", in *Electrochromic Materials* (PV 90-2), M.K. Carpenter and D.A. Corrigan (eds.), pp. 261-273, *Proceedings of the Symposium on Electrochromic Materials, The 176th Meeting of The Electrochemical Society*, Hollywood, Florida, U.S.A., 16-18 October, 1989, The Electrochemical Society, Pennington, NJ, 1990.

M.B. Armand, "Intercalation electrodes", in *Materials for Advanced Batteries*, D.W. Murphy, J. Broadhead and B.C.H. Steele (eds.), pp. 145-161, Plenum Press, New York, 1980.

P.V. Ashrit, K. Benaissa, G. Bader, F.E. Girouard and V.V. Truong, "All-solid electrochromic system for smart window application", *Proceedings of SPIE - Optical Materials Technology for Energy Efficiency and Solar Energy Conversion XI*, A. Hugot-Le Goff, C.G. Granqvist and C.M. Lampert (eds.), Toulouse-Labege, France, 19 May, 1992, Vol. 1728, pp. 232-240, The Society of Photo-Optical Instrumentation Engineers, Bellingham, Washington, U.S.A., 1992.

ASTM E 179-81, "Standard practice for selection of geometric conditions for measurement of reflectance and transmittance", 1981.

ASTM E 1585-93, "Standard test method for measuring and calculating emittance of architectural flat glass products using spectrometric measurements", 1993.

A. Azens, E. Avendaño, J. Backholm, L. Berggren, G. Gustavsson, R. Karmhag, G.A. Niklasson, A. Roos and C.G. Granqvist, "Flexible foils with electrochromic coatings: Science, technology and applications", *Materials Science and Engineering B*, **119**, 214-223, 2005.

R. Baetens, B.P. Jelle and A. Gustavsen, "Properties, requirements and possibilities of smart windows for dynamic daylight and solar energy control in buildings: A state-of-the-art review", *Solar Energy Materials and Solar Cells*, **94**, 87-105, 2010(a).

R. Baetens, B.P. Jelle, J.V. Thue, M.J. Tenpierik, S. Grynning, S. Uvsløkk and A. Gustavsen, "Vacuum insulation panels for building applications: A review and beyond", *Energy and Buildings*, **42**, 147-172, 2010(b).

R. Baetens, B.P. Jelle and A. Gustavsen, "Aerogel insulation for building applications: A state-of-the-art review", *Energy and Buildings*, **43**, 761-769, 2011.

D.N. Batchelder, "Colour and chromism of conjugated polymers", *Contemporary Physics*, **29**, 3-31, 1988.

G. Beni and J.L. Shay, "Ion-insertion electrochromic displays", in *Image Pickup and Display*, B. Kazan (ed.), Vol. 5, pp. 83-136, Academic Press, 1982.

S. Bhadra, D. Khastgir, N.K. Singha and J.H. Lee, "Progress in preparation, processing and applications of polyaniline", *Progress in Polymer Science*, **34**, 783-810, 2009.

I. Bouessay, A. Rougier, B. Beaudoin and J.B. Leriche, "Pulsed laser-deposited nickel oxide thin films as electrochromic anodic materials", *Applied Surface Science*, **186**, 490-495, 2002.

C. Breivik, B.P. Jelle, B. Time, Ø. Holmberget, J. Nygård, E. Bergheim and A. Dalehaug, "Large-scale experimental wind-driven rain exposure investigations of building integrated photovoltaics", *Solar Energy*, **90**, 179-187, 2013.

J.N. Bullock, C. Bechinger, D.K. Benson and H.M. Branz, "Semi-transparent a-SiC:H solar cells for self-powered photovoltaic-electrochromic devices", *Journal of Non-Crystalline Solids*, **198-200**, 1163-1167, 1996.

M.K. Carpenter, R.S. Conell and D.A. Corrigan, "The electrochromic properties of hydrous nickel oxide", *Solar Energy Materials*, **16**, 333-346, 1987.

M.K. Carpenter and R.S. Conell, "A single-film electrochromic device", *Journal of Electrochemical Society*, **137**, 2464-2467, 1990.

C.-Y. Chen and Y.-L. Lo, "Integration of a-Si:H solar cell with novel twist nematic liquid crystal cell for adjustable brightness and enhanced power characteristics", *Solar Energy Materials and Solar Cells*, **93**, 1268-1275, 2009.

K.-C. Chen, C.-Y. Hsu, C.-W. Hu and K.-C. Ho, "A complementary electrochromic device based on prussian blue and poly(ProDOT-Et$_2$) with high contrast and high coloration efficiency", *Solar Energy Materials and Solar Cells*, **95**, 2238-2245, 2011.

Z. Chen, Y. Gao, L. Kang, J. Du, Z. Zhang, H. Luo, H. Miao and G. Tan, "VO$_2$-based double-layered films for smart windows: Optical design, all-solution preparation and improved properties", *Solar Energy Materials and Solar Cells*, **95**, 2677-2684, 2011.

J.-C. Chiang and A.G. MacDiarmid, "'Polyaniline': Protonic acid doping of the emeraldine form to the metallic regime", *Synthetic Metals*, **13**, 193-205, 1986.

CIE No 89/3:1990, "On the deterioration of exhibited museum objects by optical radiation", 1990.

S.F. Cogan, T.D. Plante, M.A. Parker and R.D. Rauh, "Electrochromic solar attenuation in crystalline and amorphous Li$_x$WO$_3$", *Solar Energy Materials*, **14**, 185-193, 1986.

S.F. Cogan, R.D. Rauh, T.D. Plante, N.M. Nguyen and J.D. Westwood, "Morphology and electrochromic properties of V$_2$O$_5$ films", in *Electrochromic Materials* (PV 90-2), M.K. Carpenter and D.A. Corrigan (eds.), pp. 99-115, *Proceedings of the Symposium on*

Electrochromic Materials, The 176th Meeting of The Electrochemical Society, Hollywood, Florida, U.S.A., 16-18 October, 1989, The Electrochemical Society, Pennington, NJ, 1990.

S.I. Córdoba de Torresi, A. Gorenstein, R.M. Torresi and M.V. Vázquez, "Electrochromism of WO_3 in acid solutions. An electrochemical, optical and electrogravimetric study", *Journal of Electroanalytical Chemistry*, **318**, 131-144, 1991.

S.I. Córdoba de Torresi and A. Gorenstein, "Electrochromic behaviour of manganese dioxide electrodes in slightly alkaline solutions", *Electrochimica Acta*, **37**, 2015-2019, 1992.

CRC Handbook of Chemistry and Physics 1989-1990, R.C. Weast, D.R. Lide, M.J. Astle, W.H. Beyer (Eds.), 70th Ed., CRC Press, Boca Raton, Florida, p. F-167, 1989-1990.

S.G. Croll and A.D. Skaja, "Quantitative spectroscopy to determine the effects of photodegradation on a model polyester-urethane coating", *Journal of Coatings Technology*, **75**, 85-94, 2003.

D. Cupelli, F.P. Nicoletta, S. Manfredi, G. De Filpo and G. Chidichimo, "Electrically switchable chromogenic materials for external glazing", *Solar Energy Materials and Solar Cells*, **93**, 329-333, 2009.

A.W. Czanderna, D.K. Benson, G.J. Jorgensen, J.-G. Zhang, C.E. Tracy and S.K. Deb, "Durability issues and service lifetime prediction of electrochromic windows for buildings applications", *Solar Energy Materials and Solar Cells*, **56**, 419-436, 1999.

M.G. Davies, "Building heat transfer", John Wiley & Sons, 2004.

S.K. Deb, S.-H. Lee, C.E. Tracy, J.R. Pitts, B.A. Gregg and H.M. Branz, "Stand-alone photovoltaic-powered electrochromic smart window", *Electrochimica Acta*, **46**, 2125-2130, 2001.

S.K. Deb, "Opportunities and challenges in science and technology of WO_3 for electrochromic and related applications", *Solar Energy Materials and Solar Cells*, **92**, 245-258, 2008.

B. Di Pietro, M. Patriarca and B. Scrosati, "On the use of rocking chair configurations for cyclable lithium organic electrolyte batteries", *Journal of Power Sources*, **8**, 289-299, 1982.

EN 410:1998 E, "Glass in building - Determination of luminous and solar characteristics of glazing", 1998.

EN 673:1997 E, "Glass in building - Determination of thermal transmittance (U value) - Calculation method", 1997.

EN 674:1997 E, "Glass in building - Determination of thermal transmittance (U value) - Guarded hot plate method", 1997.

EN 675:1997-E, "Glass in building - Determination of thermal transmittance (U value) - Heat flow meter method", 1997.

EN 1946-2:1999 E, "Thermal performance of building products and components - Specific criteria for the assessment of laboratories measuring heat transfer properties - Part 2: Measurements by guarded hot plate method", 1999.

EN 1946-3:1999 E, ”Thermal performance of building products and components - Specific criteria for the assessment of laboratories measuring heat transfer properties - Part 3: Measurements by heat flow meter method”, 1999.

EN 1946-4:2000 E, ”Thermal performance of building products and components - Specific criteria for the assessment of laboratories measuring heat transfer properties - Part 4: Measurements by hot box methods”, 2000.

EN 12898:2001 E, ”Glass in building - Determination of the emissivity”, 2001.

EN-ISO 6946:1996, ”Building components and building elements. Thermal resistance and thermal transmittance. Calculation method”, 1996.

A.L. Fahrenbruch and R.H. Bube, ”Fundamentals of solar cells. Photovoltaic solar energy conversion”, pp. 26-31, Academic Press, 1983.

M. Fantini and A. Gorenstein, ”Electrochromic nickel hydroxide films on transparent / conducting substrates”, *Solar Energy Materials*, **16**, 487-500, 1987.

B.W. Faughnan and R.S. Crandall, ”Electrochromic displays based on WO_3”, in *Display Devices*, J.I. Pankove (ed.), Topics in Applied Physics, Vol. 40, pp. 181-211, Springer-Verlag, 1980.

R. Flavell and C. Smale, ”Studio glassmaking”, Van Nostrand Reinhold Company, 1974.

S.M. Fufa, B.P. Jelle, P.J. Hovde and P.M. Rørvik, ”Coated wooden claddings and the influence of nanoparticles on the weathering performance”, *Progress in Organic Coatings*, **75**, 72-78, 2012.

R.J. Gale, ”Spectroelectrochemistry. Theory and practice”, pp. 193-205, Plenum Press, 1988.

L.-P. Gao, G.-J. Ding, Y.-C. Wang and Y.-L. Yang, ”Preparation of UV curing crosslinked polyviologen film and its photochromic and electrochromic performances”, *Applied Surface Science*, **258**, 1184-1191, 2011.

T. Gao, L.I.C. Sandberg, B.P. Jelle and A. Gustavsen,”Nano insulation materials for energy efficient buildings: A case study on hollow silica nanospheres”, in *Fuelling the Future: Advances in Science and Technologies for Energy Generation, Transmission and Storage*, A. Mendez-Vilas (ed.), BrownWalker Press, pp. 535-539, 2012.

T. Gao, B.P. Jelle, L.I. Sandberg and A. Gustavsen, ”Monodisperse hollow silica nanospheres for nano insulation materials: Synthesis, characterization, and life cycle assessment”, *ACS Applied Materials and Interfaces*, **5**, 761-767, 2013.

W. Gao, S.H. Lee, J. Bullock, Y. Xu, D.K. Benson, S. Morrison and H.M. Branz, ”First a-SiC : H photovoltaic-powered monolithic tandem electrochromic smart window device”, *Solar Energy Materials and Solar Cells*, **59**, 243-254, 1999.

D.J. Gardiner, S.M. Morris and H.J. Coles, ”High-efficiency multistable switchable glazing using smectic A liquid crystals”, *Solar Energy Materials and Solar Cells*, **93**, 301-306, 2009.

E.M. Geniès, A. Boule, M. Lapkowski and C. Tsintavis, "Polyaniline: A historical survey", *Synthetic Metals*, **36**, 139-182, 1990.

A. Georg, W. Graf, D. Schweiger, V. Wittwer, P. Nitz and H.R. Wilson, "Switchable glazing with a large dynamic range in total solar energy transmittance (TSET)", *Solar Energy*, **62**, 215-228, 1998.

J.L. Gerlock, C.A. Smith, V.A. Cooper, T.G. Dusbiber and W.H. Weber, "On the use of Fourier transform infrared spectroscopy and ultraviolet spectroscopy to assess the weathering performance of isolated clearcoats from different chemical families", *Polymer Degradation and Stability*, **62**, 225-234, 1998.

R.B. Goldner, D.H. Mendelsohn, J. Alexander, W.R. Henderson, D. Fitzpatrick, T.E. Haas, H.H. Sample, R.D. Rauh, M.A. Parker and T.L. Rose, "High near-infrared reflectivity modulation with polycrystalline electrochromic WO_3 films", *Applied Physics Letters*, **43**, 1093-1095, 1983.

R.B. Goldner and R.D. Rauh, "Electrochromic materials for controlled radiant energy transfer in buildings", *Solar Energy Materials*, **11**, 177-185, 1984.

R.B. Goldner, A. Brofos, G. Foley, E.L. Goldner, T.E. Haas, W. Henderson, P. Norton, B.A. Ratnam, N. Weis and K.K. Wong, "Optical frequencies free electron scattering studies on electrochromic materials for variable reflectivity windows", *Solar Energy Materials*, **12**, 403-410, 1985.

R.B. Goldner, R.I. Chapman, G. Foley, E.L. Goldner, T. Haas, P. Norton, G. Seward and K.K. Wong, "Recent research related to the development of electrochromic windows", *Solar Energy Materials*, **14**, 195-203, 1986.

R.B. Goldner, K. Wong, G. Foley, P. Norton, L. Wamboldt, G. Seward, T. Haas and R. Chapman, "Thin films for practical electrochromic windows", *Solar Energy Materials*, **16**, 365-370, 1987.

R.B. Goldner, T.E. Haas, G. Seward, K.K. Wong, P. Norton, G. Foley, G. Berera, G. Wei, S. Schulz and R. Chapman, "Thin film solid state ionic materials for electrochromic smart window glass", *Solid State Ionics*, **28-30**, 1715-1721, 1988.

R.B. Goldner, G. Seward, K. Wong, T. Haas, G.H. Foley, R. Chapman and S. Schulz, "Completely solid lithiated smart windows", *Solar Energy Materials*, **19**, 17-26, 1989.

R.B. Goldner, G. Berera, F.O. Arntz, T.E. Haas, B. Morel and K.K. Wong, "Reflectance modulation with electrochromic Li_xWO_3 films", in *Electrochromic Materials* (PV 90-2), M.K. Carpenter and D.A. Corrigan (eds.), pp. 14-22, *Proceedings of the Symposium on Electrochromic Materials, The 176th Meeting of The Electrochemical Society*, Hollywood, Florida, U.S.A., 16-18 October, 1989, The Electrochemical Society, Pennington, NJ, 1990.

R.B. Goldner, F.O. Arntz, G. Berera, T.E. Haas, G. Wei, K.K. Wong and P.C. Yu, "A monolithic thin-film electrochromic window", *Solid State Ionics*, **53-56**, 617-627, 1992.

C.G. Granqvist, "Radiative heating and cooling with spectrally selective surfaces", *Applied Optics*, **20**, 2606-2615, 1981.

C.G. Granqvist, "Spectrally selective surface coatings for energy efficiency and solar applications", *The Physics Teacher*, **22**, 372-383, September 1984.

C.G. Granqvist, "Energy-efficient windows: Options with present and forthcoming technology", in *Electricity. Efficient End-Use and New Generation Technologies, and their Planning Implications*, T.B. Johansson, B. Bodlund and R.H. Williams (eds.), pp. 89-123, Lund University Press, 1989.

C.G. Granqvist, "Energy-efficient windows: Present and forthcoming technology", in *Materials Science for Solar Energy Conversion Systems*, C.G. Granqvist (ed.), pp. 106-167, Pergamon Press, 1991.

C.G. Granqvist, "Electrochromics and smart windows", *Solid State Ionics*, **60**, 213-214, 1993.

C.G. Granqvist, "Handbook of inorganic electrochromic materials", Elsevier, Amsterdam, 1995.

C.G. Granqvist, A. Azens, J. Isidorsson, M. Kharrazi, L. Kullman, T. Lindström, G.A. Niklasson, C.-G. Ribbing, D. Rönnow, M.S. Mattsson and M. Veszelei, "Towards the smart window: Progress in electrochromics", *Journal of Non-Crystalline Solids*, **218**, 273-279, 1997.

C.G. Granqvist, "Electrochromic tungsten oxide films: Review of progress 1993-1998", *Solar Energy Materials and Solar Cells*, **60**, 201-262, 2000.

C.G. Granqvist, E. Avendaño and A. Azens, "Electrochromic coatings and devices: Survey of some recent advances", *Thin Solid Films*, **442**, 201-211, 2003.

C.G. Granqvist, "Electrochromic devices", *Journal of the European Ceramic Society*, **25**, 2907-2912, 2005.

C.G. Granqvist, "Transparent conductors as solar energy materials: A panoramic review", *Solar Energy Materials and Solar Cells*, **91**, 1529-1598, 2007.

C.G. Granqvist, "Oxide electrochromics: Why, how, and whither", *Solar Energy Materials and Solar Cells*, **92**, 203-208, 2008.

C.G. Granqvist, S. Green, G.A. Niklasson, N.R. Mlyuka, S. von Kræmer and P. Georén, "Advances in chromogenic materials and devices", *Thin Solid Films*, **518**, 3046-3053, 2010.

C.G. Granqvist, "Oxide electrochromics: An introduction to devices and materials", *Solar Energy Materials and Solar Cells*, **99**, 1-13, 2012.

S.V. Green, E. Pehlivan, C.G. Granqvist and G.A. Niklasson, "Electrochromism in sputter deposited nickel-containing tungsten oxide films", *Solar Energy Materials and Solar Cells*, **99**, 339-344, 2012(a).

S.V. Green, M. Watanabe, N. Oka, G.A. Niklasson, C.G. Granqvist and Y. Shigesato, "Electrochromic properties of nickel oxide based thin films sputter deposited in the presence of water vapor", *Thin Solid Films*, **520**, 3839-3842, 2012(b).

S. Grynning, A. Gustavsen, B. Time and B.P. Jelle, "Windows in the buildings of tomorrow: Energy losers or energy Gainers?", *Energy and Buildings*, **61**, 185-192, 2013.

A. Gustavsen, B.P. Jelle, D. Arasteh and C. Kohler, "State-of-the-art highly insulating window frames – Research and market review", Project report 6, SINTEF Building and Infrastructure, 2007.

A. Gustavsen, D. Arasteh, B.P. Jelle, C. Curcija and C. Kohler, "Developing low-conductance window frames: Capabilities and limitations of current window heat-transfer design tools", *Journal of Building Physics*, **32**, 131-153, 2008.

A. Gustavsen, S. Grynning, D. Arasteh, B.P. Jelle and H. Goudey, "Key elements of and materials performance targets for highly insulating window frames", *Energy and Buildings*, **43**, 2583-2594, 2011.

I. Hamberg and C.G. Granqvist, "Optical properties of transparent and heat-reflecting indium tin oxide films: The role of ionized impurity scattering", *Applied Physics Letters*, **44**, 721-723, 1984(a).

I. Hamberg and C.G. Granqvist, "Optical properties of transparent and heat-reflecting indium-tin-oxide films: Experimental data and theoretical analysis", *Solar Energy Materials*, **11**, 239-248, 1984(b).

E. Hecht, "Optics", 2nd ed., pp. 112, Addison-Wesley, 1987.

R. Huang, Y. Shen, L. Zhao and M. Yan, "Effect of hydrothermal temperature on structure and photochromic properties of WO_3 powder", *Advanced Powder Technology*, **23**, 211-214, 2012.

W.-S. Huang, B.D. Humphrey and A.G. MacDiarmid, "Polyaniline, a novel conducting polymer. Morphology and chemistry of its oxidation and reduction in aqueous electrolytes", *Journal of the Chemical Society, Faraday Transactions 1: Physical Chemistry in Condensed Phases*, **82**, 2385-2400, 1986.

ISO 8301:1991(E), "Thermal insulation - Determination of steady-state thermal resistance and related properties - Heat flow meter apparatus", 1991.

ISO 8302:1991(E), "Thermal insulation - Determination of steady-state thermal resistance and related properties - Guarded hot plate apparatus", 1991.

ISO/DIS 9050:2001, "Glass in building - Determination of light transmittance, solar direct transmittance, total solar energy transmittance, ultraviolet transmittance and related glazing factors", 2001.

ISO 9050:2003(E), "Glass in building - Determination of light transmittance, solar direct transmittance, total solar energy transmittance, ultraviolet transmittance and related glazing factors", 2003.

ISO 9845-1:1992(E), "Solar Energy - Reference solar spectral irradiance at the ground at different receiving conditions - Part 1: Direct normal and hemispherical solar irradiance for air mass 1.5", 1992.

ISO 10291:1994(E), "Glass in building - Determination of steady-state U values (thermal transmittance) of multiple glazing - Guarded hot plate method", 1994.

ISO 10292:1994(E), "Glass in building - Calculation of steady-state U values (thermal transmittance) of multiple glazing", 1994.

ISO 10293:1997(E), "Glass in building - Determination of steady-state U values (thermal transmittance) of multiple glazing - Heat flow meter method", 1997.

ISO 10526:1999(E), "CIE standard illuminants for colorimetry", 1999.

ISO/CIE 10527:1991(E), "CIE standard illuminants for colorimetry", 1991.

Z.D. Jastrzebski, "The nature and properties of engineering materials", 3rd ed., pp. 464-468, John Wiley & Sons, 1987.

B.P. Jelle, G. Hagen, S.M. Hesjevik and R. Ødegård, "Transmission through an electrochromic window based on polyaniline, tungsten oxide and a solid polymer electrolyte", *Materials Science and Engineering B*, **13**, 239-241, 1992(a).

B.P. Jelle, G. Hagen and R. Ødegård, "Transmission spectra of an electrochromic window based on polyaniline, tungsten oxide and a solid polymer electrolyte", *Electrochimica Acta*, **37**, 1377-1380, 1992(b).

B.P. Jelle, G. Hagen, S. Sunde and R. Ødegård, "Dynamic light modulation in an electrochromic window consisting of polyaniline, tungsten oxide and a solid polymer electrolyte", *Synthetic Metals*, **54**, 315-320, 1993(a).

B.P. Jelle, G. Hagen and S. Nødland, "Transmission spectra of an electrochromic window consisting of polyaniline, prussian blue and tungsten oxide", *Electrochimica Acta*, **38**, 1497-1500, 1993(b).

B.P. Jelle, G. Hagen, S.M. Hesjevik and R. Ødegård, "Reduction factor for polyaniline films on ITO from cyclic voltammetry and visible absorption spectra", *Electrochimica Acta*, **38**, 1643-1647, 1993(c).

B.P. Jelle and G. Hagen, "Transmission spectra of an electrochromic window based on polyaniline, prussian blue and tungsten oxide", *Journal of Electrochemical Society*, **140**, 3560-3564, 1993.

B.P. Jelle, "Electrochemical and spectroscopic studies of electrochromic materials", *Ph.D. thesis*, 1993:131, Department of Applied Electrochemistry, The Norwegian Institute of Technology, Trondheim, Norway, 1993.

B. P. Jelle and G. Hagen, "Solar modulation in an electrochromic window using polyaniline, prussian blue and tungsten oxide", in *Electrochromic Materials II*, (PV 94-2), K. C. Ho and D. A. MacArthur (eds.), pp. 324-338, *Proceedings of the Symposium on Electrochromic Materials, The 184th Meeting of The Electrochemical Society*, New Orleans, Louisiana, U.S.A., 10-15 October, 1993, The Electrochemical Society, Pennington, NJ, 1994.

B.P. Jelle, G. Hagen and Ø. Birketveit, "Transmission properties for individual electrochromic layers in solid state devices based on polyaniline, prussian blue and tungsten oxide", *Journal of Applied Electrochemistry*, **28**, 483-489, 1998.

B.P. Jelle and G. Hagen, "Electrochemical multilayer deposition of polyaniline and prussian blue and their application in solid state electrochromic windows", *Journal of Applied Electrochemistry*, **28**, 1061-1065, 1998.

B.P. Jelle and G. Hagen, "Performance of an electrochromic window based on polyaniline, prussian blue and tungsten oxide", *Solar Energy Materials and Solar Cells*, **58**, 277-286, 1999(a).

B.P. Jelle and G. Hagen, "Correlation between light absorption and electric charge in solid state electrochromic windows", *Journal of Applied Electrochemistry*, **29**, 1103-1110, 1999(b).

B.P. Jelle, A. Gustavsen, T.-N. Nilsen and T. Jacobsen, "Solar material protection factor (SMPF) and solar skin protection factor (SSPF) for window panes and other glass structures in buildings", *Solar Energy Materials and Solar Cells*, **91**, 342-354, 2007.

B.P. Jelle, A. Gustavsen and R. Baetens, "Beyond vacuum insulation panels - How may it be achieved?", *Proceedings of the 9th International Vacuum Insulation Symposium (IVIS 2009)*, London, England, 17-18 September, 2009.

B.P. Jelle, A. Gustavsen and R. Baetens, "The path to the high performance thermal building insulation materials and solutions of tomorrow", *Journal of Building Physics*, **34**, 99-123, 2010.

B.P. Jelle and T.-N. Nilsen, "Comparison of accelerated climate ageing methods of polymer building materials by attenuated total reflectance Fourier transform infrared radiation spectroscopy", *Construction and Building Materials*, **25**, 2122-2132, 2011.

B.P. Jelle, "Traditional, state-of-the-art and future thermal building insulation materials and solutions - Properties, requirements and possibilities", *Energy and Buildings*, **43**, 2549-2563, 2011.

B.P. Jelle, A. Hynd, A. Gustavsen, D. Arasteh, H. Goudey and R. Hart, "Fenestration of today and tomorrow: A state-of-the-art review and future research opportunities", *Solar Energy Materials and Solar Cells*, **96**, 1-28, 2012(a).

B.P. Jelle, C. Breivik and H.D. Røkenes, "Building integrated photovoltaic products: A state-of-the-art review and future research opportunities", *Solar Energy Materials and Solar Cells*, **100**, 69-96, 2012(b).

B.P. Jelle, T.-N. Nilsen, P.J. Hovde and A. Gustavsen, "Accelerated climate aging of building materials and their characterization by Fourier transform infrared radiation analysis", *Journal of Building Physics*, **36**, 99-112, 2012(c).

B.P. Jelle and C. Breivik, "State-of-the-art building integrated photovoltaics", *Energy Procedia*, **20**, 68-77, 2012(a).

B.P. Jelle and C. Breivik, "The path to the building integrated photovoltaics of tomorrow", *Energy Procedia*, **20**, 78-87, 2012(b).

B.P. Jelle, "Accelerated climate ageing of building materials, components and structures in the laboratory", *Journal of Materials Science*, **47**, 6475-6496, 2012.

A. Jonsson and A. Roos, "Evaluation of control strategies for different smart window combinations using computer simulations", *Solar Energy*, **84**, 1-9, 2010.

S.S. Kalagi, S.S. Mali, D.S. Dalavi, A.I. Inamdar, H. Im and P.S. Patil, "Limitations of dual and complementary inorganic-organic electrochromic device for smart window application and its colorimetric analysis", *Synthetic Metals*, **161**, 1105-1112, 2011.

A. Karuppasamy and Subrahmanyam, "Studies on electrochromic smart windows based on titanium doped WO_3 thin films", *Thin Solid Films*, **516**, 175-178, 2007.

K.I. Kimura, "Scientific basis of air conditioning", pp. 99-105, Applied Science Publishers, London, 1977.

M. Kitao, S. Yamada, S. Yoshida, H. Akram and K. Urabe, "Preparation conditions of sputtered electrochromic WO_3 films and their infrared absorption spectra", *Solar Energy Materials and Solar Cells*, **25**, 241-255, 1992.

C.M. Lampert, "Thin film electrochromic materials for energy efficient windows", Lawrence Berkeley Laboratory, Berkeley, California, U.S.A., LBL-10862, October 1980.

C.M. Lampert, "Electrochromic materials and devices for energy efficient windows", *Solar Energy Materials*, **11**, 1-27, 1984.

C.M. Lampert, T.R. Omstead and P.C. Yu, "Chemical and optical properties of electrochromic nickel oxide films", *Solar Energy Materials*, **14**, 161-174, 1986.

C.M. Lampert (ed.), "Failure and degradation modes in selected solar materials: A review", *The International Energy Agency, Solar Heating and Cooling Program, Task 10: Solar Materials R&D*, May 1989.

C.M. Lampert and Y.-P. Ma, "Advanced glazing technology: Fenestration 2000 project-Phase III: Glazing Materials", Lawrence Berkeley Laboratory, Berkeley, California, U.S.A., LBL-31616, June 1992.

C.M. Lampert, "Smart switchable glazing for solar energy and daylight control", *Solar Energy Materials and Solar Cells*, **52**, 207-221, 1998.

C.M. Lampert, A. Agrawal, C. Baertlien and J. Nagai, "Durability evaluation of electrochromic devices - An industry perspective", *Solar Energy Materials and Solar Cells*, **56**, 449-463, 1999.

C.M. Lampert, "Large-area smart glass and integrated photovoltaics", *Solar Energy Materials and Solar Cells*, **76**, 489-499, 2003.

C.M. Lampert, "Chromogenic smart materials", *Materials Today*, **7**, 28-35, 2004.

E.S. Lee and D.L. DiBartolomeo, "Application issues for large-area electrochromic windows in commercial buildings", *Solar Energy Materials and Solar Cells*, **71**, 465-491, 2002.

E.S. Lee, D.L. DiBartolomeo and S.E. Selkowitz, "Daylighting control performance of a thin-film ceramic electrochromic window: Field study results", *Energy and Buildings*, **38**, 30-44, 2006(a).

E.S. Lee, S.E. Selkowitz, R.D. Clear, D.L. DiBartolomeo, J.H. Klems, L.L. Fernandes, G.J. Ward, V. Inkarojrit, M. Yazdanian, "Advancement of electrochromic windows", California

Energy Commission, PIER, Publication number CEC-500-2006-052, Lawrence Berkeley National Laboratory, 2006(b).

N. Leventis and Y.C. Chung, "Polyaniline-prussian blue novel composite material for electrochromic applications", *Journal of Electrochemical Society*, **137**, 3321-3322, 1990.

S.-Y. Li, G.A. Niklasson and C.G. Granqvist, "Thermochromic fenestration with VO_2-based materials: Three challenges and how they can be met", *Thin Solid Films*, **520**, 3823-3828, 2012.

Y.K. Lim, "Introduction to classical electrodynamics", p. 242, World Scientific, 1986.

R. Loudon, "The quantum theory of light", 2nd ed., pp. 24-30, Oxford University Press, 1990.

Y. Makimura, A. Rougier and J.-M. Tarascon, "Cobalt and tantalum additions for enhanced electrochromic performances of nickel-based oxide thin films grown by pulsed laser deposition", *Applied Surface Science*, **252**, 4593-4598, 2006.

A.F. McKinlay and B.L. Diffey, "A reference action spectrum for ultraviolet induced erythema in human skin", CIE Journal, **6**, pp. 17-22, 1987.

D.H. Mendelsohn and R.B. Goldner, "Ellipsometry measurements as direct evidence of the Drude model for polycrystalline electrochromic WO_3 films", *Journal of Electrochemical Society*, **131**, 857-860, 1984.

M. Mennig, K. Fries, M. Lindenstruth and H. Schmidt, "Development of fast switching photochromic coatings on transparent plastics and glass", *Thin Solid Films*, **351**, 230-234, 1999.

K. Midtdal and B.P. Jelle, "Self-cleaning glazing products: A state-of-the-art review and future research pathways", *Solar Energy Materials and Solar Cells*, **109**, 126-141, 2013.

N.R. Mlyuka, G.A. Niklasson and C.G. Granqvist, "Mg doping of thermochromic VO_2 films enhances the optical transmittance and decreases the metal-insulator transition temperature", *Applied Physics Letters*, **95**, 171909-1 - 171909-3, 2009.

P.M.S. Monk, R.J. Mortimer and D.R. Rosseinsky, "Electrochromism: Fundamentals and applications", VCH, 1995.

P.M.S. Monk, S.P. Akhtar, J. Boutevin and J.R. Duffield, "Toward the tailoring of electrochromic bands of metal-oxide mixtures", *Electrochimica Acta*, **46**, 2091-2096, 2001.

R.J. Mortimer, D.R. Rosseinsky and A. Glidle, "Polyelectrochromic prussian blue: A chronoamperometric study of the electrodeposition", *Solar Energy Materials and Solar Cells*, **25**, 211-223, 1992.

R.J. Mortimer, "Organic electrochromic materials", *Electrochimica Acta*, **44**, 2971-2981, 1999.

R.J. Mortimer, A.L. Dyer and J.R. Reynolds, "Electrochromic organic and polymeric materials for display applications", *Displays*, **27**, 2-18, 2006.

R.J. Mortimer and T.S. Varley, "Quantification of colour stimuli through the calculation of CIE chromaticity coordinates and luminance data for application to in situ colorimetry studies of electrochromic materials", *Displays*, **32**, 35-44, 2011.

R.J. Mortimer and T.S. Varley, "In situ spectroelectrochemistry and colour measurement of a complementary electrochromic device based on surface-confined prussian blue and aqueous solution-phase methyl viologen", *Solar Energy Materials and Solar Cells*, **99**, 213-220, 2012.

H. Moulki, D.H. Park, B.-K. Min, H. Kwon, S.-J. Hwang, J.-H. Choy, T. Toupance, G. Campet, A. Rougier, "Improved electrochromic performances of NiO based thin films by lithium addition: From single layers to devices", *Electrochimica Acta*, **74**, 46-52, 2012.

J. Nagai, T. Kamimori and M. Mizuhashi, "Transmissive electrochromic device", *Solar Energy Materials*, **14**, 175-184, 1986.

J. Nagai, G.D. McMeeking and Y. Saitoh, "Durability of electrochromic glazing", *Solar Energy Materials and Solar Cells*, **56**, 309-319, 1999.

S. Park and J.W. Hong, "Polymer dispersed liquid crystal film for variable-transparency glazing", *Thin Solid Films*, **517**, 3183-3186, 2009.

S. Passerini, B. Scrosati and A. Gorenstein, "The intercalation of lithium in nickel oxide and its electrochromic properties", *Journal of Electrochemical Society*, **137**, 3297-3300, 1990.

N. Penin, A. Rougier, L. Laffont, P. Poizot, J.-M. Tarascon, "Improved cyclability by tungsten addition in electrochromic NiO thin films", *Solar Energy Materials and Solar Cells*, **90**, 422-433, 2006.

A. Piccolo, "Thermal performance of an electrochromic smart window tested in an environmental test cell", *Energy and Buildings*, **42**, 1409-1417, 2010.

B. Rånby and J.F. Rabek, "Photodegradation, photo-oxidation and photostabilization of polymers. Principles and applications", John Wiley & Sons, 1975.

J.F. Rabek, "Polymer photodegradation. Mechanisms and experimental methods", Chapman & Hall, 1995.

J.F. Rabek, "Photodegradation of polymers. Physical characteristics and applications", Springer-Verlag, 1996.

A. Rougier, F. Portemer, A. Quédé and M. El Marssi, "Characterization of pulsed laser deposited WO_3 thin films for electrochromic devices", *Applied Surface Science*, **153**, 1-9, 1999.

A. Rougier and A. Blyr, "Electrochromic properties of vanadium tungsten oxide thin films grown by pulsed laser deposition", *Electrochimica Acta*, **46**, 1945-1950, 2001.

A. Rougier, A. Blyr, J. Garcia, Q. Zhang and S.A. Impey, "Electrochromic W-M-O (M=V, Nb) sol-gel thin films: A way to neutral colour", *Solar Energy Materials and Solar Cells*, **71**, 343-357, 2002.

M. Rubin, K. von Rottkay and R. Powles, "Window optics", *Solar Energy*, **62**, 149-161, 1998.

L.I. Sandberg, T. Gao, B.P. Jelle and A. Gustavsen, "Synthesis of hollow silica nanospheres by sacrificial polystyrene templates for thermal insulation applications", *Advances in Materials Science and Engineering*, **2013**, 6 pages, Article ID 483651, 2013.

K. Sauvet, A. Rougier and L. Sauques, "Electrochromic WO$_3$ thin films active in the IR region", *Solar Energy Materials and Solar Cells*, **92**, 209-215, 2008.

K. Sauvet, L. Sauques and A. Rougier, "IR electrochromic WO$_3$ thin films: From optimization to devices", *Solar Energy Materials and Solar Cells*, **93**, 2045-2049, 2009.

O.F. Schirmer, V. Wittver, G. Baur and G. Brandt, "Dependence of WO$_3$ electrochromic absorption on crystallinity", *Journal of Electrochemical Society*, **124**, 749-753, 1977.

A.P. Schuster, D. Nguyen and O. Caporaletti, "Solid state electrochromic infrared switchable windows", *Solar Energy Materials*, **13**, 153-160, 1986.

T. Seike and J. Nagai, "Electrochromism of 3d transition metal oxides", *Solar Energy Materials*, **22**, 107-117, 1991.

S.C. Sekhar and K.L.C. Toon, "On the study of energy performance and life cycle cost of smart window", *Energy and Buildings*, **28**, 307-316, 1998.

R.M. Silverstein, G.C. Bassler and T.C. Morrill, "Spectrometric identification of organic compounds", 4th ed., p. 307, John Wiley & Sons, 1981.

D.E. Stilwell, K.H. Park and M.H. Miles, "Electrochemical studies of the factors influencing the cycle stability of prussian blue films", *Journal of Applied Electrochemistry*, **22**, 325-331, 1992.

B. Stjerna and C.G. Granqvist, "Electrical conductivity and optical transmittance of sputter-deposited SnO$_x$ thin films", *Solar Energy Materials*, **20**, 225-233, 1990.

Surface Optics Corporation, "SOC-100 User's manual", San Diego, U.S.A., June 2009.

J.S.E.M. Svensson and C.G. Granqvist, "Electrochromic coatings for «smart windows»", *Proceedings of SPIE - Optical Materials Technology for Energy Efficiency and Solar Energy Conversion III*, C.M. Lampert (ed.), San Diego, California, U.S.A., 21-23 August, 1984, Vol. 502, pp. 30-37, The Society of Photo-Optical Instrumentation Engineers, Bellingham, Washington, U.S.A., 1984(a).

J.S.E.M. Svensson and C.G. Granqvist, "Modulated transmittance and reflectance in crystalline electrochromic WO$_3$ films: Theoretical limits", *Applied Physics Letters*, **45**, 828-830, 1984(b).

J.S.E.M. Svensson and C.G. Granqvist, "Electrochromic coatings for «smart windows»", *Solar Energy Materials*, **12**, 391-402, 1985.

A.A. Syed and M.K. Dinesan, "Review: Polyaniline – A novel polymeric material", *Talanta*, **38**, 815-837, 1991.

E. Syrrakou, S. Papaefthimiou and P. Yianoulis, "Eco-efficiency evaluation of a smart window prototype", *Science of the Total Environment*, **359**, 267-282, 2006.

K. Tajima, H. Hotta, Y. Yamada, M. Okada and K. Yoshimura, "Environmental durability of electrochromic switchable mirror glass at sub-zero temperature", *Solar Energy Materials and Solar Cells*, **104**, 146-151, 2012.

C.E. Tracy, J.-G. Zhang, D.K. Benson, A.W. Czanderna and S.K. Deb, "Accelerated durability testing of electrochromic windows", *Electrochimica Acta*, **44**, 3195-3202, 1999.

H. Tylli, C. Olkkonen and I. Forsskåhl, "A sensitivity analysis of the kinetic mechanism for the photodegradation of a model system of relevance to lignin yellowing", *Journal of Photochemistry and Photobiology, A: Chemistry*, **49**, 397-408, 1989.

S. Van Den Bergh, R. Hart, B.P. Jelle and A. Gustavsen, "Window spacers and edge seals in insulating glass units: A state-of-the-art review and future perspectives", *Energy and Buildings*, **58**, 263-280, 2013.

R. Vergaz, J.-M. Sánchez-Pena, D. Barrios, C. Vázquez and P. Contreras-Lallana, "Modelling and electro-optical testing of suspended particle devices", *Solar Energy Materials and Solar Cells*, **92**, 1483-1487, 2008.

V. Wittwer, M. Datz, J. Ell, A. Georg, W. Graf and G. Walze, "Gasochromic windows", *Solar Energy Materials and Solar Cells*, **84**, 305-314, 2004.

K. Yamanaka, "Electrodeposited films from aqueous tungstic acid-hydrogen peroxide solutions for electrochromic display devices", *Japanese Journal of Applied Physics*, **26**, 1884-1890, 1987.

H. Ye, X. Meng and B. Xu, "Theoretical discussions of perfect window, ideal near infrared solar spectrum regulating window and current thermochromic window", *Energy and Buildings*, **49**, 164-172, 2012.

K. Yoshimura, Y. Yamada, S. Bao, K. Tajima and M. Okada, "Preparation and characterization of gasochromic switchable-mirror window with practical size", *Solar Energy Materials and Solar Cells*, **93**, 2138-2142, 2009.

P.C. Yu, G. Nazri and C.M. Lampert, "Spectroscopic and electrochemical studies of electrochromic hydrated nickel oxide films", *Solar Energy Materials*, **16**, 1-17, 1987.

P.C. Yu and C.M. Lampert, "In-situ spectroscopic studies of electrochromic hydrated nickel oxide films", *Solar Energy Materials*, **19**, 1-16, 1989.

C. Zerwick, "A short history of glass", Harry N. Abrams Inc. Publishers New York in association with The Corning Museum of Glass, 1990.

J. Zhang, X.L. Wang, X.H. Xia, C.D. Gu and J.P. Tu, "Electrochromic behavior of WO_3 nanotree films prepared by hydrothermal oxidation", *Solar Energy Materials and Solar Cells*, **95**, 2107-2112, 2011.

J.G. Zhang, C.E. Tracy, D.K. Benson and S.K. Deb, "The influence of microstructure on the electrochromic properties of Li_xWO_3 thin films: Part I. Ion diffusion and electrochromic properties", *Journal of Materials Research*, **8**, 2649-2656, 1993.

Appendix A - Tables for Calculation of Solar Radiation Glazing Factors

Table A1. Normalized relative spectral distribution of the ultraviolet part of global solar radiation for the calculation of the Ultraviolet Solar Transmittance (T_{uv}). The table has been drawn up with relative values so that $\Sigma S_\lambda \Delta\lambda = 1$ for the wavelength range 300-380 nm. Table values are given in ISO 9050:2003(E) (2003), based upon air mass 1.5 values (ISO 9845-1:1992(E) (1992)).

Wavelength λ (nm)	$S_\lambda \Delta\lambda$	Wavelength λ (nm)	$S_\lambda \Delta\lambda$
300	0	345	0.073326
305	0.001859	350	0.079330
310	0.007665	355	0.082894
315	0.017961	360	0.087039
320	0.029732	365	0.097963
325	0.042466	370	0.108987
330	0.062108	375	0.113837
335	0.065462	380	0.058351
340	0.071020		

Table A2. Normalized relative spectral distribution $D_\lambda V(\lambda)\Delta\lambda$ for the calculation of the Visible Solar Transmittance (T_{vis}). The table has been drawn up with relative values so that $\Sigma D_\lambda V(\lambda)\Delta\lambda = 1$ for the wavelength range 380-780 nm. Table values are given in ISO 9050:2003(E) (2003).

Wavelength λ (nm)	$D_\lambda V(\lambda)\Delta\lambda$	Wavelength λ (nm)	$D_\lambda V(\lambda)\Delta\lambda$
380	0	590	0.063306
390	0.000005	600	0.053542
400	0.000030	610	0.042491
410	0.000103	620	0.031502
420	0.000352	630	0.020812
430	0.000948	640	0.013810
440	0.002274	650	0.008070
450	0.004192	660	0.004612
460	0.006663	670	0.002485
470	0.009850	680	0.001255
480	0.015189	690	0.000536
490	0.021336	700	0.000276
500	0.033491	710	0.000146
510	0.051393	720	0.000057
520	0.070523	730	0.000035
530	0.087990	740	0.000021
540	0.094427	750	0.000008
550	0.098077	760	0.000001
560	0.094306	770	0.000000
570	0.086891	780	0.000000
580	0.078994		

Table A3. Normalized relative spectral distribution of global solar radiation for the calculation of the Solar Transmittance (T_{sol}). The table has been drawn up with relative values so that $\Sigma S_\lambda \Delta\lambda = 1$ for the wavelength range 300-2500 nm. Table values are given in ISO 9050:2003(E) (2003), based upon air mass 1.5 values (ISO 9845-1:1992(E) (1992)).

Wavelength λ (nm)	$S_\lambda\Delta\lambda$	Wavelength λ (nm)	$S_\lambda\Delta\lambda$
300	0	680	0.012838
305	0.000057	690	0.011788
310	0.000236	700	0.012453
315	0.000554	710	0.012798
320	0.000916	720	0.010589
325	0.001309	730	0.011233
330	0.001914	740	0.012175
335	0.002018	750	0.012181
340	0.002189	760	0.009515
345	0.002260	770	0.010479
350	0.002445	780	0.011381
355	0.002555	790	0.011262
360	0.002683	800	0.028718
365	0.003020	850	0.048240
370	0.003359	900	0.040297
375	0.003509	950	0.021384
380	0.003600	1000	0.036097
385	0.003529	1050	0.034110
390	0.003551	1100	0.018861
395	0.004294	1150	0.013228
400	0.007812	1200	0.022551
410	0.011638	1250	0.023376
420	0.011877	1300	0.017756
430	0.011347	1350	0.003743
440	0.013246	1400	0.000741
450	0.015343	1450	0.003792
460	0.016166	1500	0.009693
470	0.016178	1550	0.013693
480	0.016402	1600	0.012203
490	0.015794	1650	0.010615
500	0.015801	1700	0.007256
510	0.015973	1750	0.007183
520	0.015357	1800	0.002157
530	0.015867	1850	0.000398
540	0.015827	1900	0.000082
550	0.015844	1950	0.001087
560	0.015590	2000	0.003024
570	0.015256	2050	0.003988
580	0.014745	2100	0.004229
590	0.014330	2150	0.004142
600	0.014663	2200	0.003690
610	0.015030	2250	0.003592
620	0.014859	2300	0.003436
630	0.014622	2350	0.003163
640	0.014526	2400	0.002233
650	0.014445	2450	0.001202
660	0.014313	2500	0.000475
670	0.014023		

Table A4. Normalized relative spectral distribution factors for the calculation of the Solar Material Protection Factor (SMPF). The table has been drawn up with relative values so that $\Sigma C_\lambda S_\lambda \Delta\lambda = 1$ for the wavelength range 300-600 nm. Table values are given in ISO 9050:2003(E) (2003), based upon air mass 1.5 values (ISO 9845-1:1992(E) (1992)).

Wavelength λ (nm)	$C_\lambda S_\lambda \Delta\lambda$	Wavelength λ (nm)	$C_\lambda S_\lambda \Delta\lambda$
300	0	410	0.057799
305	0.001003	420	0.052317
310	0.003896	430	0.044328
315	0.008597	440	0.045896
320	0.013402	450	0.047150
325	0.018028	460	0.044062
330	0.024831	470	0.039108
335	0.024648	480	0.035167
340	0.025183	490	0.030034
345	0.024487	500	0.026650
350	0.024949	510	0.023893
355	0.024551	520	0.020373
360	0.024278	530	0.018671
365	0.025734	540	0.016517
370	0.026962	550	0.014665
375	0.026522	560	0.012799
380	0.025624	570	0.011108
385	0.023656	580	0.009522
390	0.022418	590	0.008208
395	0.025529	600	0.003695
400	0.043742		

Table A5. Normalized relative spectral distribution factors for the calculation of the Solar Skin Protection Factor (SSPF). The table has been drawn up with relative values so that $\Sigma E_\lambda S_\lambda \Delta\lambda = 1$ for the wavelength range 300-400 nm. Table values are given in ISO 9050:2003(E) (2003), based upon air mass 1.5 values (ISO 9845-1:1992(E) (1992)).

Wavelength λ (nm)	$E_\lambda S_\lambda \Delta\lambda$	Wavelength λ (nm)	$E_\lambda S_\lambda \Delta\lambda$
300	0	355	0.019298
305	0.168176	360	0.017028
310	0.230555	365	0.016157
315	0.187429	370	0.015108
320	0.102699	375	0.013298
325	0.050895	380	0.011471
330	0.034134	385	0.009440
335	0.030432	390	0.008009
340	0.027729	395	0.008165
345	0.024094	400	0.003953
350	0.021930		

Table A6. Wavelengths for determining normal reflectance (R_n) for the emissivity (ε) determination in Eq.22 at 283 K (ISO 10292:1994(E) (1994), EN 12898:2001 E (2001)).

No. i	Wavelength λ_i (µm)	No. i	Wavelength λ_i (µm)
1	5.5	16	14.8
2	6.7	17	15.6
3	7.4	18	16.3
4	8.1	19	17.2
5	8.6	20	18.1
6	9.2	21	19.2
7	9.7	22	20.3
8	10.2	23	21.7
9	10.7	24	23.3
10	11.3	25	25.2
11	11.8	26	27.7
12	12.4	27	30.9
13	12.9	28	35.7
14	13.5	29	43.9
15	14.2	30	50.0

Table A7. Corresponding correction coefficient ($\varepsilon/\varepsilon_n$) and normal emissivity (ε_n) values, for determination of corrected emissivity (ε) values according to Eq.23, i.e. $\varepsilon = c_{corr} \cdot \varepsilon_n = \varepsilon/\varepsilon_n \cdot \varepsilon_n$. Other values may be obtained with sufficient accuracy by linear interpolation or extrapolation (ISO 10292:1994(E) (1994), EN 12898:2001 E (2001)).

Normal emissivity ε_n	0.03	0.05	0.1	0.2	0.3	0.4	0.5	0.6	0.7	0.8	0.89
Correction coefficient $\varepsilon/\varepsilon_n$	1.22	1.18	1.14	1.10	1.06	1.03	1.00	0.98	0.96	0.95	0.94

Table A8. Gas properties required for calculation of the Nusselt number (Nu) (Eq.56), which is part of the calculation of the thermal conductance (Λ) (Eq.52) (ISO 10292:1994(E) (1994)). Equation 31 gives the relationship between the absolute mean temperature T_m in K and the mean temperature θ in ºC: $\theta = (T_m - 273.15 \text{ K}) \text{ ºC/K}$.

Gas	Temperature θ (ºC)	Mass density ρ (kg/m³)	Dynamic viscosity μ (10^{-5} kg/(ms))	Thermal conductivity κ (10^{-2} W/(mK))	Specific heat c_m (10^3 J/(kgK))
Air	-10 0 +10 +20	1.326 1.277 1.232 1.189	1.661 1.711 1.761 1.811	2.336 2.416 2.496 2.576	1.008
Argon (Ar)	-10 0 +10 +20	1.829 1.762 1.699 1.640	2.038 2.101 2.164 2.228	1.584 1.634 1.684 1.734	0.519
SF₆	-10 0 +10 +20	6.844 6.602 6.360 6.118	1.383 1.421 1.459 1.497	1.119 1.197 1.275 1.354	0.614
Krypton (Kr)	-10 0 +10 +20	3.832 3.690 3.560 3.430	2.260 2.330 2.400 2.470	0.842 0.870 0.900 0.926	0.245

Table A9. Values of the constants A and n, depending on the space inclination, for calculation of the Nusselt number (Nu), Eq.56 (ISO 10292:1994(E) (1994)).

Space inclination	A	n
Vertical	0.035	0.38
45º	0.10	0.31
Horizontal	0.16	0.28

Table A10. Values of $U_{r,i}^*$, $V_{r,i}^*$ and $W_{r,i}^*$ for the test colours lighted by the standard illuminant D65, applicable in calculation of the colour rendering factor CRF (EN 410:1998 E (1998)).

Test colour number i	$U_{r,i}^*$	$V_{r,i}^*$	$W_{r,i}^*$
1	31.92	8.41	60.48
2	15.22	23.76	59.73
3	-8.34	36.29	61.08
4	-33.29	18.64	60.25
5	-26.82	-6.55	61.41
6	-18.80	-28.80	60.52
7	9.77	-26.50	60.14
8	28.78	-16.24	61.83

Table A11. Relative spectral energy distribution of illuminant D65 for wavelengths between 380 nm to 780 nm normalized to the value of 100 at 560 nm, applicable in calculation of the colour rendering factor CRF (EN 410:1998 E (1998)).

Wavelength λ (nm)	$(d\Phi/d\lambda)\Delta\lambda$	Wavelength λ (nm)	$(d\Phi/d\lambda)\Delta\lambda$
380	50.0	590	88.7
390	54.6	600	90.0
400	82.8	610	89.6
410	91.5	620	87.7
420	93.4	630	83.3
430	86.7	640	83.7
440	104.9	650	80.0
450	117.0	660	80.2
460	117.8	670	82.3
470	114.9	680	78.3
480	115.9	690	69.7
490	108.8	700	71.6
500	109.4	710	74.3
510	107.8	720	61.6
520	104.8	730	69.9
530	107.7	740	75.1
540	104.4	750	63.6
550	104.0	760	46.4
560	100.0	770	66.8
570	96.3	780	63.4
580	95.8		

Table A12. Spectral reflectance $\beta_i(\lambda)$ of the eight test colours (i from 1 to 8) for calculation of the colour rendering factor CRF (EN 410:1998 E (1998)).

λ (nm)	Test colour number i							
	1	2	3	4	5	6	7	8
380	0.219	0.070	0.065	0.074	0.295	0.151	0.378	0.104
390	0.252	0.089	0.070	0.093	0.310	0.265	0.524	0.170
400	0.256	0.111	0.073	0.116	0.313	0.410	0.551	0.319
410	0.252	0.118	0.074	0.124	0.319	0.492	0.559	0.462
420	0.244	0.121	0.074	0.128	0.326	0.517	0.561	0.490
430	0.237	0.122	0.073	0.135	0.334	0.531	0.556	0.482
440	0.230	0.123	0.073	0.144	0.346	0.544	0.544	0.462
450	0.225	0.127	0.074	0.161	0.360	0.556	0.522	0.439
460	0.220	0.131	0.077	0.186	0.381	0.554	0.488	0.413
470	0.216	0.138	0.085	0.229	0.403	0.541	0.448	0.382
480	0.214	0.150	0.109	0.281	0.415	0.519	0.408	0.352
490	0.216	0.174	0.148	0.332	0.419	0.488	0.363	0.325
500	0.223	0.207	0.198	0.370	0.413	0.450	0.324	0.299
510	0.226	0.242	0.241	0.390	0.403	0.414	0.301	0.283
520	0.225	0.260	0.278	0.395	0.389	0.377	0.283	0.270
530	0.227	0.267	0.339	0.385	0.372	0.341	0.265	0.256
540	0.236	0.272	0.392	0.367	0.353	0.309	0.257	0.250
550	0.253	0.282	0.400	0.341	0.331	0.279	0.259	0.254
560	0.272	0.299	0.380	0.312	0.308	0.253	0.260	0.264
570	0.298	0.322	0.349	0.280	0.284	0.234	0.256	0.272
580	0.341	0.335	0.315	0.247	0.260	0.225	0.254	0.278
590	0.390	0.341	0.285	0.214	0.232	0.221	0.270	0.295
600	0.424	0.342	0.264	0.185	0.210	0.220	0.302	0.348
610	0.442	0.342	0.252	0.169	0.194	0.220	0.344	0.434
620	0.450	0.341	0.241	0.160	0.185	0.223	0.377	0.528
630	0.451	0.339	0.229	0.154	0.180	0.233	0.400	0.604
640	0.451	0.338	0.220	0.151	0.176	0.244	0.420	0.648
650	0.450	0.336	0.216	0.148	0.175	0.258	0.438	0.676
660	0.451	0.334	0.219	0.148	0.175	0.268	0.452	0.693
670	0.453	0.332	0.230	0.151	0.180	0.278	0.462	0.705
680	0.455	0.331	0.251	0.158	0.186	0.283	0.468	0.712
690	0.458	0.329	0.288	0.165	0.192	0.291	0.473	0.717
700	0.462	0.328	0.340	0.170	0.199	0.302	0.483	0.721
710	0.464	0.326	0.390	0.170	0.199	0.325	0.496	0.719
720	0.466	0.324	0.431	0.166	0.196	0.351	0.511	0.725
730	0.466	0.324	0.460	0.164	0.195	0.376	0.525	0.729
740	0.467	0.322	0.481	0.168	0.197	0.401	0.539	0.730
750	0.467	0.320	0.493	0.177	0.203	0.425	0.553	0.730
760	0.467	0.316	0.500	0.185	0.208	0.447	0.565	0.730
770	0.467	0.315	0.505	0.192	0.215	0.469	0.575	0.730
780	0.467	0.314	0.516	0.197	0.219	0.485	0.581	0.730

Table A13.   Abridged set of spectral tristimulus values $\bar{x}(\lambda), \bar{y}(\lambda)$ and $\bar{z}(\lambda)$ for the CIE 1931 standard colourimetric observer, for wavelengths between 380 nm to 780 nm at 10 nm intervals, applicable in calculation of the colour rendering factor CRF (EN 410:1998 E (1998)).

Wavelength λ (nm)	$\bar{x}(\lambda)$	$\bar{y}(\lambda)$	$\bar{z}(\lambda)$
380	0.0014	0.0000	0.0065
390	0.0042	0.0001	0.0201
400	0.0143	0.0004	0.0679
410	0.0435	0.0012	0.2074
420	0.1344	0.0040	0.6456
430	0.2839	0.0116	1.3856
440	0.3483	0.0230	1.7471
450	0.3362	0.0380	1.7721
460	0.2908	0.0600	1.6692
470	0.1954	0.0910	1.2876
480	0.0956	0.1390	0.8130
490	0.0320	0.2080	0.4652
500	0.0049	0.3230	0.2720
510	0.0093	0.5030	0.1582
520	0.0633	0.7100	0.0782
530	0.1655	0.8620	0.0422
540	0.2904	0.9540	0.0203
550	0.4334	0.9950	0.0087
560	0.5945	0.9950	0.0039
570	0.7621	0.9520	0.0021
580	0.9163	0.8700	0.0017
590	1.0263	0.7570	0.0011
600	1.0622	0.6310	0.0008
610	1.0026	0.5030	0.0003
620	0.8544	0.3810	0.0002
630	0.6424	0.2650	0.0000
640	0.4479	0.1750	0.0000
650	0.2835	0.1070	0.0000
660	0.1649	0.0610	0.0000
670	0.0874	0.0320	0.0000
680	0.0468	0.0170	0.0000
690	0.0227	0.0082	0.0000
700	0.0114	0.0041	0.0000
710	0.0058	0.0021	0.0000
720	0.0029	0.0010	0.0000
730	0.0014	0.0005	0.0000
740	0.0007	0.0002	0.0000
750	0.0003	0.0001	0.0000
760	0.0002	0.0001	0.0000
770	0.0001	0.0000	0.0000
780	0.0000	0.0000	0.0000

Appendix B - Tables for Calculation of Thermal Conductance

Table B1.　Actual given and calculated values applied in the calculations of the thermal conductance Λ for different cases, which are hence applied in the calculations of the solar factors (SF). The emissivity values $\varepsilon_{float} = 0.836$, $\varepsilon_{lowe} = 0.071$ and $\varepsilon_{silver} = 0.543$, for the float glass, low emittance glass and dark silver coated glass, respectively, were measured by hemispherical directional reflectance. Two-layer window pane with air in the gas space. G = glass, LE = low emittance coating, S = dark silver coating, A = air cavity.

Properties – Two-layer window with air	G/A/G	G/A/LE/G	G/A/S/G	G/LE/A/LE/G	G/LE/A/G	G/S/A/G	G/S/A/LE/G	G/S/A/S/G
Stefan-Boltzmann's constant (10^{-8} W/(m^{2}K^4))	5.6696	5.6696	5.6696	5.6696	5.6696	5.6696	5.6696	5.6696
External heat transfer coefficient (W/(m^{2}K))	23	23	23	23	23	23	23	23
Internal heat transfer coefficient (W/(m^{2}K))	8	8	8	8	8	8	8	8
Thickness of each material (glass) (m)	0.004	0.004	0.004	0.004	0.004	0.004	0.004	0.004
Thermal resistivity of each material (glass) (mK/W)	1	1	1	1	1	1	1	1
Number of spaces	1	1	1	1	1	1	1	1
Number of materials (glass panes)	2	2	2	2	2	2	2	2
Gas thermal conductivity at +10°C (W/(mK))	0.02496	0.02496	0.02496	0.02496	0.02496	0.02496	0.02496	0.02496
Space width of gas (m)	0.012	0.012	0.012	0.012	0.012	0.012	0.012	0.012
Gas mean temperature (K)	283	283	283	283	283	283	283	283
Corrected emissivity for material 1 (glass 1)	0.836	0.836	0.836	0.071	0.071	0.543	0.543	0.543
Corrected emissivity for material 2 (glass 2)	0.836	0.071	0.543	0.071	0.836	0.836	0.071	0.543
Space inclination constant	0.035	0.035	0.035	0.035	0.035	0.035	0.035	0.035
Space inclination exponent	0.38	0.38	0.38	0.38	0.38	0.38	0.38	0.38
Gas mass density at +10°C (kg/m^3)	1.232	1.232	1.232	1.232	1.232	1.232	1.232	1.232
Gas dynamic viscosity at +10°C (10^{-5} kg/(ms))	1.761	1.761	1.761	1.761	1.761	1.761	1.761	1.761
Gas specific heat capacity per unit mass (J/(kgK))	1008	1008	1008	1008	1008	1008	1008	1008
Temperature difference on either side of glazing (K)	15	15	15	15	15	15	15	15
Prandtl number	0.71117308	0.71117308	0.71117308	0.71117308	0.71117308	0.71117308	0.71117308	0.71117308
Grashof number	4397.64606	4397.64606	4397.64606	4397.64606	4397.64606	4397.64606	4397.64606	4397.64606
Nusselt number	0.7451477	0.7451477	0.7451477	0.7451477	0.7451477	0.7451477	0.7451477	0.7451477
Corrected Nusselt number	1	1	1	1	1	1	1	1
Gas conductance (W/(m^{2}K))	2.08	2.08	2.08	2.08	2.08	2.08	2.08	2.08
Radiation conductance (W/(m^{2}K))	3.69168821	0.35993398	2.52238676	0.18918985	0.35993398	2.52238676	0.34436941	1.91563161
Gas space conductance (W/(m^{2}K))	5.77168821	2.43993398	4.60238676	2.26918985	2.43993398	4.60238676	2.42436941	3.99563161
Total gas space resistance (m^{2}K/W)	0.17325953	0.40984715	0.21727857	0.44068591	0.40984715	0.21727857	0.41247839	0.25027332
Material resistance (m^{2}K/W)	0.004	0.004	0.004	0.004	0.004	0.004	0.004	0.004
Total material resistance (m^{2}K/W)	0.008	0.008	0.008	0.008	0.008	0.008	0.008	0.008
Thermal conductance (W/(m^{2}K))	5.51695123	2.3932196	4.43894869	2.22873055	2.3932196	4.43894869	2.37824348	3.87186717
Thermal transmittance - U-value (W/(m^{2}K))	2.85928493	1.70553753	2.5396385	1.62031441	1.70553753	2.5396385	1.69791782	2.34328363

Table B2.   Actual given and calculated values applied in the calculations of the thermal conductance Λ for different cases, which are hence applied in the calculations of the solar factors (SF). The emissivity values $\varepsilon_{float} = 0.836$, $\varepsilon_{lowe} = 0.071$ and $\varepsilon_{silver} = 0.543$, for the float glass, low emittance glass and dark silver coated glass, respectively, were measured by hemispherical directional reflectance. Three-layer window pane with air in the two gas spaces, where each gas space is treated in each column. G = glass, LE = low emittance coating, S = dark silver coating, A = air cavity, e = exterior side (gas space), i = interior side (gas space).

Properties – Three-layer window with air	G/A/G e	G/A/G i	G/A/LE/G i	G/A/LE/G e	G/LE/A/LE/G e	G/S/A/G e	G/S/A/LE/G e	G/S/A/S/G e	G/A/S/G i
Stefan-Boltzmann's constant (10^{-8} W/(m^{2}K^4))	5.6696	5.6696	5.6696	5.6696	5.6696	5.6696	5.6696	5.6696	5.6696
External heat transfer coefficient (W/(m^{2}K))	23	23	23	23	23	23	23	23	23
Internal heat transfer coefficient (W/(m^{2}K))	8	8	8	8	8	8	8	8	8
Thickness of each material (glass) (m)	0.003	0.003	0.003	0.003	0.003	0.003	0.003	0.003	0.003
Thermal resistivity of each material (glass) (mK/W)	1	1	1	1	1	1	1	1	1
Number of spaces	1	1	1	1	1	1	1	1	1
Number of materials (glass panes)	2	2	2	2	2	2	2	2	2
Gas thermal conductivity at +10°C (W/(mK))	0.02496	0.02496	0.02496	0.02496	0.02496	0.02496	0.02496	0.02496	0.02496
Space width of gas (m)	0.012	0.012	0.012	0.012	0.012	0.012	0.012	0.012	0.012
Gas mean temperature (K)	279.25	286.75	286.75	279.25	279.25	279.25	279.25	279.25	286.75
Corrected emissivity for material 1 (glass 1)	0.836	0.836	0.836	0.836	0.071	0.543	0.543	0.543	0.836
Corrected emissivity for material 2 (glass 2)	0.836	0.836	0.071	0.071	0.071	0.836	0.071	0.543	0.543
Space inclination constant	0.035	0.035	0.035	0.035	0.035	0.035	0.035	0.035	0.035
Space inclination exponent	0.38	0.38	0.38	0.38	0.38	0.38	0.38	0.38	0.38
Gas mass density at +10°C (kg/m^3)	1.232	1.232	1.232	1.232	1.232	1.232	1.232	1.232	1.232
Gas dynamic viscosity at +10°C (10^{-5} kg/(ms))	1.761	1.761	1.761	1.761	1.761	1.761	1.761	1.761	1.761
Gas specific heat capacity per unit mass (J/(kgK))	1008	1008	1008	1008	1008	1008	1008	1008	1008
Temperature difference on either side of glazing (K)	7.5	7.5	7.5	7.5	7.5	7.5	7.5	7.5	7.5
Prandtl number	0.71117308	0.71117308	0.71117308	0.71117308	0.71117308	0.71117308	0.71117308	0.71117308	0.71117308
Grashof number	2228.35064	2170.06772	2170.06772	2228.35064	2228.35064	2228.35064	2228.35064	2228.35064	2170.06772
Nusselt number	0.57550938	0.56974236	0.56974236	0.57550938	0.57550938	0.57550938	0.57550938	0.57550938	0.56974236
Corrected Nusselt number	1	1	1	1	1	1	1	1	1
Gas conductance (W/(m^{2}K))	2.08	2.08	2.08	2.08	2.08	2.08	2.08	2.08	2.08
Radiation conductance (W/(m^{2}K))	3.54686986	3.84039582	0.37443275	0.34581441	0.18176827	2.42343802	0.33086041	1.8404848	2.62399287
Gas space conductance (W/(m^{2}K))	5.62686986	5.92039582	2.45443275	2.42581441	2.26176827	4.50343802	2.41086041	3.9204848	4.70399287
Total gas space resistance (m^{2}K/W)	0.1777187	0.16890763	0.40742612	0.41223269	0.44213194	0.22205257	0.41478967	0.2550705	0.21258536
Material resistance (m^{2}K/W)	0.003	0.003	0.003	0.003	0.003	0.003	0.003	0.003	0.003
Total material resistance (m^{2}K/W)	0.006	0.006	0.006	0.006	0.006	0.006	0.006	0.006	0.006
Thermal conductance (W/(m^{2}K))	5.44310403	5.71730361	2.41881188	2.39101348	2.23148565	4.38495381	2.37648418	3.83038305	4.57487189
Thermal transmittance - U-value (W/(m^{2}K))	2.83932035	2.9121756	1.71849541	1.7044168	1.62177011	2.52187198	1.6970209	2.32802443	2.58355463